

Review

Advanced Applications of Carbonaceous Materials in Sustainable Water Treatment, Energy Storage, and CO₂ Capture: A Comprehensive Review

Md Sumon Reza ^{1,2,3,*}, Shammya Afroze ⁴, Kairat Kuterbekov ⁴, Asset Kabyshev ⁴,
Kenzhebatyr Zh. Bekmyrza ^{4,*}, Md Naimul Haque ², Shafi Noor Islam ⁵, Md Aslam Hossain ⁶, Mahbub Hassan ⁷,
Hridoy Roy ⁸, Md Shahinoor Islam ^{8,9}, Md Nahid Pervez ¹⁰ and Abul Kalam Azad ³

- ¹ Research Institute of New Chemical Technologies, Faculty of Natural Sciences, L.N. Gumilyov Eurasian National University, Astana 010008, Kazakhstan
 - ² Department of Civil Engineering, East West University, Dhaka 1212, Bangladesh; naimul@ewubd.edu
 - ³ Faculty of Integrated Technologies, Universiti Brunei Darussalam, Jalan Tungku Link, Gadong BE1410, Brunei; abul.azad@ubd.edu.bn
 - ⁴ Faculty of Physics and Technical Sciences, L.N. Gumilyov Eurasian National University, Astana 010008, Kazakhstan; afroze_sh@enu.kz (S.A.); kuterbekov_ka@enu.kz (K.K.); kabyshev_am_1@enu.kz (A.K.)
 - ⁵ Geography and Environmental Studies, Faculty of Arts and Social Sciences (FASS), Universiti Brunei Darussalam, Jalan Tungku Link, Gadong BE1410, Brunei; shafi.islam@ubd.edu.bn
 - ⁶ DPS Group Global 175 Regency Wds Pl Suite 400, Cary, NC 27518, USA; aslam.hossain@dpsgroupglobal.com
 - ⁷ School of Chemical and Biomolecular Engineering, Faculty of Engineering, University of Sydney, Camperdown 2006, Australia; m.hassan@sydney.edu.au
 - ⁸ Department of Chemical Engineering, Bangladesh University of Engineering and Technology, Dhaka 1000, Bangladesh; hridoyroy@che.buet.ac.bd (H.R.); shahinoorislam@che.buet.ac.bd (M.S.I.)
 - ⁹ Department of Textile Engineering, Daffodil International University, Dhaka 1341, Bangladesh
 - ¹⁰ Sanitary Environmental Engineering Division (SEED), Department of Civil Engineering, University of Salerno, Via Giovanni Paolo II 132, 84084 Fisciano, SA, Italy; mpervez@unisa.it
- * Correspondence: reza_m@enu.kz (M.S.R.); bekmyrza_kzh@enu.kz (K.Z.B.)



check for updates

Citation: Reza, M.S.; Afroze, S.; Kuterbekov, K.; Kabyshev, A.; Zh. Bekmyrza, K.; Haque, M.N.; Islam, S.N.; Hossain, M.A.; Hassan, M.; Roy, H.; et al. Advanced Applications of Carbonaceous Materials in Sustainable Water Treatment, Energy Storage, and CO₂ Capture: A Comprehensive Review. *Sustainability* **2023**, *15*, 8815. <https://doi.org/10.3390/su15118815>

Academic Editor: Agostina Chiavola

Received: 8 March 2023

Revised: 5 May 2023

Accepted: 25 May 2023

Published: 30 May 2023



Copyright: © 2023 by the authors. Licensee MDPI, Basel, Switzerland. This article is an open access article distributed under the terms and conditions of the Creative Commons Attribution (CC BY) license (<https://creativecommons.org/licenses/by/4.0/>).

Abstract: The demand for energy has increased tremendously around the whole world due to rapid urbanization and booming industrialization. Energy is the major key to achieving an improved social life, but energy production and utilization processes are the main contributors to environmental pollution and greenhouse gas emissions. Mitigation of the energy crisis and reduction in pollution (water and air) difficulties are the leading research topics nowadays. Carbonaceous materials offer some of the best solutions to minimize these problems in an easy and effective way. It is also advantageous that the sources of carbon-based materials are economical, the synthesis processes are comfortable, and the applications are environmentally friendly. Among carbonaceous materials, activated carbons, graphene, and carbon nanotubes have shown outstanding performance in mitigating the energy crisis and environmental pollution. These three carbonaceous materials exhibit unique adsorption properties for energy storage, water purification, and gas cleansing due to their outstanding electrical conductivity, large specific surface areas, and strong mechanical strength. This paper reviews the synthesis methods for activated carbons, carbon nanotubes, and graphene and their significant applications in energy storage, water treatment, and carbon dioxide gas capture to improve environmental sustainability.

Keywords: activated carbons; carbon nanotubes; graphene; water treatment; energy storage; CO₂ capture

1. Introduction

“Where nature finishes producing its own species, man begins, using natural things and, with the help of this nature, to create an infinity of species”, as the great scientist/artist Leonardo da Vinci said. In this regard, the synthesis and application of carbonaceous

materials towards environmental solicitations are the main goals for scientists [1]. Energy, the most valuable resource for humans, forges close ties between nature and life. For the social and economic development of a nation, there are no substitutes for energy. Given this, the need for energy is increasing daily [2,3]. The primary source of energy is fossil fuels, which are depleting with time and producing greenhouse gases, particularly carbon dioxide (CO₂), during combustion [4,5]. With the escalation of CO₂ levels, energy generation and utilization are polluting water sources tremendously, as there is a strong positive relationship between energy and environmental pollution (air and water) [6]. Therefore, it is highly important to protect the environment by mitigating energy problems. Carbonaceous materials offer some of the best solutions to resolve these issues for environmental sustainability [7].

Carbon (C), the sixth most abundant element in the universe, was first applied by the Egyptians in 3750 BC in the form of coal to absorb pungent vapors from wounds [8]. The allotropes of carbon are commonly known as activated carbons, graphite, nanotubes, diamond, graphene, fullerenes, etc. [9]. Among these materials, activated carbons (ACs), graphene, and carbon nanotubes (CNTs) are considered the most effective adsorbents due to their high surface areas and distinct chemical and physical properties [10–12]. An AC is an amorphous, dense carbonaceous material with a three-dimensional arrangement of carbon and has a large porous surface area and a variety of functional groups [13]. Activated carbons (ACs) are highly effective for adsorption, purification, and filtration processes [14]. The low-cost byproducts from biomass processing industries have been established as possible sources of activated carbons [15]. The performances of activated carbons in the carbon capture and storage (CCS) process are also very promising with respect to reducing CO₂ emissions from point sources [16].

Graphene is referred to as a single sheet of sp² hybridized carbon atoms arranged in a 2D honeycomb configuration. A single-atom-thick layer of virgin graphene provides unique mechanical, thermal, optical, and electrical properties [17]. Graphene has gained a lot of attention in recent years for its exceptional and distinctive qualities, which include excellent electrical conductivity, a sizable theoretical specific surface area, and high mechanical strength. Graphene oxide (GO), a single layer of graphite oxide, has also shown effective performance due to the multiple oxygen-containing functional groups embedded in it (carboxyl, phenol, quinone, and lactone at the sheet edges) [18].

Carbon nanotubes (CNTs) are 1D crystals of sp² bonded carbon and are normally used in the nanotechnology industry [9]. Due to their high electrical conductivity, perfect structure, and chemical stability, they are mostly proposed as emitters in the electron field [19]. Carbon nanotubes consist of single-walled carbon nanotubes (SWCNTs) and multi-walled carbon nanotubes (MWCNTs) [20]. When CNTs have only one graphitic shell, they are called single-walled carbon nanotubes, and when they have many concentric graphitic shells, they are called multi-walled carbon nanotubes [21]. They are electrochemically intercalated, as they possess large irreversible capacities and voltage hysteresis [22]. CNTs are also potential theranostics and carriers of drug delivery systems owing to their simple cell membrane permeability [23].

Another significant application of carbon nanotubes is water treatment for the appropriate control of organic, inorganic, and biological water pollutants [24]. Regarding energy storage applications, MWCNTs and SWCNTs have been used for electrochemical hydrogen storage [25] and some redox reactions, which can be used for fuel cells [26,27]. Furthermore, CNTs have been recognized for their excellent adsorbing capacity in capturing CO₂, while MWCNTs have been found to be better adsorbents compared to SWCNTs [28]. The role of carbon nanotubes as adsorbents can be distinguished from those of other adsorbents by the van der Waals forces between pollutants and nanotubes, as they stick and agglomerate in the form of clusters [29]. A new family of carbon-only compounds called fullerenes, which were initially known as buckminsterfullerenes and include 60 carbon atoms (C₆₀) grouped in a soccer-ball configuration, are also carbon-based materials [30]. However, due

to their higher price compared to two-dimensional graphene and one-dimensional carbon nanotubes (CNTs), they have received less attention than other carbon materials [31].

Energy storage is one of the great challenges of the twenty-first century because of the vast expansion of energy technology. Storage is most essential in remote locations and depends on the ability to store kinetic energy [32]. To cover the base load for urban society and evolving ecology, it is critical to find portable, lightweight, low-cost, and environmentally sustainable energy storage solutions [33]. Storage systems are used in major energy devices, such as solar panels, batteries, fuel cells, electrolytic capacitors, supercapacitors, and hydrogen storage. In the present day, energy storage technology, batteries, and supercapacitors show high performance and efficiency due to their high-power capabilities and long cycle life [34]. Supercapacitors offer higher peak currents, lower cyclic costs, good reversibility, and low material toxicity, whereas batteries have lower purchase costs and stable voltage with complex electronic control. Activated carbons, graphene, and carbon nanotubes have the ability to increase the capacity of a supercapacitor with better stability [35].

Along with energy, water is another element that is vital to life, as it maintains the regulation of the ecosystem of the earth. However, unexpectedly, there is a continual decrease in the accessibility of safe and clean water, as water pollution has risen tremendously [36]. Some of the factors that heighten the contamination of water are the growth of the world population, household and cultivation activities, and booming factories, which are directly or indirectly related to energy [37]. As water pollution poses a considerable threat not only to human health but also to the environment, it is considered one of the most severe issues these days [38]. It is highly important to develop an efficient, reliable, and cost-effective water treatment process and technology [39].

Sea water is significantly polluted in a similar manner to terrestrial water. The percentages of significant pollutants entering the oceans annually are shown in Figure 1. To purify water and maintain environmental cleanliness, a unique strategy for developing an effective adsorbent is required [40]. Since the early history of science, adsorption has been used as the standard for separation due to its efficiency and user-friendly approach. Additionally, this process can treat wastewater by removing all harmful pollutants from the waste [41]. Besides ACs, nanomaterials are also effective in eliminating pollutants from wastewater via different chemical functions and are characterized by high sorption capacities, non-toxicity, and recyclability [42,43].

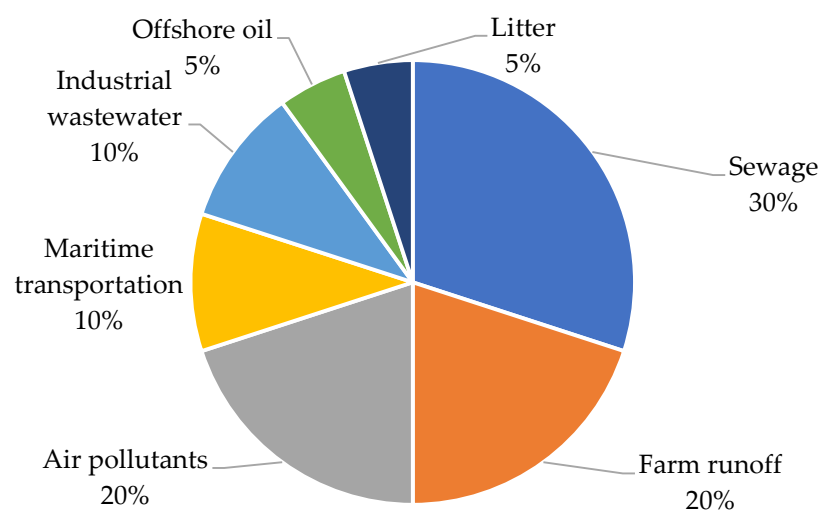


Figure 1. Pollutants entering the oceans [44].

Similar to water pollution, air pollution is a critical issue regarding the sustainability of the environment. The main cause of air pollution is carbon dioxide, which is emitted from vehicles during the combustion of fossil fuels for electricity production [45]. CO₂ capture

and storage processes have increased significantly in response to global warming and climate change. According to the Intergovernmental Panel on Climate Change, greenhouse gases are responsible for more than 95% of unavoidable global warming. From 1970 to 2010, CO₂ emissions from fossil fuels and manufacturing activities contributed about 78% of overall greenhouse gas emissions. Several technologies, including physical absorption, chemical absorption, adsorption, cryogenic separation, and membranes, are currently used to capture and isolate CO₂ gases [46].

The rise in global CO₂ emissions over time is demonstrated in Figure 2 [47]. Due to its low energy demand, cost–benefit ratio, and ease of use, adsorption is considered one of the most effective methods for capturing carbon dioxide. The effectiveness of the process is contingent on the production of adsorbents with high CO₂ adsorption capability as well as the ease of regeneration. Activated carbons, carbon nanotubes, graphene sheets, graphene oxide, and other adsorbents for CO₂ capture are extremely efficient [46]. At low concentrations and ambient temperatures, carbonaceous materials have proved excellent for CO₂ adsorption. At high temperatures, the potential adsorption capabilities decrease [48]. Since CO₂ (Lewis acid) has a poor acidic position, adding Lewis bases to carbon surfaces would improve the capturing efficiency. Surface oxidation adds electron-acceptor properties to the carbon surface since the oxygen surface groups have an acidic character [49]. The overall performances of activated carbons, graphene, and carbon nanotubes in capturing carbon dioxide are promising.

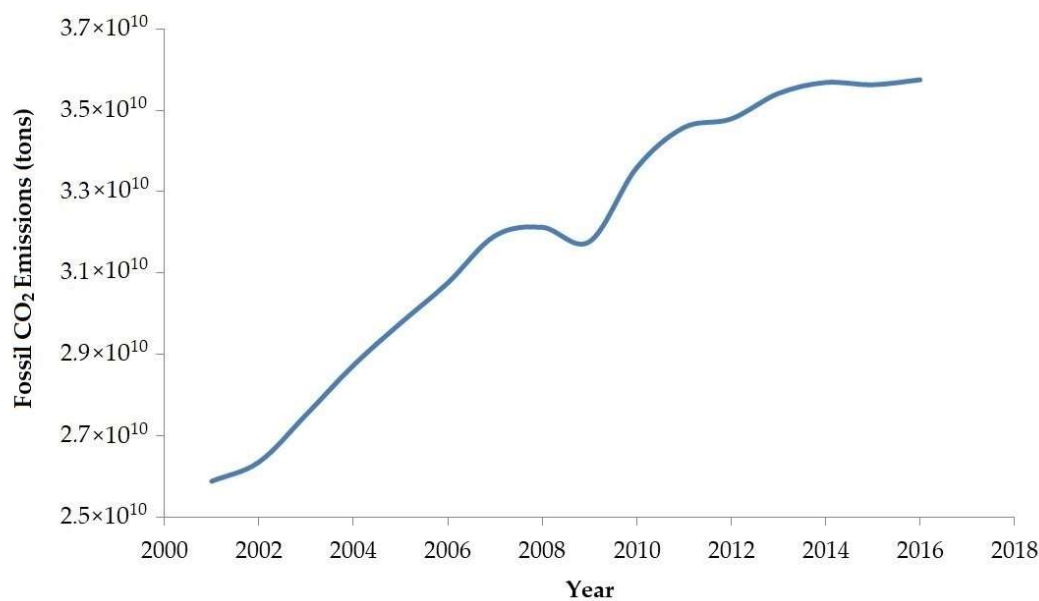


Figure 2. Global CO₂ emissions from fossil fuels [47].

The aim of this review is to accumulate information about the methods of synthesizing activated carbons, graphene, and carbon nanotubes and their potential applications in energy storage, water treatment, and CO₂ removal for environmental sustainability.

2. Synthetization of Carbonaceous Materials

There are several methods for synthesizing or preparing carbonaceous materials, and the most important, effective, and common methods are discussed here.

2.1. Activated Carbons (ACs)

Activated carbons refers to materials with a high carbon content and well-developed internal pores. They have many properties that make them flexible substances that can be used in a variety of applications. Activated carbons are perceived as the oldest and most commonly used adsorbents in wastewater purification [50]. Owing to their highly defined porosity, broad surface area (which can exceed 3000 m²/g), high degree of surface reactivity,

and variable surface-chemistry characteristics, they are noted for their effectiveness as adsorbents [51]. They were applied as adsorbents in industrialized and metropolitan wastewater, solvent retrieval, and pollution regulators, removing color, taste, and odor. Furthermore, they have also been used in gas adsorption or gas storage in electronic devices, such as capacitors [52]. Not only are they used as adsorbents; other applications include catalysts for the removal of various contaminants from gases and liquids [53].

Generally, activated carbons are produced from agricultural wastes, woody biomass, and coal through thermochemical conversion and activation at higher temperatures. The functional groups of activated carbons are bonded to fused aromatic rings. As a result, the functional groups of the carbon structures may be adjusted using heat, chemical treatments, or a combination of the two for various applications. The physical and chemical properties of raw materials and the activation methods are important factors in sorption efficiency [54]. Due to their abundance, renewability, and affordability, some significant precursors, including agricultural residues, sewage sludge, and forestry wastes, are used as sources of activated carbons [55]. Moreover, it was found that wastes from agriculture and forests have a higher carbon content and a lower ash content (0.2–10 wt%), which is important for the production of activated carbons [56].

Recently, the application of activated carbons produced from biochar using biomass resources has gained much attention [57]. Biochar is produced from biomass via thermochemical conversion processes at low temperatures (<700 °C) under oxygen-limited conditions. Such thermochemical methods include pyrolysis, hydrothermal carbonization, gasification, and flash carbonization [40]. Biochar is beneficial for carbon sequestration, soil improvement [58], and pollution control [59]. Biochar is a potential carbon source material for activated carbons due to its high reactivity and other distinct properties [60]. Biochar made from biomass has the potential to be used as an alternative precursor for activated carbon production due to its advantages. As a result, the number of technologies for water treatment, energy conservation, and CO₂ reduction has grown significantly [61]. Sometimes, the activated carbons derived from biochar perform equally well or even better than commercially available activated carbons [62].

There are four main methods to produce activated carbons: physical, chemical, physiochemical, and microwave activation (Figure 3) [14]. The chemical activation method is generally favored due to its higher yield, shorter activation time, simplicity, low temperature, and the porous structure it produces.

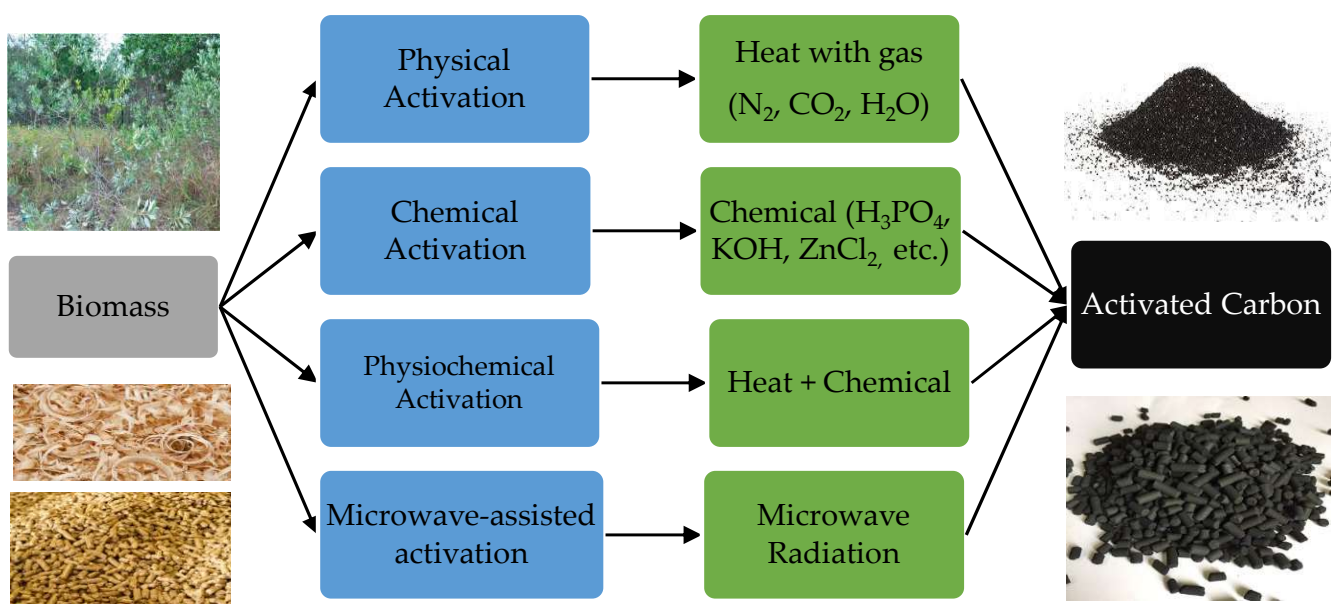
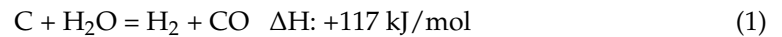


Figure 3. The synthesis process of activated carbons [14].

2.1.1. Physical Activation

Physical activation consists of two steps: carbonization and activation via carbon dioxide or steam [14]. The reaction mainly consists of carbon oxidation during the activation process. The reaction occurs as per Equations (1) and (2) [63]:



The physical activation procedure is described in Figure 4a [64], which includes carbonization, activation, cleaning, drying, and sieving. The heat produced during the process can be used for vapor production and drying. Moreover, waste gases, such as steam and CO₂, are less polluting for the environment.

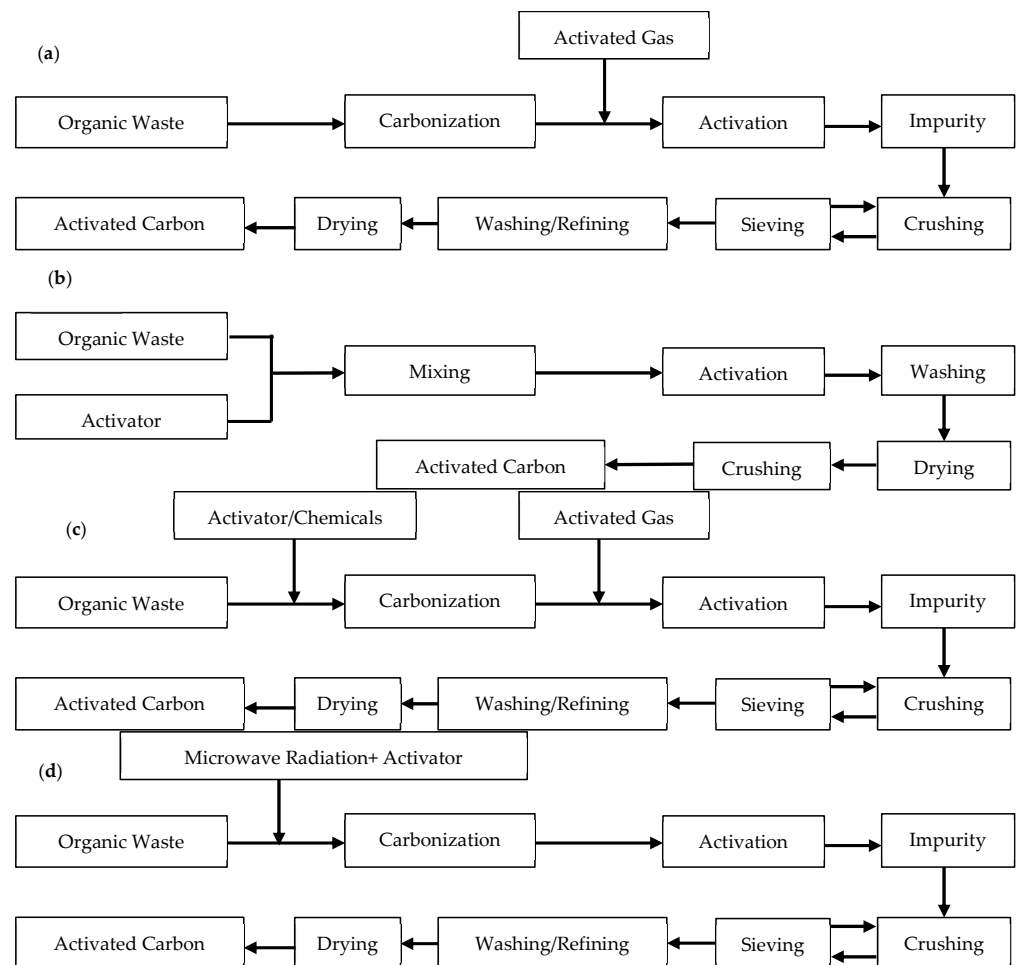


Figure 4. (a) Physical activation process [64]. (b) Chemical activation process [64]. (c) Physiochemical activation process [14]. (d) Microwave activation process [14].

This method could optimize the surface structure of biochar effectively. Some notable physical variations can be achieved, such as changes in pore volume, surface area, and pore structures. Additionally, physical activation may also influence surface characteristics (outside functional group, polarity, and hydrophobicity). There are two most common physical activations: steam activation and gas activation. Steam activation is commonly used after the carbonization of biomass. This method increases the existing porosity of biochar. During the activation procedure of the reaction between steam and carbon [65], three situations occur, which include:

- (a) The omission of volatile matter and the degradation of tar;

- (b) The establishment of new micropores;
- (c) Additional expansion of the pores present.

During gas activation, similar to steam activation, the surface area can be increased with higher numbers of pores reacting to the char and gas. This develops the structure with micropores and mesopores [66]. Carbon dioxide, steam, and nitrogen gases are normally used for this activation, CO₂ being the most effective, as the characteristics of the obtained material are outstanding [63]. The longer activation time, limited adsorption capacity, and high energy consumption of the process are the major drawbacks [67].

2.1.2. Chemical Activation

In the chemical activation process, carbonization and activation occur simultaneously with the utilization of an activating agent. The basic process of chemical activation is shown in Figure 4b [64]. In this process, the wastes are mixed with the activator or activating agent to be activated by methods such as carbonization, activation, washing, and drying [14,63]. Changing the ratios of activating agents to biomass alters the properties of the resultant activated carbons [68]. The factors affecting the carbonization reaction, the structure, and the features of the activated carbons are the reaction time, temperature, and impregnation ratio. In this method, acid, alkali, and oxidation treatments are applied to enhance the physicochemical properties of biochar. Some of the acids used in the acid treatment are HNO₃, H₂SO₄, H₃PO₄, and HCl. Some salts are also used to produce activated carbons, such as K₂SiO₃, Na₂SiO₃, K₂B₄O₇, Na₂Al₂O₄, etc. Among these alkaline activating agents, KOH is the most effective activating agent in preparing ACs with an extremely high specific surface area.

There are two significant changes after acid treatment. Firstly, there is a development of the surface area, porosity, and pore properties of biochar because of the elimination of contaminants on the exterior of the char. Secondly, functional groups, such as carboxylic groups and amino groups, may be established or increased on the biochar surface. Some standard bases for alkali treatment include KOH, NaOH, and K₂CO₃, which enhance pore characteristics and biochar function [14,63,65]. One drawback of this process is the requirement for a prolonged and repeated washing procedure to remove the activating agents from the final mixture after the activation process is executed [67].

2.1.3. Physiochemical Activation

This method involves a combination of physical and chemical activation. Generally, biomasses are treated with activators before physical activation using high-temperature activating gases. Chemical activating agents affect organic waste or biomass by increasing the reactivity of the raw materials and assisting the activating gas in passing through the precursor, thus enhancing the porosity of the activated carbon. Both physical and chemical activators perform concurrently in the physiochemical activation process after carbonization [40]. The physiochemical activation process is described in Figure 4c, which was generated from Reza et al.'s study [14]. The activation occurred mostly at a higher temperature of 600–850 °C in the presence of chemicals, such as H₃PO₄, ZnCl₂, KOH, CO₂, or H₂O (steam). Physiochemical activation can produce activated carbons with substantial surface qualities, despite the process being expensive and time-consuming. The joint activation process will cause pore opening, resulting in a well-built porous structure. For instance, KOH with CO₂ gasification can create larger macropore and mesopore structures within the AC matrix [69]. In this process, the use of zinc chloride, which is used in the pharmaceutical and food industries, is not recommended for activated carbons, as zinc contaminates the product [70].

2.1.4. Microwave-Assisted Activation

Microwave (MW) activation has recently become a feasible replacement for conventional methods due to the rapid, steady, adequate heating; the control; and the indirect interaction between the heat generator and heated material [40]. Moreover, the dimensions

of the equipment are compact due to the rapid reaction speed of microwave radiation [71]. There are numerous advantages to this method, including higher carbon yield, high energy efficiency, refinement of the quality of activated carbon, and decreased formation and emissions of dangerous materials [72]. The MW process is described in Figure 4d, which was generated from Reza et al.'s study [14]. This process produces activated carbons with varying pore structures and surface areas, despite the fact that it only provides heat during the activation process. This is due to the mechanism of pore formation by microwave plasma [73]. Appropriate activation methods and enhancing parameters can result in better properties of activated carbons by developing porosity and favorable surface functionalities [74]. The major drawback of this process is the inaccurate temperature control and possible leakage of microwaves [75].

2.2. Carbon Nanotubes

Carbon nanotubes were invented accidentally by Iijima in 1991 and gained recognition in the scientific community [76]. After two years, in 1993, Iijima and Ichihashi and the Bethune group synthesized the other type of carbon nanotube, which was the single-walled carbon nanotube [77]. There are numerous tens of graphitic shells, also termed multi-walled carbon nanotubes, in the nanotubes, with diameters of around 1 nm and a high length/diameter ratio, respectively, and adjoining shell separation of approximately 0.34 nm [78].

Generally, three main procedures are used to produce MWCNTs and SWCNTs: arc discharge, laser ablation, and catalytic growth [79]. Owing to their high Young's modulus values and tensile strength, they were considered potential composite materials with enhanced mechanical properties [80]. Their number of layers can differentiate SWCNTs from MWCNTs. They have received considerable attention due to their unique one-dimensional structures, extraordinary electronic properties, outstanding mechanical properties, and potential applications [81]. The current and best-known methods that are used to synthesize CNTs include electrolysis, chemical vapor deposition, mechano-thermal methods, laser ablation, flame synthesis, and arc discharge (Figure 5). These methods have the same purpose: to provide energy to a carbon source to create CNTs from carbon atoms.

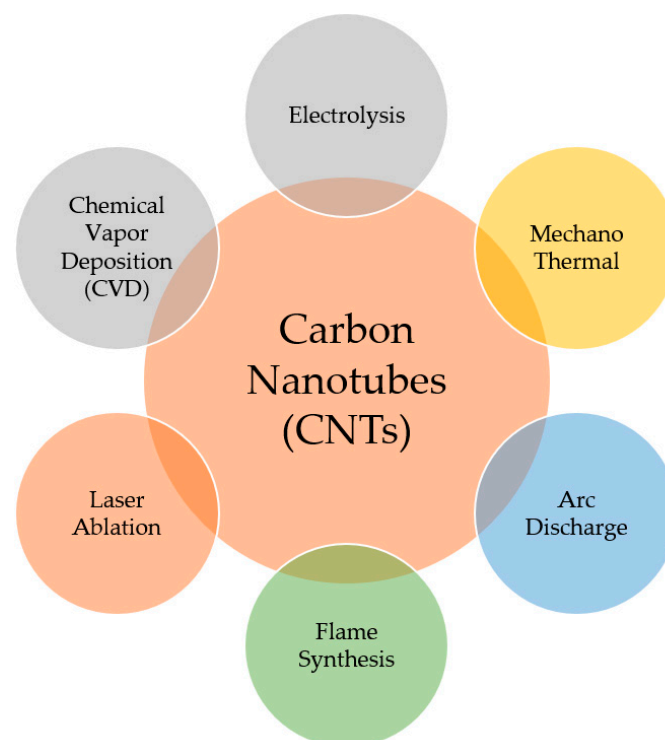


Figure 5. Synthesis of carbon nanotubes [82].

2.2.1. Electrolysis

The electrolysis method was invented in 1995 by the deployment of the electrowinning process of alkali and alkaline earth metals with the CNT-based molten chloride salt phase. The process occurred between two liquid alkali-alkaline earth metal electrodes through a DC voltage application, which created multi-walled carbon nanotubes [83]. The formation reaction is as per Equation (3) [84]:



CNTs can be synthesized in liquid form by creating lithium carbide (Li_2C_2) molecules 2–10 nm in diameter and 0.5 μm in length. The CNTs produced via this method are normally multi-walled or single-walled [85]. Different salts, such as NaCl, KCl, LiCl, and LiBr, can be used to produce carbon nanotubes. Salt density, current flow, electrolysis systems, time, and temperature are the major parameters related to the quality and quantity of CNTs. Productivity can be achieved at low temperatures with an efficiency of up to 40% by optimizing process parameters [86]. The drawbacks of the electrolysis method are the cracking difficulty of the graphite cathode and the buildup of chlorine gas, alkaline metal, and carbon nanomaterials in the chamber [76].

2.2.2. Chemical Vapor Deposition (CVD)

The best procedure to manufacture CNTs on a large scale is chemical vapor deposition at low temperatures and ambient pressure [87]. Chemical vapor deposition is a process in which the precursors are carbon-based gases, such as CO_2 , C_2H_4 , C_2H_2 , and other hydrocarbons, with high temperatures of 350 to 1000 $^\circ\text{C}$. The operating time, temperature, catalyst type, and reactant gases are the parameters influencing CNT production in this process [88]. The usual CVD methods for CNT production are plasma-enhanced chemical vapor deposition, aerosol-assisted chemical vapor deposition, laser chemical vapor deposition, water-assisted chemical vapor deposition, oxygen-assisted chemical vapor deposition with plasma, and catalytic chemical vapor deposition [89]. Apart from CNTs, the CVD method has been extensively used for the synthesis of fullerenes, carbon nanofibers, graphene, etc. [90].

Many researchers have reported that the CVD process with aerosol as a catalyst could enhance the process of synthesizing high-quality single- and multi-walled CNTs [91]. The efficiency of aerogel-based CVD can reach more than 100% for single-walled CNTs with alumina as a catalyst. Alcohol-based CVD with Fe and Co as catalysts can produce better-quality CNTs (1 nm in diameter) with higher efficiency and at lower operating temperatures. This is one of the most effective methods for obtaining high-purity products with low production costs and high efficiency [92]. In water-assisted CVD, the CNTs can be 2.5 mm in length [93]. In oxygen-supported CVD, high-quality, single-walled CNTs can be synthesized with higher efficiency using a small amount of oxygen gas. Single-walled CNTs can be easily achieved by adding oxygen, as it increases the purity and efficiency and stops damage to the sp^2 bonds by removing the amorphous carbons, impurities, and other destructive precursors [94]. The disadvantage of this process is that the CNTs produced in the CVD process are usually defective [95].

2.2.3. Mechano-Thermal Methods

The mechanical–thermal process consists of two major steps: producing amorphous carbon initially and strengthening it in the vacuum furnace [96]. The high-energy ball milling process can produce amorphous carbon. The operating time, type of gas (argon or air), cup speed (300 rpm or more), number of balls, and ball-to-powder ratio are the major parameters related to the quality and quantity of the CNTs. Increasing the ball milling time decreases the crystallite sizes, and amorphous carbon is finally produced [97]. Produced amorphous carbon was placed in a vacuum furnace at 1400 $^\circ\text{C}$ for a few hours to connect the carbon atoms to form CNTs. These CNTs normally have a multi-walled

structure with a springy shape. The process is simple, enables mass production at a lower cost, and does not require heavy equipment; however, it is time-consuming [96]. Though the process is simple in operation, the CNTs can be damaged depending on the variation in the parameters [76].

2.2.4. Laser Ablation

Another technique is laser ablation, which was first reported in 1995 [98]. In the laser ablation process, continuous lasers or waves strike the graphite for nucleation to occur and the development of CNTs [86]. Initially, the matter is hot but is cooled down instantly. During cooling, the carbon atoms are condensed quickly and form larger clusters by van der Waals forces, and CNTs are synthesized. To produce MWCNTs, pure graphite rods are used, and for SWCNTs, a composite block of graphite with a metal catalyst (Fe, Ni, Co, He-H₂, or Ar) is normally used [99]. In the pulsed laser method, laser lights with higher intensity are used, where the CNTs are 4–30 nm in diameter and about 1 µm in length. Most common catalysts, such as Co, Pt, Cu, Co/Ni, Co/Pt, Co/Cu, Nb, Ni, and Ni/Pt, are used in this method. The quality of the CNTs depends on the power and properties of the laser beam, the type of catalyst, the type of gas, the temperature of the reactions, and the distance between the target and substrate. The laser ablation methods mainly produce SWCNTs because they are costly. Although the production method is expensive, CNTs produced by this method are highly pure and have a higher yield [89]. One of the drawbacks of this process is that it is expensive, as it requires expensive lasers and high power [95].

2.2.5. Flame Synthesis

To synthesize CNTs via the flame synthesis method, direct combustion of the carbon sources (methane, acetylene, ethanol, and ethylene) is performed in the presence of oxygen gas. There are three basic steps: first, the carbon sources are produced from hydrocarbons through hydrolysis; second, the carbon atoms are diffused by a metallic catalyst; and third, the CNTs are nucleated on the surface of the catalyst [100]. The type of flame, the temperature, the composition of the gas, and the types of catalysts have an essential role in determining the quality of the CNTs produced. This process is economical for higher production of single-walled CNTs, but the growth rate is relatively low [101]. In the flame synthesis of CNTs, it is crucial to establish and maintain a perfect balance between the optimum carbon supply and the flame temperature, since an excess of carbon leads to the creation of amorphous carbon [76].

2.2.6. Arc Discharge

The arc discharge method was the first method recognized and utilized for CNT synthesis. It uses high temperatures (above 1700 °C) and produces CNTs with fewer structural defects compared to CNTs produced by other procedures. The tools used include a boiler, a stainless-steel vacuum chamber, graphite electrodes, a water-cooled trap, and a high-voltage power supply. The CNTs produced have high crystallinity and perfection due to the high temperature used; they also have a higher yield per unit of time than CNTs produced via other processes [82]. In the arc discharge method, two pure graphite rods are used as an anode and cathode in the direct current flow. For the power of the produced arc, the carbons are separated from the anode towards the cathode to form coal [102]. This process can be performed in liquid nitrogen, toluene, non-ionized water, and different gas situations (argon, helium), or the plasma spinning arc discharge process can be used. Plasma spinning is economical and considered a high-yield synthesis method, as the centrifugal force from rotation accelerates the evaporation of the anode by forming a stable arc. The major CNTs produced in this method are multi-walled, but single-walled CNTs can be made by penetrating the graphite rods and metal catalysts. Steam compartment pressure and flow rates are the key factors in controlling procedure productivity. The speed of the process is high, and the conditions can be handled easily, but the efficiency of this

process is low [89]. This process requires extensive purification, as the CNTs produced are short, dragged, and random in direction [95].

2.3. Graphene

Graphene was successfully synthesized first in 2004 as single-layer graphene sheets by Profs. Geim and Novoselov by repeatedly peeling graphite crystals [103]. The synthesis of graphene can be carried out in two main ways: top-down or bottom-up. Top-down methods depend on the attack of powdered raw graphite, which ultimately separates its layers to produce graphene sheets. This method is categorized into mechanical exfoliation, chemical reduction, and chemical exfoliation processes. At the same time, bottom-up approaches involve the use of carbonaceous gases to produce graphene. The bottom-up strategy includes pyrolysis, chemical vapor deposition, epitaxial growth, and plasma synthesis [104]. The following subsections describe different graphene synthesis processes [105].

2.3.1. Mechanical Exfoliation

Mechanical exfoliation is one of the most well-known and widely used processes for producing graphene sheets. As layered materials are subjected to transverse or longitudinal stress, this method is used. Graphite is formed when a single graphene layer is created by weak van der Waals forces [104]. Van der Waals forces stack partially filled p orbital overlaps on the planes of boards, causing piling. Exfoliation is the reversal of stack formation for weak bonding, in which the lattice spacing is increased in the vertical direction. With limited spacing, the hexagonal lattice arrangement creates higher bondage [106]. Around $300 \text{ nN}/\mu\text{m}^2$ of force has to be applied to separate the graphite into a single atomic layer [104]. By implementing this method, the layers can be of graphitic substances can be removed to form graphene sheets with different thicknesses. The exfoliation method can be executed by ultra-sonication, an electric field, using scotch tape, or the transfer printing process [107]. The drawback of this method is that it cannot be used at a large-scale for industrial manufacturing [108].

2.3.2. Chemical Reduction of Graphite

In 1962, the first single-layer graphene sheets were produced through the reduction of graphite. Chemical reduction is another method used to generate a higher amount of graphene from graphite. The oxidation of graphite with oxidants, including potassium permanganate, nitric acid, and condensed sulfuric acid, produces graphene oxide. The reduction of GO and sonication are two other synthesis methods for producing graphene. Reducing agents include NaBH_4 , ascorbic acid, hydroxylamine, glucose, phenyl-hydrazine, pyrrole, hydroquinone, and alkaline solutions [107]. Graphene production can be carried out via the electrochemical reduction process by sonicating the graphite oxide into GO nanoplatelets. Finally, the oxygen groups can be removed by implementing the reducing agent (hydrazine) [109]. Even then, the flacks may provide some extra oxygen. For a single- or double-layered GO, sonication in water can be used first, followed by filtration to deposit the GO onto the surfaces. In addition, forming reduced graphene in an organic solvent using solvothermal reduction is a simple method [110]. In the direct sonication of graphite, the production yield is very low, and the separation process is quite tough [104].

2.3.3. Chemical Exfoliation

Chemical exfoliation is the most effective way to increase graphene production in the top-down phase. It involves two simple stages. Using oxidants such as potassium permanganate, nitric acid, and powdered sulfuric acid, the interlayer spacing is initially improved by reducing van der Waals forces. Finally, the graphene is exfoliated in single or multi-layers through fast heating or sonication [104]. After its invention in 1860, graphene was synthesized using three different methods: the Brodie, Staudenmaier, and Hummers methods [107]. Owing to the low toxicity and well-organized structure of the graphene

produced, the Hummers process has proven to be the best method [111]. In this process, the cost of ionic liquids is very high [112].

2.3.4. Pyrolysis

Additionally, graphene can be synthesized by the pyrolysis process, which is a bottom-up method. For example, ethanol and sodium (1:1 molar ratio) can be placed in a reactor throughout the pyrolysis process. Similarly, sodium ethoxide can also be pyrolyzed through the sonication process [113]. The class of the graphene sheet can be examined by Raman spectroscopy, electron diffraction, and transmission electron microscopy. It was found that the formation of multi-layered graphene sheets derived from pyrolytic carbon can have an average length of 1–3 μm and a width of 200–350 nm [114]. Large-scale production of graphene is not possible using this technology [112].

2.3.5. Chemical Vapor Deposition (CVD)

Another bottom-up technique for producing graphene is chemical vapor deposition, which involves the deposition of gaseous reactants onto substrates [115]. The films form on the exterior of the substrate as the substrate is mixed with the gases in the heated compartment. The temperature of the substrate is the main parameter in executing the reactions. In this process, the coating is smaller in extent and has a lower micron thickness. Then, the vaporization of solid substances towards condensation onto the substrate is carried out [116]. Two CVD processes are available for graphene synthesis: low-pressure chemical vapor deposition (LPCVD) and ultra-high vacuum chemical vapor deposition (UHCVD). LPCVD is carried out at sub-atmospheric pressures to boost performance while preventing unwanted reactions, whereas UHCVD is carried out at very low atmospheric pressures (around 6–10 Pascal) [117]. The small scale of production is the major disadvantage of this method [112].

2.3.6. Epitaxial Growth

Epitaxial growth is one of the strategies implemented for the growth of graphene on surfaces. The epitaxial growth process, which involves heating and cooling a silicon carbide (SiC) crystal, can be used to make graphene. On the Si face of the crystal, single- or multilayer graphene is formed, while the C face produces just a few layers of graphene [118]. The outcome depends on the temperature, pressure, and heating rate of the process. The silicon carbide (SiC) lattice can be made from nickel (III) surfaces through the nickel diffusion process by evaporation, as their constant lattice difference is about 1.3% [119]. Carbon diffusion occurs through the nickel coating during heating, forming graphene or graphite on the soil. In comparison to the silicon carbide lattice without nickel, the produced graphene is easy to distinguish from the exterior. The graphene generated in this way is not completely homogeneous as a result of grain boundaries and defects [107]. To increase the economic and practical feasibility, the technical issue of high temperatures and the expensive cost of SiC should be considered [108].

2.3.7. Plasma Synthesis

Plasma synthesis, which includes both plasma-enhanced chemical vapor deposition (PECVD) and the plasma doping technique, is another bottom-up method for producing graphene [120]. Various kinds of plasma are used in the synthesis process, including energetic particles, electrons, extremely reactive radicals, and photons. Direct current plasma-enhanced chemical vapor deposition (DC-PECVD), inductively coupled plasma-enhanced chemical vapor deposition (ICP-PECVD), and microwave plasma-enhanced chemical vapor deposition (MPECVD) are the three forms of PECVD [107]. In the DC-PECVD process, plasma ions and atoms strike the cathode, causing sputtered atoms to disperse through the plasma and cause impure atoms during graphene processing. Wave heating is used to remove impurities in the ICP-PECVD phase, which produces plasma in the absence of electrodes. Pressure, temperature, and gas flow rate are all factors that

influence reaction activity [121]. The plasma is generated in the MW-PECVD using wave heating and wet etching on graphene films with no polymer contamination, metallic impurities, or metal catalysts. This plasma synthesis method has many benefits, including a lower energy requirement, a shorter processing time, increased catalyst stimulation, minimal environmental pollution, and consistent properties during the process [120]. Despite the fact that gas-phase precursor materials are used, the process is expensive [104].

3. Water Treatment

Treating water is indispensable due to domestic, industrial, commercial, and agricultural activities in both developed and developing countries [122]. It was found that around 2.2 million people die each year due to the consumption of polluted water [123]. The cost of treating waterborne diseases around the world is approximately USD 7.3 million [124]. At least 2 billion people utilize polluted water sources worldwide. More than 2 billion people reside in nations with water scarcity, and the situation is predicted to worsen in some areas due to population growth and climate change [125].

The water treatment process for the main carbonaceous materials (activated carbons, graphene, and carbon nanotubes) is explained in Figure 6 [11]. The severity of water pollution is predicted to increase, as it is affected by human activities. Hence, with the growth of population and population density, water shortages add to the danger of polluted water [126]. By 2025, it is expected that 4 billion people will suffer from extreme water shortage if the current population trend and usage patterns continue [127]. Consequently, practical and economical technology is essential for water treatment, reuse, and reclamation.

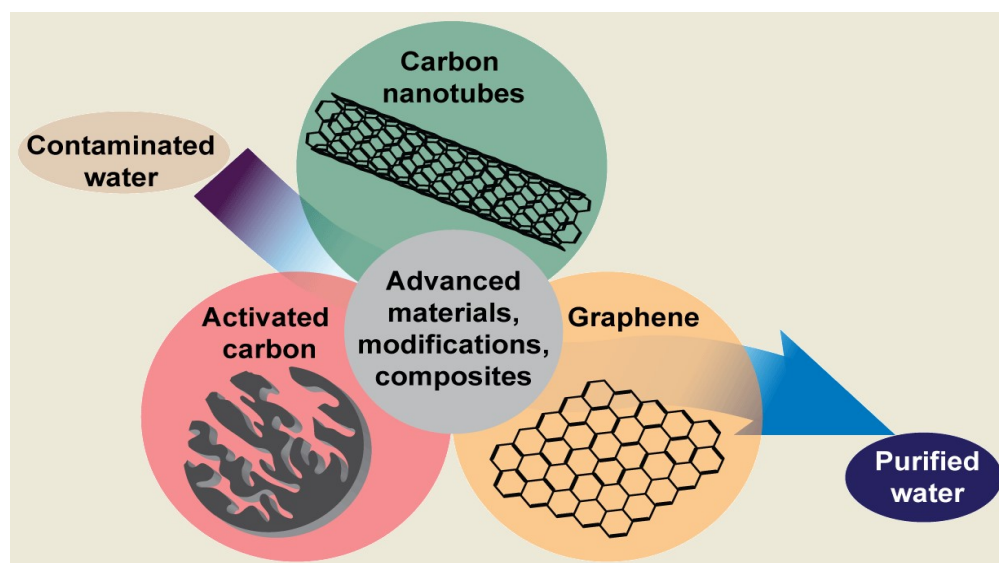


Figure 6. The major carbonaceous materials for water treatment [11].

3.1. Activated Carbons in Water Treatment

The discharge of untreated wastewater into the environment has devastating effects on humans and can cause difficulties during conventional water treatment. Traditional water treatment aims to reduce contaminant levels in water and provide safe and filtered water for consumption and disposal. Some conventional water treatment methods are coagulation, sedimentation, membrane or media filtration, adsorption by activated carbons, biological therapy, and oxidation. The most common and widespread method in industrial wastewater and water treatment is utilizing an activated carbon as an adsorbent [128]. There have been numerous reports on the capability of activated carbons to adsorb various types of pollutants. Activated carbons are also excellent adsorbents that are more effective in removing organic compounds than metals and other inorganic contaminants. Many approaches are still in progress to significantly enhance carbon surface potential by using

distinct chemicals or appropriate treatment techniques to improve AC performance for specific contaminants [50].

3.1.1. Dye Removal

Some of the factors affecting the adsorption capability of biochar with respect to numerous pollutants include the activation method, which could enhance the chemical/physical properties of the biochar. When these properties change, their surface areas change as well. Pore shapes are improved, surface functional groups are introduced, and surface hydrophobicity changes. The most notably refined properties of physical and chemical activation are pore volume and surface area, to different extents [129]. As the surface areas and pore structures are modified, there is a possible improvement in the removal of contaminants, as the surface area can be increased and microporous and mesoporous structures can be created. This is due to the increased availability of contact sites between activated carbons and contaminants, coupled with the formation of pores that are easily accessible for pollutants [130].

When the functional groups (hydroxyl, carboxyl, amino, etc.) increase, there are additional bonding positions for heavy metals, which boosts the driving strength of the metal adsorption in the biochar, which includes ion exchange, outside complexation, and electrostatic attraction [131]. Biochar hydrophobicity could increase with the improvement of the interconnection between the organic pollutants and the surface of the biochar [132]. After the activation step, the activated carbon surface can also be improved by three types of modifications for water treatment applications: chemical amendment, physical change, and biological modification. Other surface alteration methods include oxidative and non-oxidative processes [133]. Some examples of complexing groups that are incorporated into the surfaces of activated carbons are carboxylic, lactonic, and phenolic groups. There have been studies reporting the coupling of activated carbons with the coagulation procedure, resulting in the enhanced elimination of natural organic matter (NOM) by 70% [134].

Furthermore, activated carbons can also eliminate the hydrophilic fraction of natural organic matter, which cannot be well removed by the coagulation process [135]. Due to activated carbons (ACs) being widely used as adsorbents, some of the regular applications include the adsorption of organic materials, such as phenol, dyes, and heavy metal ions (mercury, chromium, cadmium, arsenic, and lead). The dye adsorption capacities of the activated carbons derived from lignocellulosic biomass are shown in Table 1. In modern industry, vast amounts of wastewater containing phenolic compounds and dyes are generated, the organic compounds and dyes being considered harmful to the environment. Moreover, most of the colors are found to be entirely unsusceptible to biodegradation processes [136]. The surface chemical properties of activated carbons are important when it comes to adsorbing dyes. According to Table 1, wild olive cores activated by H_3PO_4 have the highest dye adsorption capability of 781.25 mg/g. The dye removed is basic 46 at a pH of 4. Flamboyant pods have the second-highest dye adsorption capacity in Table 1. They remove acid yellow 6 at a pH of 2 and have an adsorption capacity of 673.68 mg/g. Date stones are next, as they have an adsorption capability of 398.19 mg/g. The carbon is activated using $ZnCl_2$ to remove methylene blue at pH 7.

Table 1. Removal of dyes and heavy metals by activated carbons.

Dye Adsorption by Activated Carbons						
Dye	Activating Agent	Raw Material	S_{BET} (m^2/g)	pH	Adsorption Capacity (mg/g)	Ref.
Methylene blue	KOH	Water hyacinth	6.6	587.92	1765.52	[137]
Methylene blue	$NaHCO_3$	<i>Medulla tetrapanacis</i>	9	923	1116.94	[138]
Anionic	Phosphoric acid	Raffia palm shells	2	-	1762.93	[139]
Methyl orange	HNO_3	Coffee grounds	3	658	-	[140]

Table 1. Cont.

Dye Adsorption by Activated Carbons						
Dye	Activating Agent	Raw Material	S _{BET} (m ² /g)	pH	Adsorption Capacity (mg/g)	Ref.
Basic green 4	CO ₂	Durian peel	-	3	312.5	[141]
Reactive red 120	H ₃ PO ₄	Jute fiber	-	6	200	[142]
Malachite green (mg)	K ₂ CO ₃ /CO ₂	Bamboo	1724	5	263.58	[143]
Methylene blue	CO ₂ /steam	Oil palm wood	1084	-	90.9	[144]
Acid yellow 6	NaOH	Flamboyant pods	-	2	673.68	[145]
Eriochrome black T	Thermal	Rice hulls	-	2	0.04	[146]
Acid red 114	H ₂ SO ₄	Sesame	229.65	3	102.4	[147]
Malachite green	ZnCl ₂	Coconut coir	205.27	-	27.44	[148]
Methylene blue	ZnCl ₂	Date stones	1045.61	7	398.19	[149]
Basic red 46	H ₃ PO ₄	Wild olive cores	969	4	781.25	[150]
Methylene blue	ZnCl ₂	Pineapple waste	914.67	-	288.34	[151]
Methylene blue	HCl	Acacia fumosa seeds	-	6	10.49	[152]
Acid red 114	H ₂ SO ₄	Pongam seeds	324.79	3	3.33	[147]
Malachite green	NaOH	Tea leaves	134	4	256.4	[153]
Yellow 18	ZnCl ₂	Sour cherry	1704	2	75.76	[154]
Methyl violet	CO ₂	Kapok	647–897	-	160.3	[155]
Amido black 10b	H ₂ SO ₄	Palm flower	9.57	-	4.04	[156]
Malachite green	HNO ₃	Oakwood	68.5180	-	4.34	[157]
Methylene blue	H ₃ PO ₄	Vetiver roots	1004–1185	-	394	[158]
Malachite green	H ₂ SO ₄	Ricinus communis	-	7	27.78	[159]
Heavy Metal Adsorption by Activated Carbons						
Heavy Metal	Activating Agent	Raw Material	S _{BET} (m ² /g)	pH	Adsorption Capacity (mg/g)	Ref.
Cr (VI)	Citric acid	Waste walnut shells	4.2	75.26	602.47	[160]
Pb (II)	Cs ₂ CO ₃	Palm tree (<i>Phoenix Dactylifera</i>)	7	-	2704	[161]
Cr (VI)	KOH	Leather industry waste	5	41.6	0.124	[162]
As (V)	KOH	Apricot stones	7.3	75.9	733.6	[163]
Fe (III)	HNO ₃	Bulgarian lignite	2.7	-	293	[164]
Pb	ZnCl ₂	Hazelnut husks	1092	5.7	13.05	[165]
Pb	H ₃ PO ₄	Sugar cane bagasse	-	4	8.58	[166]
Pb	ZnCl ₂	Van apple pulp	1067	4.0	17.77	[167]
Pb	H ₃ PO ₄	Lemna minor	531.9	6	170.9	[168]
Pb	ZnCl ₂	Coffee residue	890	5.8	63	[169]
Cr	Ozone	Rice husks	380	2	8.5	[170]
Cr	Thermal	Olive bagasse	718	2	109.89	[171]
Cr	NaOH	Longan seeds	1511.8	3	169.5	[172]
Cr	H ₂ SO ₄	Date palm seeds	-	1	120.48	[173]
Cr	KOH	Peanut shells	95.51	2	16.26	[174]

Table 1. Cont.

Heavy Metal Adsorption by Activated Carbons						
Heavy Metal	Activating Agent	Raw Material	S _{BET} (m ² /g)	pH	Adsorption Capacity (mg/g)	Ref.
Hg	ZnCl ₂	Walnut shells	780	2	151.5	[175]
Hg	H ₂ SO ₄	Rice straw	-	5	142.88	[176]
Hg	H ₂ SO ₄	Sago waste	625	5	55.6	[177]
Hg	ZnCl ₂	Residue of liquorice	1492.4	8	24.78	[178]
Hg	KOH	Coconut pith	505	-	0.74 mmol/g	[179]
Cd	KOH	Olive stones	1280.71	6	11.72	[180]
Cd	HNO ₃	Oak wood	68.518	9	3.31	[157]
Cd	H ₃ PO ₄	Nutshells	1556.9	10	104.17	[181]
Cd	H ₃ PO ₄	Aguaje	1202	5	26.33	[182]
Cd	H ₃ PO ₄	Olive fruit stones	1283	5	24.83	[182]

3.1.2. Heavy Metal Removal

Heavy metals pose a danger to human health, animals, and plants. Hence, they are widely studied to minimize the harmful effects they cause. They usually exist in the waste discharges produced from the mining, petrochemical, tannery, and textile industries [183]. Activated carbons extracted from lignocellulosic materials have been successfully used by researchers all over the world to study the adsorption of heavy metals, such as iron, chromium, arsenic, and cadmium. Table 1 reveals that Lemna minor has the largest adsorption potential for the removal of lead, with 170.9 mg/g. Phosphoric acid and a pH of 6 are used to activate it [168]. Lead must be avoided because prolonged exposure can cause edema, mental retardation, liver and kidney injury, decreased hemoglobin synthesis, miscarriage, and abnormalities in pregnant women [184]. As for chromium removal, longan seed activated using NaOH at a pH of 3 is found to adsorb the heavy metal at the highest adsorption capacity of 169.5 mg/g [172].

Chromium is considered one of the top-priority toxic heavy metals in wastewater. There are two stable oxidation states of chromium, which are Cr (III) and Cr (VI). Cr (VI) is found to be more noxious than Cr (III), as it is very soluble and can be easily absorbed and accumulated in the body, especially in the kidneys, stomach, and liver [185]. The other heavy metal adsorbed is mercury, and it is regarded as one of the most dangerous metals. The MCLG (Maximum Contaminant Level Goal) for mercury is set at 2 parts per billion (ppb). According to the Environmental Protection Agency (EPA), at that level, mercury would not lead to any potential health problems. Based on Table 1, the walnut shells activated using ZnCl₂ at pH 2 were found to remove mercury with the highest adsorption capability of 151.5 mg/g [175]. Nutshells were found to be the best absorbers of cadmium, which is a non-biodegradable heavy metal that travels through the food chain. It was found that concentrations of 10–326 mg Cd²⁺/L of cadmium are severely harmful; however, non-fatal symptoms were reported. The nutshells used were activated using phosphoric acid at a pH of 10. This study also concluded that the adsorption of cadmium on the adsorbents is pH-dependent, and the pH range of 8–12 is that in which the maximum adsorption takes place [181].

3.1.3. Removal of Pesticides

Pesticides are important for modern agriculture, but they can contaminate water when they are used. In agriculture and gardening, pesticides such as bentazon, carbofuran, and 2,4-Dichloro-phenoxyacetic acid are widely used. Their optimum water concentrations are set at certain thresholds because of their carcinogenicity and mutagenicity, which are

deliberate dangers to the natural ecosystem and human health. For bentazon, carbofuran, and 2,4-Dichloro-phenoxyacetic acid, the maximum allowable concentrations in water are 0.05 mg/L, 0.09 mg/L, and 0.1 mg/L, respectively [186]. In light of this, one of the most powerful separation methods for removing chemicals from water supplies is adsorption [69]. Table 2 also summarizes how date stones, olive kernels, soya stalks, etc., were commonly used as pesticide adsorption predecessors. El Bakouri et al. [187] investigated the adsorption of date-stone ACs on various forms of drin pesticides from aqueous solutions, including dieldrin, aldrin, and endrin. The highest adsorption capabilities for endrin, dieldrin, and aldrin were 228.05 mg/g, 295.30 mg/g, and 373.23 mg/g, respectively, indicating an improvement in adsorption potential from endrin to aldrin. Since aldrin had the lowest solubility in this experiment, it can be inferred that the rise in adsorption was caused by a decline in pesticide solubility in water.

The adsorption capabilities of physiochemically stimulated date-seed activated carbons were investigated by Salman et al. [188]. Date seeds were treated physiochemically with CO₂ and KOH, resulting in adsorption of bentazon and carbofuran of 137.04 mg/g and 86.26 mg/g, respectively. The disparity in adsorption capacities can be explained by the fact that the molecular size of carbofuran is smaller than that of bentazon, allowing for easier diffusion and binding to the AC surfaces. Another researcher repeated the experiment and obtained comparable findings, with bentazon containing 78.13 mg/g and carbofuran containing 175.4 mg/g. There was also an observation of the adsorption of 2,4-Dichloro-phenoxyacetic acid. According to the report, ACs can remove the pesticides at 175.4 mg/g from an aqueous solution [186]. Physical activation of olive kernels, soya stalks, and rapeseed stalks developed ACs for the removal of Bromopropylate. The ACs were stated in the study to have elimination efficacies of up to 100% for all of the feedstock [189].

3.1.4. Phenolic Removal

The chemical and petrochemical sectors produce the majority of phenolic compound-containing effluents. These contaminants are extremely harmful and carcinogenic, posing a direct danger to the marine environment and living species [190]. As a result, environmental and health authorities have specifically restricted phenolic compound concentrations in water sources, and these contaminants have been prioritized for removal. The Environmental Protection Agency (EPA) has set a limit of 0.1 mg/L in industrial wastes for these toxins, while the World Health Organization has set a limit of 0.001 mg/L for phenols in water for consumption [70]. The various forms of adsorbents that were used to remove phenolic compounds, as well as their adsorption capabilities, are illustrated in Table 2. The adsorption of Bisphenol A by argan-nutshell ACs was investigated by Zbair et al. (2018) at 293 K, and the optimum adsorption potential was found to be 1250 mg/g [191]. As compared to commercial ACs, the generated ACs performed better in terms of adsorption. Durian peel is sometimes used as a precursor for this adsorption. However, despite the adsorption process lasting a day, the adsorption found with durian-peel ACs was 4.2 mg/g [192].

Table 2. Applications of ACs in phenolic and pesticide removal from water.

Applications of ACs in Phenolic Removal from Water						
Adsorbent	Activator	Adsorbate	S _{BET} (m ² /g)	pH	Q _m (mg/g)	Ref.
<i>Acacia mangium</i> ACs	H ₃ PO ₄	Phenol	1767	3	53.8	[193]
Soybean-curd-residue ACs	KOH	Phenol	253.14	2	-	[194]
Antibiotic-mycelial-residue ACs	-	Phenol	1369.76	-	-	[195]
Kenaf-rapeseed ACs	CO ₂	Phenol	1112	10	84.1	[196]
Date-pit ACs	CO ₂	Phenol	-	-	161.8	[69]

Table 2. Cont.

Applications of ACs in Phenolic Removal from Water						
Adsorbent	Activator	Adsorbate	S _{BET} (m ² /g)	pH	Q _m (mg/g)	Ref.
Avocado-kernel ACs	CO ₂	Phenol	206	6	90	[196]
Açaí-seed ACs	Ar/CO ₂	Phenol	496	3.5–8	133	[197]
Baobab-wood ACs	H ₃ PO ₄	Phenol	1682	3	240	[198]
Date-pit ACs	ZnCl ₂	Phenol	-	7	169.5	[69]
Coconut-husk ACs	KOH	2,4,6-trichlorophenol	-	2	716.10	[196]
Loosestrife ACs	H ₃ PO ₄	2,4,6-trichlorophenol	1255.75	-	367.65	[199]
Date-pit ACs	H ₃ PO ₄	o-Nitrophenol	-	-	142.9	[69]
Date-pit ACs	KOH	p-Cresol	-	-	322.5	[69]
Avocado-seed ACs	H ₂ SO ₄	Resorcinol, 3-aminophenol	1432	7	Resorcinol: 407 3-aminophenol: 454	[192]
Durian-peel ACs	H ₂ SO ₄	Bisphenol A	-	-	4.2	[192]
Argan-nutshell ACs	H ₃ PO ₄	Bisphenol A	1372	-	1250	[191]
Elimination of Pesticides by ACs						
Activated Carbon Sources	Activator	Adsorbate	S _{BET} (m ² /g)	pH	Q _m (mg/g)	Ref.
Coconut charcoal	Methanol	Monocrotophos	79.4	7	103.9	[200]
Navel orange (<i>Citrus sinensis</i> L.)	H ₃ PO ₄	Chlorpyrifos	94.26	6.8	-	[201]
Dates (<i>Phoenix dactylifera</i> L.)	H ₃ PO ₄	Chlorpyrifos	111.75	6.8	-	[201]
Pomegranates (<i>Punicagranatum</i> L.)	H ₃ PO ₄	Chlorpyrifos	183.89	6.8	-	[201]
Bananas (<i>Musa</i> sp.)	H ₃ PO ₄	Chlorpyrifos	289.86	6.8	-	[201]
Date stones	Steam	Aldrin	-	-	373.23	[187]
Date stones	Steam	Dieldrin	-	-	295.30	[187]
Date stones	Steam	Endrin	-	-	228.05	[187]
Date seeds	CO ₂ /KOH	Bentazon	1322	5.5	86.26	[188]
Date seeds	CO ₂ /KOH	Carbofuran	-	-	135.14	[186]
Date seeds	CO ₂ /KOH	Bentazon	-	-	78.13	[186]
Date seeds	CO ₂ /KOH	Dichlorophenoxyacetic acid	-	3.6	238.10	[69]
Olive kernels	Steam	Bromopropylate	600	-	Up to 100% removal	[189]
Soya stalks	Steam	Bromopropylate	570	-	Up to 100% removal	[189]
Rapeseed stalks	Steam	Bromopropylate	490	-	Up to 100% removal	[189]

The adsorption of phenols was achieved using lignocellulosic biomass, such as date pits, avocado kernels, kenaf rapeseed, and Aça seeds. H₃PO₄-activated baobab-wood ACs are said to be the strongest adsorbents among these ACs. At 50 °C and an optimum pH of 3, maximum adsorption was achieved in 24 h. In their analysis, Bansal et al. [202] found that acidic functional groups on AC surfaces reduced adsorption efficacies, while non-acidic or essential functional groups increased adsorption. Another study found that date-pit ACs were activated with both KOH and H₃PO₄ to remove phenolic compounds (o-Nitrophenol and p-Cresol). The alkali-treated ACs could extract 322.5 mg/g of phenolic compounds, while the acid-treated ACs could only eliminate 142.9 mg/g [69].

3.1.5. Pharmaceutical Component Removal

Pharmaceutical compounds are emerging contaminants in the atmosphere, with widespread application in human, agricultural, and aquaculture activities. The increasing use of pharmaceuticals has resulted in their persistent discharge into marine ecosystems over time. They can be persistent in water due to their high steadiness and hydrophilicity, posing a danger to the ecosystem. Despite the fact that pharmaceuticals have very low concentrations in water, usually trace amounts, they may also have negative effects on the atmosphere [203–205]. The removal of pharmaceutical compounds by activated carbons is explained in Table 3.

Table 3. Activated carbons for pharmaceutical-compound elimination.

Adsorbent	Activator	Adsorbate	S _{BET} (m ² /g)	pH	Q _m (mg/g)	Ref.
Paper-mill-sludge ACs	KOH	Carbamazepine, sulfamethoxazole, and ibuprofen	795	8	154 ± 11, 167 ± 12 and 147 ± 8	[206]
Coconut-shell ACs	HNO ₃ , H ₂ SO ₄	2, 2'-azino-bis 3-ethylbenzothiazole-6-sulphonic acid	1100	5	180.5–735.2	[207]
Granular activated carbons	-	Peroxymonosulfate and peroxydisulfate	1040	7.13	-	[208]
Cork-powder ACs	Steam	Ibuprofen	-	2–11	378.1	[204]
Mung-bean-husk ACs	Steam	Ibuprofen	-	2	62.5	[204]
Cork-powder ACs	K ₂ CO ₃	Ibuprofen	-	2–11	145.2	[204]
Mugwort-leaf ACs	H ₂ SO ₄	Ibuprofen	-	2	16.95	[204]
Waste-apricot ACs	ZnCl ₂	Naproxen	-	5.82	106.4	[204]
Olive-waste ACs	H ₃ PO ₄	Naproxen	-	4.1	39.5	[204]
Olive-waste ACs	H ₃ PO ₄	Ketoprofen	-	4.1	24.7	[204]
Sawdust ACs	ZnCl ₂	PC	-	-	226.71	[209]
Primary-paper-mill-sludge ACs	HCl	PAR	-	-	405	[209]
Lagenaria vulgaris-shell ACs	-	Ranitidine	665	2–11	315.5	[210]
Date-stone ACs	-	Levofloxacin	817	2–12	100.4	[210]
Cyclamen persicum ACs	-	Diclofenac	799–880	2–12	22.22	[210]
Paper-mill-sludge ACs	K ₂ CO ₃	SMX, CBZ, PAR	1583	-	SMX = 75% CBZ = 85% PAR = 84%	[211]

Ahmed et al. [204] gathered information on and investigated the various forms of precursors used to remove ibuprofen from aqueous solutions. ACs are made by physically and chemically activating olive stones, mung-bean husks, cork powder, and mugwort leaves. The best finding was confirmed to be steam-activated cork powder, which was capable of dissolving 378.1 mg of ibuprofen in one gram of water. As opposed to K₂CO₃-treated cork powder, steam-activated cork powder came out on top. CO₂-powered olive stones performed better than the other activated carbons, with an adsorption potential of 282.6 mg/g compared to 200 mg/g for the others.

In terms of naproxen elimination, the activated carbons from waste apricots and waste olives can be contrasted. After an adsorption time of 26 h, ZnCl₂-treated waste-apricot ACs absorbed 106.4 mg/g of the pharmaceuticals, while H₃PO₄-treated olive-

waste ACs removed just 39.5 mg/g. The adsorption of naproxen and ketoprofen was also tested for olive waste. The adsorption capacities of ACs were compared using the same precursor (olive waste) and treatment (phosphoric acid). Olive-waste ACs adsorb naproxen (39.5 mg/g) more than ketoprofen (24.7 mg/g), according to the findings. Olive-waste ACs were not to be suitable adsorbents for medicinal composites, as the findings were disappointing. Primary-paper-mill-sludge ACs, on the other hand, were shown to be strong adsorbents, with a higher adsorption potential of 405 mg/g for paroxetine and elimination efficiencies of 75.0, 85.0, and 84.0% for carbamazepine (CBZ), sulfamethoxazole (SMX), and paroxetine (PAR), respectively [209,211].

3.2. Carbon Nanotubes

Carbon nanotubes are used in a variety of applications due to their smooth construction and almost cylindrical shape. They are suitable for use as single-walled nanotubes and multi-walled nanotubes due to their thermal, mechanical, electrical, and physical properties. Carbon-nanotube manufacturing has exploded in recent years due to their high performance. Nanomaterials have received greater recognition as being utilizable in advanced water treatment technologies [212]. They are normally defined as materials that are less than 100 nm in at least one direction. Owing to their huge surface areas and modifiable pore sizes, carbon-based nanomaterials, such as charcoal, activated carbons, carbon nanotubes, and graphene, have been used for filtration and adsorption [213]. There have been numerous studies on carbon nanomaterials in wastewater treatment.

3.2.1. Dye Removal

Since the surface-area-to-volume ratios of carbon nanotubes are greater than those of other adsorbents, their mechanical, electrical, and physical properties significantly affect dye adsorption. As a result, the reactions between dye molecules and CNTs are more efficient, resulting in increased interaction across the surface area and an increase in adsorbent performance [214]. The adsorption capabilities of carbon nanotubes for different dyes are shown in Table S1 [215–230]. Regarding the most used dyes, malachite green and methylene blue, carbon nanotubes adsorbed 13.95 and 188.68 mg/g, respectively, in normal pH conditions [215,217]. The basic red 46 dye was eliminated at 38.35 mg/g for 100 min of experiments with pH 9 [218]. For the elimination of reactive black 4 and reactive black 5, the performance of MWCNTs was effective, with values of 502.5 and 1082.07 mg/g, respectively [222,223]. The multi-walled carbon nanotubes showed a removal of acid blue 161 of 1000 mg/g for 60 min operation periods [227]. CNTs are made up of graphene or graphitic sheets with a unique sidewall curve and a conjugative structure that has a highly hydrophobic surface. The key pathways for CNTs to absorb various dyes are determined by the cationic or anionic properties of the dyes [231]. The dye adsorption potential of CNTs is rarely straightforward. Dye-removal performance is affected by hydrophobic behavior, van der Waals forces, piling, hydrogen bonding, and electrostatic interactions occurring together or separately [232].

3.2.2. Heavy Metal Removal

CNTs have been used in a variety of studies to remove inorganic pollutants from aqueous solutions [233]. The vast surface area, porosity, surface functional groups, and interactions between contaminants and CNTs all influence the adsorption potential of CNTs against inorganic contaminants [234]. Combined CNTs with polymeric membranes improve the removal performance of heavy metals and arsenic by adsorption into the CNT membranes due to these properties. Internal sites, interstitial channels, grooves, and outer surfaces are the most common sites for pollutant adsorption onto the CNTs. The numerous sorption sites present on the CNT surfaces bind the heavy metals, causing the adsorption of heavy metals into CNTs [235]. The electrostatic interaction force between the negative charge on the surface of CNTs and divalent metal ions is predicted to result in strong CNT

adsorption [236]. Solution pH is essential for the metal adsorption of CNT membranes because of the protonation and deprotonation of CNTs [237].

Cation adsorptions are more efficient at raising negative charges on CNT surfaces at higher pH (alkaline). Due to the protonation of functional groups on CNTs, removal efficiency is reduced at lower pH (acidic) [238]. The oxidation doping of MWCNT materials to remove cadmium from an aqueous solution was highly dependent on pH, while ethylenediamine-functionalized MWCNTs had a high removal efficiency for Cd in the pH range of 8–9 [239]. The elimination of metal ions is based on the competitive influence of metal cations and anions on CNTs, in addition to pH. Studies found that the attraction between divalent cation ions, such as Pb^{2+} and anionic surfactants, led to the successful removal of metal ions from CNTs in the presence of sodium dodecylbenzene sulfonate. In the presence of benzalkonium chloride, on the other hand, the adsorption of Pb^{2+} decreases dramatically [240].

Furthermore, owing to the presence of negative and positive charges, the interactions between CNTs and heavy metals vary. Adsorption of Cr(III) with nitrogen-doped magnetic CNTs, for example, occurred due to chemical adsorption, while adsorption of Cr(III) with acid-modified CNTs occurred due to electrostatic interactions between CNTs and Cr (III). The unique surface areas of CNTs are available for inorganic pollutant adsorption, and the productivity improves as the diameter of the CNTs decreases. As a result of the interaction, metal ion adsorption on CNTs is determined by the functional groups present on CNT surfaces rather than CNT distance. The adsorption of As(III) and As(V) by CNTs of the same diameter with two separate functional groups (zirconia nanohybrid and iron oxide) was studied, and it was discovered that both As(III) and As(V) were strongly associated with CNTs for zirconia nanohybrids relative to iron oxide-coated CNTs [241]. The removal efficiency of heavy metals by different CNTs is explained in Table 4.

Table 4. Experimental observations were obtained by utilizing multifunctional CNTs.

Material Type	Surface Area (m ² /g)	Pollutant	Effect on Water Purification	Ref.
NiO/MWCNTs	245.3	Cadmium (Cd) (II)	-	[242]
CNTs-TMPDET	120	Platinum (Pt) (IV)	260 mg/g	[243]
CNTs-MnO ₂	110.4	Silver (Hg) (II)	58.8 mg/g	[244]
CNTs/Fe ₃ O ₄ -NH ₂	90.7	Lead (Pb) (II)	75.0 mg/g	[245]
AA-CNTs	203.0	Chromium (Cr) (VI)	264.5 mg/g	[246]
SWCNTs	400.0	Cadmium (Cd) (II)	21.2 mg/g	[247]
OH-SWCNTs/RGO	-	Copper (Cu) (II)	256 mg/g	[248]
Purified SWCNTs	423.0	Zinc (Zn) (II)	41.8 mg/g	[249]
Oxidized CNTs	-	Cobalt (Co) (II)	85.7 mg/g	[250]

CNTs can be utilized for physical adsorption owing to the Van der Waal forces; physical and chemical adsorption are also possible when surface functional groups are present [251]. Carbon nanotubes have exceptional performance as adsorbent media for multiple organic (drug particles, insecticides, dyes, and other organ halides), inorganic, and biological (fungi and algae) water pollutants. CNTs have different functions in photocatalysis, disinfection, desalination, composites, hybrids, and detection. As for doped CNTs, they have been utilized for desalinating seawater and brackish water [252]. Their ideal adsorption material is due to their structure, as they have bigger surface areas and a robust hollow structure. According to one study, it was found that the morphologies of carbon nanotubes have a significant influence on their adsorption capabilities [253].

There have been many studies carried out on CNTs as adsorbents. Recently, a study compared the adsorption capability of copper ions (Cu^{2+}) from water by non-functionalized and functionalized carbon nanotubes. It was found that CNTs functionalized with sul-

furic acid (H_2SO_4) and HNO_3 showed better removal efficiency. The CNTs were able to remove up to 94.5% in the ideal conditions (pH 5 and 0.2 g) for 101 min of contact time at a temperature of 90 °C [254]. Another study reviewed the different types of raw and surface-oxidized CNTs used to adsorb metal ions (Cu^{2+} , Cd^{2+} , Zn^{2+} , Ni^{2+} , Pb^{2+} , etc.) from a water solution [255]. The results showed that oxidized CNTs from NaOCl, KMnO_4 , and HNO_3 adsorbed better than raw CNTs. The contact of ions on the CNT surfaces by hydroxyl, carboxyl, and carbonyl functional groups, which are available after the functionalized procedure, as well as metal ions, constitutes the mechanism of adsorption. It was also reported that MWCNTs can be used as sound absorbents for the elimination of Reactive Red M-2BE textile dye from aqueous solutions [224], as they removed at least 98.7% of the dye in a high-saline-concentration medium.

Other than heavy metals discharged by industry as a major water pollution source, bacteria and viruses have also been recognized as significant contaminants. Researchers have studied the effect of CNTs on removing these contaminants from water. They applied severe cytotoxicity and pulmonary poisoning to animal cells. SWCNTs were found to have the highest toxicity level, followed by MWCNTs, quartz, and C60 [256]. Some factors need to be taken into account to maximize the disinfecting ability of CNTs, including the degree of aggregation, the correlating stabilization effects by NOM, and the bioavailability of the CNTs [257]. CNTs with a very high purity level exhibit reliable antimicrobial performance [258], with dangerous destruction to cell membranes occurring; this is due to the straight interaction with SWCNTs.

3.2.3. Pathogen Removal

Bacteria, viruses, and protozoa are the most common pathogenic microorganisms present in drinking water and drainage effluents [259]. CNTs have the capability to inactivate or remove bacteria (*Micrococcus lysodeikticus*, *Salmonella*, *Escherichia coli*, and *Streptococcus mutans*), viruses (MS2 bacteriophages), and protozoa (*Tetrahymena pyriformis*). SWCNTs were found to effectively inactivate *E. coli*, such that they could penetrate the cell walls. Chemically engineered CNTs have a greater affinity for microorganism cell walls than pristine CNTs and polymeric membranes. Microorganisms in direct interaction with CNTs can have negative effects on metabolic function, cell-wall integrity, and bacterial (*E. coli*) morphology. The ability of CNTs to inactivate bacteria depends on their ability to penetrate the cell wall of the microorganisms [260].

Bacterial removal performance can be improved by using functionalized CNTs with silver nanoparticles. For example, three distinct forms of Ag-doped CNTs with different impregnation ratios (1, 10, and 20 wt.%) effectively removed 100% of *E. coli* bacteria. The toxic effects of nanosized Ag-CNTs are attributed to their ability to destroy or remove microorganisms from water. The diameter of CNTs was found to play a significant role in the elimination of bacteria and other microbes from wastewater in the majority of studies performed [261]. The removal characteristics of microorganisms by CNTs are demonstrated in Table S2 [262–269]. It goes without saying that the surface areas, pore volumes, and structures of CNTs are not the only factors that influence microorganism adsorption performance. Some factors simultaneously increase and decrease the potential of CNTs. Other factors, such as environmental chemical characteristics, such as pH, temperature, toxins, and ionic water pressure, may also play a role in changing the adsorption rate of CNTs. As a result, for a thorough understanding of CNT adsorption, all parameters should be double-checked [270].

3.2.4. Removal of Other Contaminants

Organic contaminants in the form of dissolved materials with a wide molecular-weight range may be present in water, causing animal, plant, and human decay [238]. Based on their preference for nonionic resin and aquagenic activity, organic matter that forms in water is known as hydrophilic or hydrophobic. Pedogenic, hydrophobic, and aquagenic polysaccharides are among these entities, and they play a significant role in

natural organic matter [271]. Organics, such as poisons, herbicides, and pharmaceuticals, are introduced into water as a result of human activities. Since these organics have harmful health consequences, it is important to handle water in which they are present with CNTs, since organics are difficult to extract using conventional low-pressure membranes, such as RO and NF [272]. As a result, developing novel CNT membranes with high permeability is critical for efficiently removing organic pollutants from water.

For small dissolved organics and depth filtration, CNT membranes are effective at removing natural organic matter through filtration [273]. CNTs were able to remove 95% of pharmaceuticals and personal-care items (PPCPs) by increasing the aromatic rings and surface areas [274]. The π - π interactions, chemical adsorption, hydrogen bonding, and van der Waals forces between them all contribute to the removal performance of CNT membranes with respect to organic contaminants. Due to the higher electrostatic repulsion forces and lower interactions, the adsorption of natural organic matter by CNTs reduces as the number of oxygenated functional groups on the surfaces increase. The same thing happened when the pH was raised, which increased the electrostatic repulsion force between CNTs and organic matter [275]. The broad surface areas of CNT membranes and the π - π interactions between the aromatic rings of CNT membranes and natural organic matter resulted in a high removal of natural organic matter by CNTs [276]. Removal efficiencies of organic contaminants by CNT membranes are presented in Table 5.

Table 5. Removal of organic contaminants by CNT membranes.

Adsorbate	Pollutants	Removal Efficiency	Ref.
MgAl ₂ O ₄ @CNTs	MgAl ₂ O ₄	100%	[277]
CNTs	Polyacrylonitrile	Above 95%	[278]
CNTs	Polyaniline	93.4%	[279]
CNT nanocomposites	PPCP	Improvement of 45%	[280]
CNT nanocomposites	PPCP	95%	[274]
M-MWCNTs coated with Calcium	Humic acid	90.2%	[281]
Functionalized CNT buckypaper	Humic acid	>93%	[276]
Polyelectrolyte CNTs	Bovine serum albumin (BSA)	99.9%	[282]
b-cyclodextrin grafted MWCNTs (MWCNT-g-CDs)	Polychlorinated biphenyls	>96%	[283]

The adsorption competition between organic chemicals in water and CNT surfaces in organic pollutant removal is similar to that which occurs in inorganic pollutant removal [284]. The proportion of organic pollutants removed will often be unaffected by the initial concentration of the feeds. As a result, tailoring the surface properties of CNTs is critical for increased adsorption of various organic materials and improved water treatment. Similarly, wastewater pretreatment may be an effective way to address these issues. Pre-coagulation of wastewater effluents, for example, is successful for NOM removal through competitive adsorption [239].

3.3. Graphene-Based Materials

Antibiotic-polluted water, as well as other biological and inorganic contaminants, can be successfully treated with graphene-based adsorbents. Graphene-based products demonstrate the economic and environmental benefits of graphene-based technology. For contaminants in the adsorption phase, single-layered graphene has two basal planes [285]. Since the functional groups are responsible for the adsorption of metal ions by GO pads, this is a significant advantage of the material. Graphene-based materials were used to remove toxins from aqueous fluids in a number of experiments [286]. Graphene, as an

adsorbent, has excellent removal properties. First, graphene is made up of a single-layered carbon structure, which means that all of the atoms are exposed to the atmosphere on both sides, making it possible for them to come into contact with antibiotics (primarily through π - π interactions). Second, in contrast to conventional adsorbents, graphene adsorbents have a porous structure and a large surface area, making them an excellent candidate for quicker antibiotic diffusion or surface reactions, resulting in quick and efficient adsorption. Third, although the adsorption capabilities of antibiotics are equal, the cost of large-scale processing of graphene adsorbents is lower than that of other high-performance adsorbents (e.g., carboxyl multi-walled carbon nanotubes and single-walled carbon nanotubes). There has been significant progress in the development of graphene adsorbents, but they do have some intrinsic drawbacks which need to be overcome [287].

3.3.1. Heavy Metal Removal

The majority of studies have focused on using graphene oxide (GO) to remove metal ions from water [288]. The significance of oxygen-containing functional groups was identified by comparing the adsorption of Pb (II) by pristine and oxidized graphene sheets [289]. Metal oxides can be mixed with GO and graphene nanosheets (GNs) to form composite materials. Metal oxide and GO composites have distinct properties and can be used as effective adsorbents for the treatment of various contaminants. Zn^{2+} , Cd^{2+} , and Pb^{2+} ions were removed from water using flower-like TiO_2 on a GO hybrid (GO- TiO_2) [290]. The Zn^{2+} , Cd^{2+} , and Pb^{2+} adsorption capacities of the GO- TiO_2 hybrid were 88.9 mg/g, 72.8 mg/g, and 65.6 mg/g, respectively [291]. Several graphene-based nanocomposites for heavy-metal ion and organic ion elimination are presented in Table 6.

Table 6. Graphene-based nanocomposites for the elimination of heavy metals and organics.

Graphene Based Nanocomposites for the Elimination of Heavy Metals				
Adsorbate	Adsorbent	S _{BET} (m ² /g)	Adsorption Capacity (mg/g)	Ref.
Lead (II)	GO-MnFe ₂ O ₄	196	673	[292]
Uranium (VI)	ZrO ₂ /GO	37.86	128	[293]
Copper (II)	GO/Fe ₃ O ₄	-	18.3	[294]
Cadmium (II)	GO/Fe ₃ O ₄ /sulfanilic acid	-	55.4	[295]
Chromium (VI)	CdO-GO	-	399	[296]
Lead (II)	rGO/COFe ₂ O ₄	169.9	299.4	[297]
Cadmium (II) and copper (II)	GO/Mn-doped Fe(III)oxide	180	87.2 and 129.7	[298]
Chromium (VI)	GO/SiO ₂	-	181.81	[299]
Copper (II)	GO/Fe ₃ O ₄ /sulfanilic acid	92.79	50.7 and 56.8	[300]
Copper, lead, and cadmium	GO/Fe ₃ O ₄	49.9	23.1, 38.5 and 4.4	[301]
Lead (II)	TiO ₂ /GO	-	65.6	[291]
Lead (II)	SiO ₂ -GNs	252.5	113.6	[302]
Organic Pollutant Adsorption Using Graphene-Based Materials				
Organic Pollutants	Adsorbent	S _{BET} (m ² /g)	Adsorption Capacity (mg/g)	Ref.
Methylene blue	PDOP-GO	20	270	[303]
Ethylene glycol	GO-Fe ₃ S ₄	7.71	21.87	[304]
Methylene blue	rGO	>1000	174	[305]
Methylene blue	Polyethersulfone/GO	24.98	62.50	[306]
Methylene blue, Neutral Red (NR)	Fe ₃ O ₄ /GO hybrids	-	167.2, 171.3	[307]
Rhodamine B (RhB), Methylene blue	Reduced GO-MFe ₂ O ₄ hybrids	-	92% and 100%	[308]
Methylene blue, methyl violet (MV)	GO sponge	48.409	397, 467	[309]
Methylene blue, Congo Red (CR)	Fe ₃ O ₄ -GNs	118.175	45.3, 33.7	[310]
Methylene blue	GO	28	351	[311]
Methylene blue	Reduced-GO	0.60	2000	[312]
Methylene blue	GNs	295.56	154–204	[313]

For the available carboxyl groups to improve the adsorption process, graphene, GNS500, and GNS700 (exfoliation at temperatures of 500 or 700 °C) revealed higher adsorp-

tion of Pb(II) compared to pristine graphene [289]. Heavy metal removal from wastewater is influenced by a number of factors, including initial dosage, graphene properties, metal ions, pH, temperature, interaction length, acidic organic ligands, and coexisting ions [314]. Strong metals (cadmium (II), lead (II), copper (II), chromium (VI), and other toxic heavy metals) are removed using graphene and graphene oxide-based products. Heavy metals are also non-biodegradable and therefore dangerous to living beings. Fe₃O₄/mesoporous silica/GO, magnetic manganese-doped iron(III) oxide nanoparticle implanted graphene, and iron(III) oxide/graphene oxide/1-ethyl-3-methylimidazolium tetrafluoroborate will be eliminated [107].

The products used to remove lead include antimicrobial graphene polymers, few-layered GO, manganese ferrite/graphene oxide, ethylenediaminetetraacetic acid/magnetic graphene oxide, chitosan/graphene oxide, hyperbranched polyethylenimine/graphene oxide (HPE), and amino-functionalized graphene oxide. The products used to remove copper ions are L-tryptophan-functionalized graphene oxide, chitosan/sulfhydryl-functionalized graphene oxide, chitosan/graphene oxide (Chitosan-GO), poly (allylamine hydrochloride)/graphene oxide, and polyethylenimine-adapted magnetic graphene oxide with Fe₃O₄ nanoparticles.

In addition, the elimination of chromium (VI) ions necessitates research into materials such as graphene oxide-alpha cyclodextrin-polypyrrole nanocomposites, chitosan/graphene oxide, reduced graphene oxide/nickel oxide (RGO/NiO), magnetic ionic liquid/chitosan/graphene, 2-imino-4-thiobiuret-partially reduced graphene oxide, and graphene oxide functionalized with magnetic cyclodextrin-chitosan. Such heavy metals as cobalt, uranium (U(VI)), and rhenium (Re(VII)) can be extracted using graphene oxide-based nanomaterials [107].

3.3.2. Organic Pollutants

In addition, graphene-based compounds are used to remove different organic contaminants from liquids. Table 6 shows how graphene-based adsorbents remove organic compounds from water. Polyethersulfone/GO can remove methylene blue (MB) at 62.50 mg/g [306], while Fe₃O₄/GO hybrids showed removal efficiencies for methylene blue and neutral red of 167.2 mg/g, and 171.3 mg/g, respectively [307]. Reduced GO-MFe₂O₄ hybrids exhibited removal efficiencies for rhodamine B and methylene blue of 92% and 100%, respectively [308]. An excellent removal capability was achieved for methylene blue (397 mg/g) and methyl violet (467 mg/g) with a GO sponge. The Fe₃O₄-GNs, GO, and GNs also showed better performance in eliminating methylene blue from aqueous solutions [313]. At pH 7.0, modified GO developed by the Hummers process effectively removes brilliant green and methylene blue at 416.67 mg/g and 476.19 mg/g, respectively [315]. The π - π interactions or electrostatic attraction between positively charged dyes and negatively charged GO is used to remove the dyes [316]. Without sonication, fabricated GO-chitosan demonstrated a high adsorption potential for MB (402.6 mg/g) which was equivalent to those of other GO materials [317].

3.3.3. Pharmaceutical Compound Removal

Given their adsorption potential in various laboratory environments, graphene-based materials are effective adsorbents for treating pharmaceutical-laden wastewater [314]. The removal of pharmaceutical pollutants by graphene-based materials is demonstrated in Table 7.

Table 7. Pharmaceutical pollutant adsorption by graphene-based materials.

Pharmaceutical Pollutants	Adsorbent	Adsorption Capacity (mg/g)	Ref.
AlFum-CoFe ₂ O ₄ /GO	Tetracycline and Doxycycline	230	[318]
Ag ₃ PO ₄ /Fe ₃ O ₄ /graphene oxide	Carbamazepine	-	[319]
CNC-PVAm/rG	Diclofenac	605.87	[318]
Tetracycline	Graphene oxide	313.48	[320]
Doxycycline	GO	398.40	[320]
Oxytetracycline	F-GO with MNPs	45.0	[321]
Chlortetracycline	F-GO with MNPs	42.6	[321]
Doxycycline	F-GO with MNPs	35.5	[321]
Tetracycline	GO	381.77	[322]
Ciprofloxacin	Single-layer GO	379	[323]
Ciprofloxacin	KOH-activated graphene	194.6	[324]
Ciprofloxacin	Porous graphene hydrogel	235.6	[325]

Graphene oxides (GOs) and reduced graphene oxides (RGOs) are two essential branches of graphene materials with oxygen functional groups that have a lattice of heavy hydroxyl, epoxy, and carboxyl groups. These organizations enable the GOs to form stable suspensions in an aqueous solution, allowing for further possibilities for antibiotic adsorption due to dispersion. GOs and RGOs are made from various negatively charged inorganic and organic reducing agents with fewer oxygen atoms [287]. At pH 5.0, both ciprofloxacin (CIP) and sulfamethoxazole (SMX) were adsorbed by GOs with capacities of 379 and 240 mg/g, respectively [323]. Other research has shown that GOs can efficiently remove tetracycline (TC) through π - π interactions [322]. Furthermore, both doxorubicin (DOX) (1428.57 mg/g) [326] and levofloxacin (LEV) (256.6 mg/g) adsorb better with GOs. The ability of RGOs to remove sulfonamide antibiotics from water is also encouraging [327]. As a result, GOs and RGOs have a high capacity for consuming various medicinal compounds.

3.3.4. Other Pollutants

GO mixed with lanthanum-substituted manganese ferrites (LMFs) can remove perfluorooctanoic acid (PFOA) from aqueous solutions in an effective way. The electrostatic interaction and hydrogen bonding properties of PFOA and GO are shown by the surface charge densities and crystalline changes. Additionally, the PFOA adsorption by these nanohybrids was unaffected by coexisting pollutants, such as anions, cations, and other organic compounds [328]. A multifunctional, chitosan-attached, plasmonic Au NP-conjugated GO was designed and created for the delivery of safe and sanitary drinking water. The three-dimensional porous membrane was used to separate pharmaceutical toxins from water and destroy methicillin-resistant *Staphylococcus aureus*. Using an extremely porous membrane, this GO substance can quickly capture MRSA bacteria. It shows around 100% removal of MRSA by killing through the porous membrane [329]. Single-layered graphene with nanopores was shown to effectively sieve NaCl salt from vapor. Moreover, chemical groups bonded to graphene edges might roughly increase water fluidity due to their hydrophilic nature [329]. For magnetic separation applications, a GO nanocomposite demonstrated higher antibacterial performance against both Gram-positive and -negative bacteria [330]. Recently, graphene-based nanocatalysts (G-, GO-, and rGO-based) were studied for the modification of nanocomposites to demonstrate their exceptional properties in water treatment. These characteristics include surface area (2630 m²/g), good electron conductivity (7200 Sm⁻¹), high thermal/chemical stability, and excellent capacity for many nanoparticles (metal oxides, noble metals, and magnetic nanoparticles) [331].

4. Energy Storage

Energy is crucial for improving human life, influencing the development of society and the economy [332,333]. It is predicted that the demand for worldwide energy will double in about 20 years [334]. The available energy supplies are currently fossil fuels, such as oil,

coal, and gases, which are quickly depleting, and this is exacerbated by the destruction of forests and biodiversity, species degradation, and waste [335,336]. Furthermore, fossil fuels are not long-term renewable [337]. As a result, high-performance energy storage systems are needed to satisfy the rising demand for electrical energy [338], which is commonly used in electronic devices and accessories. Over the last few decades, research into alternative energy sources and electrochemical energy storage systems, such as supercapacitors, has grown [339]. In 1957, supercapacitors were first experimented with by General Electric engineers. Supercapacitors can be utilized commercially in portable electronics, transportation, and the aerospace industry [340]. Improvements have also been made to the various components of supercapacitors, such as cathodes, electrolytes, anodes, and separators, reduction in their costs having also been researched comprehensively [341].

As for the performance of supercapacitors, this is greatly affected by the electrode materials. The commonly used electrode materials are carbon-based materials, transition metals, and conducting polymers [342]. Carbon is mainly utilized due to its low cost, amplexness, and environmental benignity. Furthermore, its ability to derive a family of new carbon materials makes it an excellent choice for energy applications. Due to the high cost of preparing activated carbons from fossil sources, biomass-derived carbon electrodes are used as an alternative solution [343]. Moreover, ACs, graphene, and CNTs are also effective for supercapacitors, as they have a high specific surface area and excellent electrical conductivity, which is suitable for energy storage applications (Figure 7). Carbon nanomaterials have properties that are influenced by size and surface, which can improve energy conversion and storage performances [344].

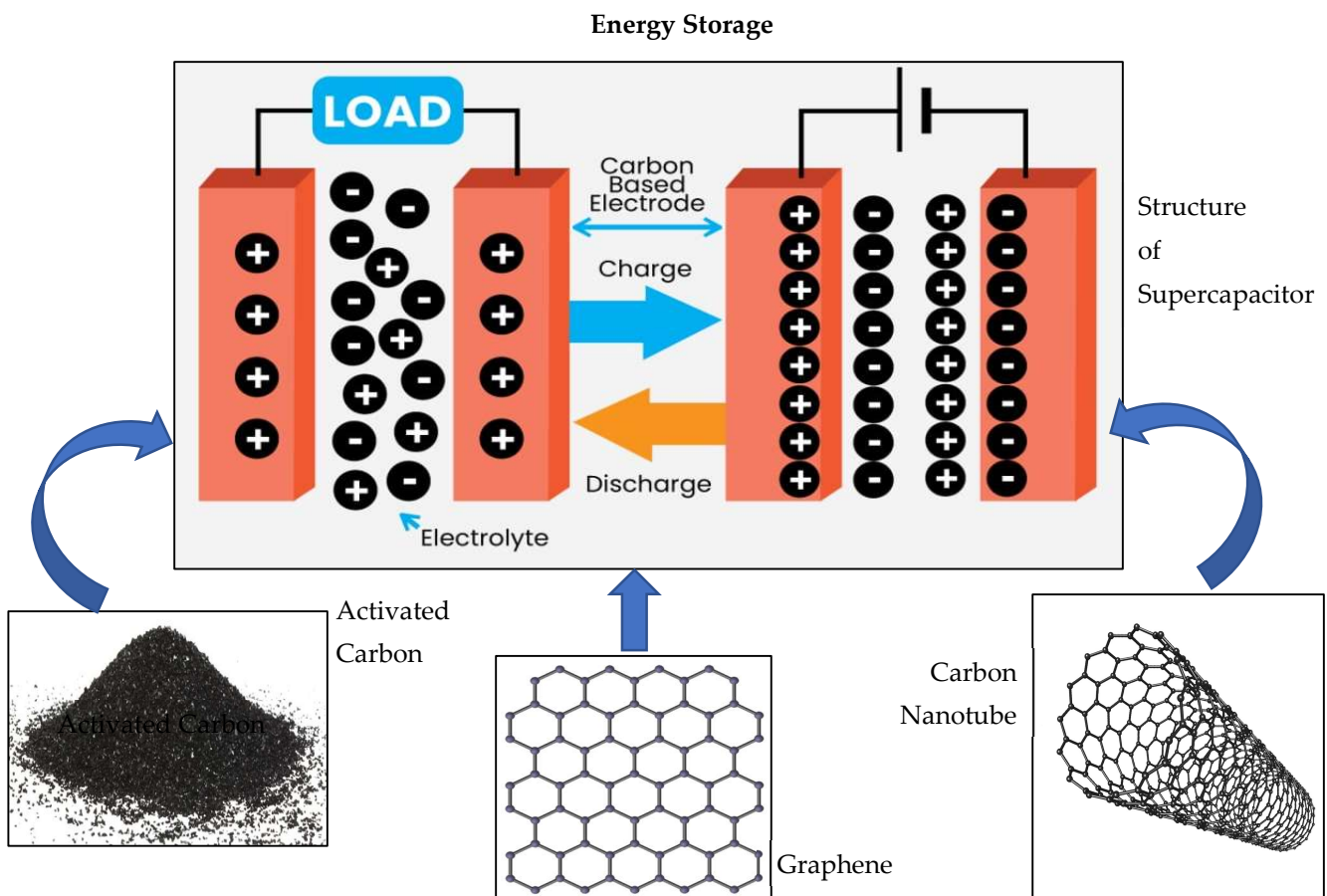


Figure 7. Use of carbon-based materials for energy storage applications with a supercapacitor.

4.1. Activated Carbons in Energy Storage

Activated carbons are the carbon-based materials that have been most studied for use as electrodes in higher-quality supercapacitors due to their upper-surface pores and

better surface areas [345]. Electrochemical double-layer capacitors (EDLCs) have excellent potential as high-power energy sources for a variety of applications that call for high cycle efficiency, high power density, and long cycle life [346]. One of the materials used in commercial EDLCs is activated carbon. The performance of activated-carbon-based materials as supercapacitors (two-electrode cell systems) is shown in Table S3 [347–363]. According to Table S3, O-rich bituminous coal-based ACs exhibited the highest capacitance of 370 F/g with a surface area of 1950 m²/g and KOH electrolyte. The excellent performance is due to the large upper surface area, high oxygen content, superior electronic conductivity, and broader pore size distribution. This type of activated carbon is recommended to be used as an electrode material for the EDLC industry because bituminous coal is abundant and not costly [348].

O- and N-doped ACs have exhibited a capacity of 368 F/g when added to a sulfuric acid (H₂SO₄) electrolyte. The high electrochemical performance was attributed to a wide distribution of micropores and mesopores of 2–4 nm. The existence of electrochemically active quinone oxygen groups and nitrogen functional groups also supports the operations [358]. The third highest capacitance of 279 F/g was obtained from peach-stone-derived AC with a top surface area of 2692 m²/g. The result was acquired at room temperature, which makes it an appropriate candidate for low-temperature operation in electrochemical capacitors [351]. Petroleum coke-based AC, Si-doped AC, activated carbon aerogel, activated templated carbon, straw-based AC, N-doped activated templated carbon, activated carbon nanoplates, activated CNTs, and activated graphene-like nanosheets can be used for supercapacitors as well.

The performance of supercapacitors depends on the porous network of activated carbon, which can be enhanced by proper activation. Moreover, it can also be improved by the presence of a microporous and mesoporous structure [364]. It was found that the capacitance notably improved by nearly 2.8 times compared to the raw biochar when using the oxygen plasma activation method. These developments are due to the formation of extensive spreading in pores and large surface areas [365]. The activated carbon electrode revealed a very high total capacitance of 222–245 F/g with a significant microporous matrix, which is attributed to its high micropore content. Another factor that is responsible for the application of supercapacitors is the altered chemical properties of activated biochar [366], which has been proven to have a seven-times-higher capacity for biochar activated in nitric acid (HNO₃) at room temperature [367]. This improvement is caused by an increase in the exposure of surface oxygen groups. It was reported that the ability of activated biochar as a supercapacitor is equal to or sometimes higher than that of other blended carbonaceous materials, such as carbon nanotubes, graphene, and commercial activated carbon [368]. Hence, activated biochar has the potential to be effective and cheap for specific applications.

4.2. Carbon Nanotubes for Energy Storage

Several decades ago, there was a significant development in alternative technologies with a shift towards using clean, sustainable energy. Research was carried out on novel carbon materials, such as carbon nanomaterials, to determine their potential as crucial additions for optically clear, electrically conductive films for solar cells [369]. Carbon nanotubes have been utilized to develop batteries and supercapacitors. CNTs also display characteristics such as not requiring uniform chirality and orientation, which gives them the potential to be used in energy storage applications [370]. Furthermore, CNTs can also be introduced into electrochemical cells for modern energy storage, as they have been shown to have suitable morphological dimensions and exceptional electricity conductivity. CNTs are recognized as attractive electrode materials for creating high-performance supercapacitors because of their unique characteristics, including high charge transfer capacity, high mesoporosity, high electrolyte accessibility, high specific surface area, and high electrical conductivity [371]. The performances of carbon nanotubes as supercapacitors are shown in Table 8.

Table 8. Performances of carbon nanotubes as supercapacitors.

Material	Operating Conditions	Capacitance	Ref.
SWNTs	KOH Solution	180 F/g	[372]
PVA/SF-SWNTs	Facile solution-cast technique	26.4 F/g	[373]
SWCNTs	350 °C-oxidized	15 to 135 F/g	[374]
CNTs	Polypyrrole treated	170 F/g	[375]
CNTs	Manganese oxide (MnO ₂)	140 F/g	[376]
SWCNTs/TiO ₂	SWCNT/TiO ₂ nanocomposites as electrodes and PVA/H ₂ SO ₄ as gel electrolyte	144 F/g	[377]
SWCNTs/phthalocyanine polymer composite	Self-nitrogen-doping	228 F/g	[378]
MnO ₂ /CNTs	Nanocomposite MnO ₂	580 F/g	[379]
MWNTs	Chemical evaporation deposition	340 mAh/g (reversible)	[380]
PANI/SnS ₂ @CNTs	Radial orientation and high chemical/physical stability	891 F g ⁻¹	[381]
NiCo ₂ S ₄ /N-CNTs		1428 F/g	[382]
NiCo ₂ S ₄		733.5 F/g	[382]
S-PANI/OCNT and S-PANI/SCNTs	Doping of long-chain protonic acids during in situ polymerization	316.8 F/g and 345.4 F/g	[383]
Cobalt hydroxide/porous graphene/functionalized MWNTs	Hydrothermal method	1426 F/g	[384]
CNTs	Nanosized lithium manganese oxide (LMO)	107 mAh/g (reversible)	[385]
Hybrid CNTs	0.5 M H ₂ SO ₄ electrolyte	145 F/g	[386]
CNTs	V ₂ O ₅	850 mAh/g	[387]
Ti ₃ C ₂ /CNTs/MnCo ₂ S ₄	Electrostatic self-assembly between positively charged multi-walled carbon nanotubes (CNTs) and negatively charged Ti ₃ C ₂ , followed by subsequent anchoring of bimetallic sulphide MnCo ₂ S ₄ nanoparticles to Ti ₃ C ₂ /CNT hybrids via a two-step hydrothermal method	823 F/g	[388]
Activated-carbon-coated MWCNTs	Nitrogen (N-AC-MWCNT)	103.1 F/g	[389]

The first type of CNT material that was examined for supercapacitors was randomly entangled CNTs, as they are easy to form. CNTs are found to only possess average specific surface areas compared to activated carbons, which have a high surface area. However, the capacitance of CNTs is higher, with SWCNTs having a capacity of 180 F/g [372], in contrast activated carbons, which have capacities of only tens of F/g. In order to measure the level of capacitance, mesoporosity was found to be the main factor. It can be demonstrated that CNTs that are very accessible to the electrolyte due to tube entanglement have a distinctive mesoporosity, which leads to a high capacitance [390].

Of the many different types of devices for energy storage, the lithium-ion battery and the supercapacitor are the center of attention and dominate the current market for energy storage devices [391]. CNTs have been widely applied in electrode production for the unique lithium-ion battery and the supercapacitor [392]. It was found that Li_xC formation has a high capacity during the lithiation process and that lithium ions that are introduced into the CNT-based electrode by the structural flaws and the interlayer rooms display good involvement regarding the energy storage capacity [393]. As for CNTs used as supercapacitors, electrodes based on CNTs have outstanding electrochemical performances due to their promising properties, such as rapid transport of charge, greater surface-area-

to-volume proportion, high electron conductivity, and larger electrolyte available capacity. However, relative to conventional materials, such as solid carbon, amorphous carbon, black carbon, and graphite, pure CNT-based electrodes are expensive and inappropriate for large-scale production due to the harsh synthesis conditions and intricate manufacturing methods required [394].

Carbon nanotubes (multi- and single-walled), which are also carbonaceous materials, have a wide variety of surface areas and capacitance values that typically range from 15 to 135 F/g [374]. There are a few methods to enhance charge storage in carbon supercapacitors. One approach allows for a greater capacity than those which can be attained by chemical or thermal (or both) char treatments. Thus, the available surface area and the functional groups can be increased. Another technique to improve the operation involves coating the carbonaceous material with conducting polymers, such as polypyrrole and polyaniline or redox-active metal oxides [395]. The effect has been displayed, for example, by polypyrrole-treated CNTs, which had a capacity of 170 F/g [375], and manganese oxide (MnO₂)-covered CNTs, which achieved a 140 F/g capacitance [376]. For electrochemical applications, it was emphasized that patterned CNTs are greatly preferred for their structures and properties, which ease their integration into devices [396]. In addition, vertically aligned CNTs were recently discovered to be better than randomly entangled CNTs for supercapacitor applications.

Hybrid carbon nanotubes performed efficiently as supercapacitors, with a capacity of 145 F/g. Modification and doping of compounds in CNTs are some of the best methods to improve the electronic properties of CNTs. This helps to insert the majority of existing materials inside carbon nanotubes with precise encapsulation. These types of modifications are highly effective for applications in electrodes, energy storage, supercapacitors, catalytic support, and bio-sensing [386].

4.3. Graphene for Energy Storage

Graphene has a layer of sp²-bonded carbon atoms that are bound tightly in a honeycomb structure with a hexagonal shape [397]. With respect to macrostructure, free-standing graphene dots and particles are zero-dimensional, fiber- and yarn-type structures are one-dimensional, graphene and graphene-based films are two-dimensional, and graphene foams and composites are three-dimensional graphene-based electrode products. Since graphene-based supercapacitors are widely utilized for energy storage devices, such as next-generation portables in the textile industry, wearables, and smart electronics, including smart watches, electronic skins, sensors, and many other devices [398–400], new avenues of research are constantly being opened on this subject. The performances of graphene-based materials as supercapacitors are detailed in Table 9.

Table 9. Performances of graphene-based materials as supercapacitors.

Materials	Synthesis Method	Electrolyte	Reference Electrode	Capacitance (F/g)	Ref.
F-rGO	Modified Hummers method	1.1 M LiPF ₆	Ag/AgCl	210.0	[401]
N-doping PG-Ni	Modified Hummers method	1.0 mol/L KOH	Saturated calomel	575.0	[402]
MnO ₂ nanoparticles on reduced graphene oxide (RGO)	Modified Hummers method	GO particles (0.5 mg·mL ⁻¹)	Saturated calomel electrode	432	[403]
ACP/GOx	-	0.8 g gel H ₃ PO ₄	Ag/AgCl (3 M KCl)	16.5	[404]
COF/rGO	Modified Hummers method	Aqueous 1 M H ₂ SO ₄	Ag/AgCl (3 M KCl)	321.0	[405]

Table 9. Cont.

Materials	Synthesis Method	Electrolyte	Reference Electrode	Capacitance (F/g)	Ref.
MoS ₂ /graphene	Surface methodology	1 M H ₂ SO _{4(aq)} solution	–	76.0	[406]
MW-GNPs	Modified Hummers' method	Solid-state electrolyte (1.0 g of PVA in 10 mL of deionized water)	–	78.1	[407]
Graphene/MnO ₂	Sonication	1 M Na ₂ SO ₄	Saturated calomel	320.0	[408]
Ni(OH) ₂ /NG	Tube furnace calcination	6 M KOH	Saturated calomel	1350.0	[409]
RG/NiO	Microwave	5 M NaOH	–	617.0	[410]
Fe ₂ O ₃ /NG	Hydrothermal	1M Na ₂ SO ₄	Saturated calomel	260.1	[411]

A number of works on graphene-based supercapacitors have already caught the attention of researchers. Tsai et al. introduced an exceptional graphene-based supercapacitor, MEGO, prepared by microwave irradiation. In their study, (PIP13-FSI)0.5 (PYR14-FSI)0.5 ionic liquid electrolyte was used to raise the specific capacitance drastically. MEGO powders, a three-electrode Swagelok[®] nylon cell, and a piston as a separator were assembled. Electrochemical characterizations were examined via cyclic voltammetry. For the specific ionic liquid electrolyte, an outstandingly high capacitance of about 150 F/g, with the highest voltage of 3.5 V, was achieved at 130 °C [412].

rGO/Ni(OH)₂ was examined to determine its performance as a supercapacitor. The modified Hummers technique was used to create composites whose shapes resembled flakes, sticks, flowers, and cubes. The positive electrode in this experiment was rGO/Ni(OH)₂, the negative electrode was rGO, the separator consisted of non-woven textiles, and the electrolyte solution consisted of 6 M KOH. With a basic capacitance of 1670.4 F/g at a charge and discharge current density of 1 A/g and a high rate capability, the nanoflake-like rGO/Ni(OH)₂ composites had the highest overall electrochemical efficiency according to Lai et al. The capacitance of the stick-like composites was 1866.8 F/g, that of the flower-like composites was 890.6 F/g, and that of the cube-like composites was 366.9 F/g [413]. A short time ago, a paper describing an aqueous fibrous supercapacitor with a graphene/PEDOT electrode and an Ag/AgCl reference electrode coupled with Pt wire as a counter electrode and 1 M H₂SO₄ as an electrolyte was published. A network resembling a continuous rose blossom was built into PSS hydrogel fiber. Galvanostatic charge/discharge (GCD) and cyclic voltammetry were used to measure the electrochemical outputs at room temperature (RT). In comparison to an aerogel fiber-based supercapacitor, the hydrogel fiber and PVA electrolyte-based all-gel-state supercapacitor had a high capacitance of 281.2 F/g (0.1 A/g) at 25 °C [414].

5. Carbon Dioxide (CO₂) Capture

Carbon dioxide is highly connected with global climate change as its level in the atmosphere increases through combustion (particularly that which occurs in fossil-fuel power plants) [415]. Due to this issue, many methods have been proposed to reduce CO₂ levels in the atmosphere. Capturing carbon dioxide is one of the techniques that can be used to manage climate change and utilize the byproducts of fossil-fuel power plants [416]. In gas-phase adsorption processes, a high micropore volume is the main requirement for an effective adsorbent. The surface area and porosity of carbonaceous materials are very significant parameters when it comes to capturing CO₂ [417]. CO₂ capture can be performed using carbonaceous materials, such as activated carbon, biochar, and carbon nanotubes. Furthermore, there are a few properties of carbonaceous materials that can be assessed by CO₂ gas, such as surface area and surface porosity [418].

Some of the proposed methods used to seize CO₂ include absorption, adsorption, membranes, and cryogenics. The global commercial method used to separate a large

quantity of CO₂ is absorption [419]. Although monoethanolamine (MEA) is the most popular and widely used absorbent, it has some drawbacks, such as oxidation degradation, energy consumption for regeneration, the decomposition of the material [420], and the complication of absorbing CO₂ diluted in flue gas streams at low concentrations. To overcome these drawbacks, porous adsorbents that can capture CO₂ effectively and release it in pressure or temperature swipec adsorption–desorption cycles [421] are receiving greater attention. Specifically, the reason adsorption is preferred is due to its specialty in handling dilute solutions. To improve the adsorption performance of CO₂, the amine group can be implanted onto the surface of adsorbents as it results in carbamate creation (-COO-), and MEA is also the standard solvent for absorbing CO₂. Some of the types of adsorbents with amine surface modification are zeolite, activated carbons, and carbon nanotubes [422].

5.1. Activated Carbon for CO₂ Capture

Activated carbon is a form of physical adsorbent with the ability to absorb CO₂ due to its unique properties. It is classified as a solid adsorber because of its ease of regeneration, low cost, high specific surface area, high mechanical efficiency, moisture impassivity, sufficient pore size distribution, high CO₂ adsorption potential at atmospheric conditions, and low energy demand [423]. Some factors, however, affect the effectiveness of activated carbon to seize CO₂, including the activation method and the nature of the raw materials used, which therefore influence properties such as porosity and surface chemistry. The activation of raw materials should be performed easily, resulting in a lower degradation rate and hence the maintenance of their physicochemical properties [424]. Therefore, the raw materials must be selected thoroughly, as the physicochemical properties will be affected by the composition of the material structures, such as carbon, nitrogen, oxygen, hydrogen, and sulfur. The CO₂ adsorption capacities of activated carbon derived from biomass are shown in Table 10.

Table 10. Carbon dioxide adsorption capacities of activated carbons.

Biomass	Production Temperature (K)	BET Surface Area (m ² /g)	Activating Agent	Adsorption Capacity (mmol/g)	Ref.
Bamboo	1073	2000	KOH	7.00	[425]
Fir bark	973	1242	KOH	6.10	[426]
Longan shells	1073	3260	KOH	5.60	[427]
Eucalyptus sawdust	1073	2850	KOH	5.20	[428]
Paulownia sawdust	1073	1555	KOH	7.14	[429]
Wheat	1073	2192	KOH	5.70	[430]
Black locust	1103	2511	KOH	5.86	[431]
Celtuce leaves	1073	3404	KOH	6.04	[432]
Pulverized semi-coke	973	120.5–590.2	HCl	1.80	[433]
Commercial activated carbon	1073	1374	ZnCl ₂	-	[434]
Soya beans	673	710–1193	KOH	4.24	[435]
Activated carbon	200–1000 °C	-		53 mg/g	[436]
African palm shells	1073	473–1361	Cu(NO ₃) ₂	103–217 mg/g	[437]
Granular activated carbon (GAC)	-	954	3-aminopropyl-triethoxysilane	34.6	[438]
GAC	-	954	3-aminopropyl-triethoxysilane	79.5 C _{in} :50%, T:25 °C	[438]

From Table 10 above, it can be concluded that Paulownia sawdust has the highest carbon dioxide adsorption capacity of 7.14 mmol/g at 273 K. It was prepared with an ideal mass ratio of 4:1 for KOH and Paulownia sawdust and activated at 700 °C for 1 h [429]. Using bamboo to prepare activated carbon resulted in the second-highest adsorption capacity of 7.00 mmol/g at 273 K among the other precursors. This was due to the formation of some narrow micropores, which are assisted by the distinctive textural structure of bamboo [425]. According to Table 10, the biomass with the third-highest adsorption capacity was fir bark, with a value of 6.10 mmol/g [426]. These three biomasses, when compared to commercial activated carbon, possess higher adsorption capacities. These results encourage the derivation of activated carbon from biomass. Other biomasses have also been used in research to determine their carbon dioxide adsorption capacities, including longan shells, eucalyptus sawdust, wheat, black locust, and celuce leaves.

Currently, the post-combustion system is a widely utilized technology for CO₂ capture. In this system, the flue gas is separated after the fossil fuel is combusted. This system is commonly adopted as it is easy to incorporate into existing power plants, and the process is adaptable to different circumstances, which still enables power plants to operate even if the capturing system malfunctions [439]. Activated carbon and zeolites are commonly the only suitable solid adsorbents for this system as the operating temperatures are low, and these adsorbents are made for low-temperature adsorption applications, in addition to their substantial applications in industrial processes [440]. Other advantages of these adsorbents are that their properties as physisorbed materials are environmentally safe and that they are reasonably priced for manufacturers [441].

However, activated carbon is found to be a better CO₂ adsorbent for the flue gas stream, which is attributed to its hydrophobicity properties, which enable the elimination of moisture before CO₂ adsorption occurs. Another application of ACs for CO₂ arrest is in sound-assisted fluidization, where CO₂ is absorbed from flue gases using fine activated carbon [442], resulting in an increase in adsorption. Although activated carbon was found to be an attractive CO₂ adsorbent, its utilization has not been broadly analyzed. Since it has not been used on a large scale, only in pilot-scale power plants, more research is needed to establish its application on a large scale and at a lower cost [443]. Regarding granular activated carbon, the character of the adsorbent was improved by modification, which enhanced the capture affinity of the CO₂ molecules and the adsorbent. It displayed a maximum removal efficiency of 79.5 mmol/g under analogous situations [438].

The CO₂ activation at 700 °C increased the surface area and micropore content of the activated carbon derived from palm kernel shells, allowing it to absorb 7.32 mmol/g of CO₂ (89.50%) [444]. ACs from almond shells and olive stones with oxygen concentrations of 3%, 5%, and 21% were successful with respect to CO₂ adsorption at temperatures of 400 and 650 degrees Celsius [417]. The different ACs produced from KOH activation suggested different CO₂ uptake performances. The association between physical properties and CO₂ adsorption potential at high pressure was verified by the different BET surface areas and pore depths [445].

The surface area and pore structure of ACs, as well as the chemical properties of both the adsorbate and adsorbents, determine their CO₂ adsorption abilities. The addition of nitrogenous functional groups to the AC surface was shown to increase CO₂ adsorption capability [446]. An AC with N-functional groups and a large surface area is beneficial for CO₂ adsorption. The biomass should be pre-deashed by HF (hydrofluoric acid) with high-temperature ammonia treatment to increase the CO₂ adsorption potential of nitrogen-enriched AC. The findings showed that primary amides, amines, azo compounds N=N, secondary amide groups, and aliphatic C-N/C-O are strong CO adsorbents [447]. For CO₂ adsorption, both the physical (surface area and pore structure) and chemical (functional group) properties of ACs are essential. They are low-cost, long-term replacements for commercially available products for CO₂ capture from flue gas and air [368].

5.2. Carbon Nanotubes for CO₂ Capture

Some of the technologies being studied to capture CO₂ are absorption, membranes, cryogenics, adsorption, and there are many more [448]. Carbon nanotubes are considered promising adsorbents that are used to eliminate the many types of organic and inorganic pollutants in air streams [449]. Moreover, sorption on the solid adsorbent is an excellent alternative to capture the CO₂ from flue gases efficiently. Due to their porous assembly and the presence of a broad range of functional groups that can be attained by thermal or chemical treatments, carbon nanotubes have been found to have a high adsorption capacity.

Not long ago, there were studies on the alterations of pore materials by adding elementary positions that resulted in higher carbon dioxide capture capability and selectivity. These alterations were attributable to the durable contact between the functional groups and CO₂. Normally, the basic groups that are introduced into pore materials are the alkaline carbonates with several amine groups [450]. Grafting can be performed to prepare the solid adsorbents, where the amine groups are chemically bonded to the support [451]. Another method that can be used is impregnation, which inactivates liquid amines within the pores of the support [452]. Comparing these two methods, impregnation is better, as its preparation procedures are simple [453]. The carbon nanotubes modified by 3-aminopropyltriethoxysilane could remove CO₂ by 40.9 mg/g [438]. The carbon dioxide adsorption capacities of carbon nanotubes are detailed in Table 11.

Table 11. Carbon dioxide adsorption capacities of carbon nanotubes.

Adsorbents	Modification Chemicals	Adsorption (mg/g)	Conditions	Ref.
CNTs	3-aminopropyl-triethoxysilane	43.3	Influent concentration mgL ⁻¹ : 15%, T:20 °C	[454]
CNTs	3-aminopropyl-triethoxysilane	114.0	Cin:50%, T:20 °C	[454]
SWCNT	-	87	C _{in} :99%, T:35 °C	[455]
Chitosan/MWCNTs	Chitosan	3 mg/g	At 45°C, 1.1 bar	[456]
CNTs	3-aminopropyl-triethoxysilane	40.9	Cin: 10%, T: 25 °C	[438]
CNTs	3-aminopropyl-triethoxysilane	96.3	Cin: 50%, T: 25 °C	[438]
CNTs	Tetraethylenepentamine (TEPA)	3.87 mmol/g	2 v.% of CO ₂ and 2 v.% of H ₂ O at 40 °C	[452]
MWCNT/Cd-nanozeolite composites	Polyethylenimine	5.7 mmol/g	At 25 °C, 1 bar	[457]
MWCNTs	Polyethylenimine (PEI)	93 mg/gfiber	PEI load at 20 wt.-%	[458]
MWCNTs	Polyaspartamide (PAA),	99.5%	100 °C	[459]
Modified carbon nanotubes (MCNTs)	Tetraethylenepentamine	5 mmol CO ₂ /g	Containing 10 vol% CO ₂ in N ₂ with 1 vol% H ₂ O	[460]
Microcrystalline cellulose	Amidoxime	3.85 mmol/g	120 °C, 1.01325 bar	[461]
CNTs	Pebax-1657 membrane	5 wt% CNTs		[462]
Functionalized carbon nanotubes	Carbon nanofibers (CNFs)	6.3 mmol g ⁻¹	At 1.0 bar and 298 K	[463]
Amine-loaded carbon nanotubes	Temperature/vacuum swing adsorption	67% after TVSA		[463]

There is a study in which CNTs were altered using 3-aminopropyltriethoxysilane (APTS), which resulted in 1 mmol/g of optimal CO₂ adsorption capacity for 15 v.% CO₂ at 20 °C [454]. Another study used the impregnation of CNTs with tetraethylenepentamine (TEPA), where adsorption capability was recorded at around 3.87 mmol/g for 2 v.% of CO₂ and 2 v.% of H₂O at 40 °C [452]. Based on these findings, it can be hypothesized that

altering CNTs improves CO₂ adsorption capability. After modification, CNTs show the largest increases in CO₂ adsorption potential (96.3 mg/g), followed by zeolites, and finally GAC [438].

The modified carbon nanotubes with tetraethylenepentamine modification eliminate 5 mmol of carbon dioxide per gram [452]. On the other hand, the functionalized carbon nanotubes can absorb 6.3 mmol of carbon dioxide per gram [463]. It was also determined that B2CNTs (6, 0) are very effective in CO₂ removal and gas separation because of their larger diameter and negative charge [464]. Pyridinic-nitrogen combinations with CNTs increased CO₂ adsorption for electron injection. The functionality of CO₂ removal can be controlled by the charge-carrying system [465].

5.3. Graphene

Graphene is another carbon nanomaterial that possesses a hierarchical porous structure with high porosity. These parameters are critical for CO₂ capture, since they allow for low-resistance pathways and micropore entry. Individual carbon nanomaterials (carbon nanotubes, graphene, and so on) were tested for CO₂ capture, and their special thermal, mechanical, electrical, and chemical properties resulted in higher efficiencies [466]. The carbon nanomaterials for CO₂ capture are described in Table S4 [467–473]. Graphene oxide-decorated biobased chitosan hybrid aerogels captured CO₂ in the range of 1.92 to 4.14 mmol/g with high stability [468]. While graphene materials are more time-consuming and costly to manufacture, they can be used to capture CO₂ with high selectivity and power. With high thermal stability and good recovery, functionalized graphene sheets will capture CO₂ at 4.3 mmol/g (25 °C, 1 atm) [474]. The copper-based graphene oxide, Cu-BTC/GO composite, could arrest 9.59 mmol/g CO₂ at normal atmospheric pressure and temperature [472].

6. Recommendations for Future Directions

The three main carbonaceous materials are being used in extremely promising ways for the purification of water, storing energy, and removing carbon dioxide from the atmosphere. The steps of the basic process for synthesizing these carbonaceous materials and their practical applications described in the current work are depicted in Figure 8. Furthermore, the recommendations for future directions are as follows:

- i. Carbonaceous materials have so many allotropes with different applications. These allotrope materials can be used for sensitive applications, such as fuel cells, medicine, cosmetics, catalysts, etc. Similarly, other carbonaceous materials (fullerene, carbon onions, peapods, nanohorns, etc.) can also be investigated.
- ii. The applications of activated carbons are concentrated mostly in water treatment, whereas the applications of ACs in energy storage and CO₂ capture are relatively few and can be further improved. Applications of activated carbons for CO₂ adsorption from soil can amend soil quality by reducing greenhouse gases.
- iii. Improving the surface properties of carbon nanotubes for precise organic matter adsorption may be a major research project in the near future to further improve water treatment. The degree of oxidation of the surface of carbonaceous adsorbents should be considered since the actual surface areas of CNTs are about 1000 m²/g (the theoretical maximum is 1315 m²/g).
- iv. Surface hydrophobicity and fast agglomeration in aqueous solutions are two major drawbacks of graphene, limiting its adsorption potential in practical applications. Therefore, the performance of graphene can be improved by functionalizing it to overcome these shortcomings. Moreover, surfactants can be used to change the surfaces of hydrophobic materials.
- v. The reduction of graphene oxide to produce graphene is a promising field for low-cost graphene production on a large scale in the future. Furthermore, the less costly graphene manufacturing technology has made little progress. As a result, new graphene synthesis techniques will increase the range of potential applica-

tions and enable the development of new green synthesis methods to regenerate sustainable resources.

- vi. Carbonaceous materials are currently being employed as catalysts in fuel cells. The improved performance of these catalysts in comparison to an industry standard may be developed by overcoming the weaknesses of the present catalytic technology and boosting lifespan to fulfill the durability criterion.
- vii. Comparisons of these carbonaceous materials can be evaluated in terms of characteristics, advantages, and disadvantages for a specific application.
- viii. Additional modifications to activated carbons, graphene, and carbon nanotubes may be made to improve properties while lowering costs and improving efficiency, and environmentally friendly paths will be built to open new trails based on the attributes, allowing for more research into highly replicable real-time applications.

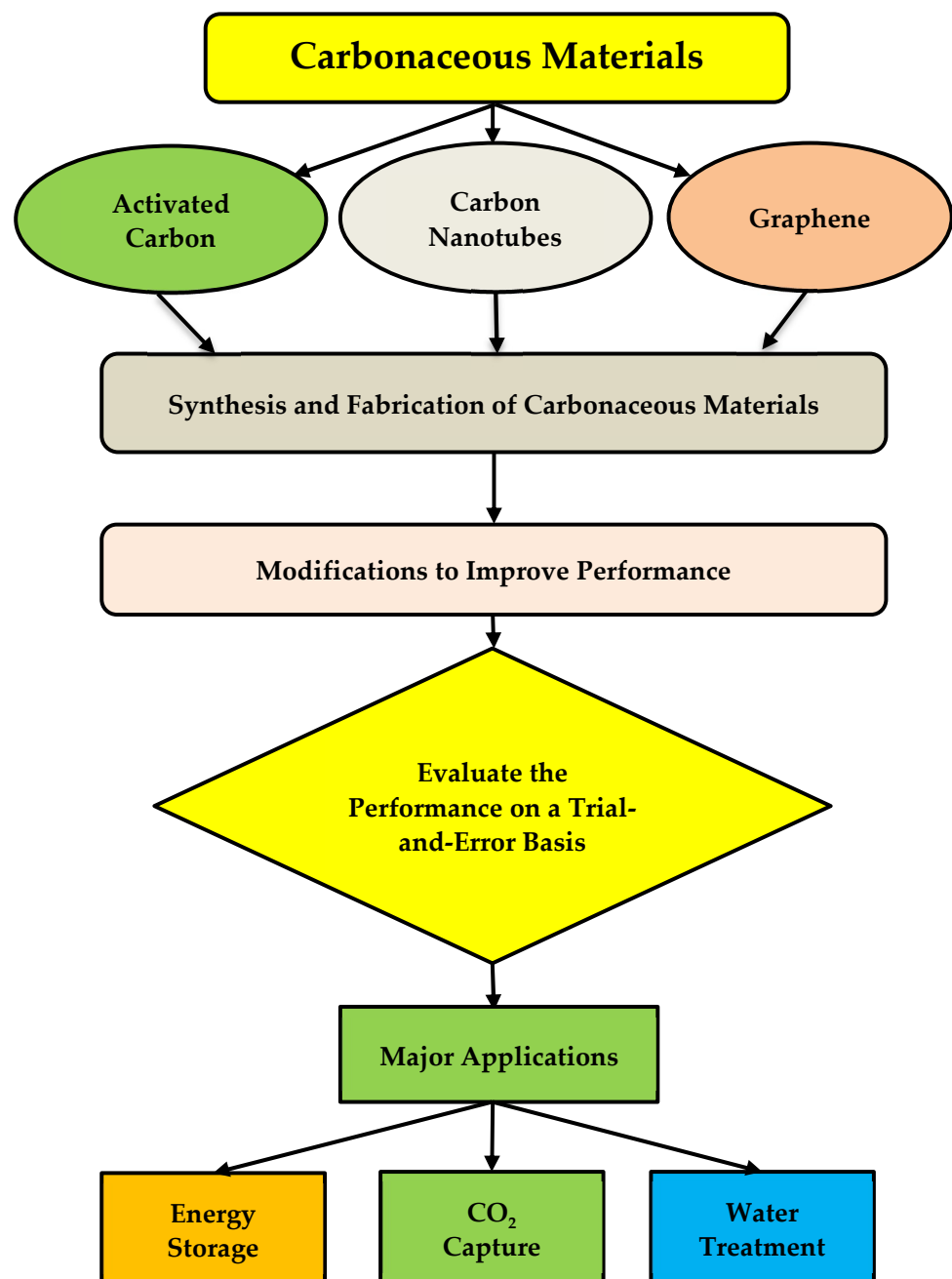


Figure 8. Pathways for processing and applications of carbonaceous materials.

7. Conclusions

In this review, three major classes of carbon allotropes (activated carbons, carbon nanotubes, and graphene) have been investigated with respect to their important synthesis methodologies and three sustainability applications (water treatment, energy storage, and carbon dioxide removal), which are connected to each other. The success of these carbon allotropes in resolving the energy crisis, water treatment, and air purification is commendable and is due to their solid mechanical strength, super chemical stability, high surface area, and enormous functional groups.

Regarding the preparation of activated carbon, it can be produced from various types of household, municipal, and industrial solid wastes through different activation processes (physical, chemical, physiochemical, and microwave). Chemical activation is more frequent than the physical activation process, as it requires a lower activation temperature and a shorter processing time. However, the chemical activation process is more corrosive and requires an additional washing step for purification. Activated carbon synthesized by physiochemical activation has a larger porosity and a higher surface area than those synthesized by other activation processes. In the activation of AC, phosphoric acid and potassium hydroxide are preferable to zinc chloride for environmental friendliness and less toxicological contamination.

In the synthesis of CNTs in a conventional process, high temperatures are applied to enable the catalyst and disintegrate the carbon sources. Arc discharge and laser ablation procedures are costly ways to synthesize CNTs on a large scale, despite the fact that they produce CNTs of high quality. The most effective and practical way to produce carbon nanotubes on a wide scale is by using CVD; however, the application is better suited to the creation of SWNTs. The synthesis of high-quality graphene is achieved using a variety of synthetic techniques, where epitaxial growth and CVD processes are more suitable. The chemical exfoliation process is highly effective for producing chemically modified graphene in high yields and has a wide range of uses. The synthesis of these carbonaceous materials mainly depends on the carbon precursor, the activation type, the activation temperature, the processing time to develop the microstructure, the textural properties, the surface chemistry, and the adsorption capacity of the produced carbons.

For water treatment, activated carbon has been counted as one of the most-usable carbon-based materials for a long time, due to its availability and economical cost of production. However, in the sophisticated filtering procedure for removing particular contaminants from water, CNTs and graphene are highly developed materials. Carbon nanotubes showed better performance in removing microorganisms from water than activated carbon and graphene. Effective pollutant neutralization by CNTs and graphene devices also provides a benefit over the action of AC in circumstances when access to treated water is constrained. One of the significant qualities of CNTs and graphene-based materials is that they require very little material to purify water effectively. The development of next-generation water filtration technologies may greatly depend on carbon-based nanomaterials or a mixture of these materials.

Regarding energy storage applications, carbonaceous materials have shown efficient performances, with mechanical stability and electronic conductivity. AC is significant in the mainstream electrochemical double-layer capacitors (EDLCs), while thin electrodes composed of CNTs or graphene structures may serve in specialized applications focused on ultra-high performance rates and competition with electrolytic capacitors. Processing CNTs and graphene into flexible, strong, and highly electrically conductive fabrics may allow them to serve as electrodes in weight-sensitive applications in aerospace or the military. CNTs and graphene may also serve as high-surface-area conductive substrates for the deposition of conductive polymers or metal oxides for higher-energy-density asymmetric capacitor applications. Porous carbon materials with an excessive number of large mesopores or macropores simply cannot compete with the microporous carbons used in commercial supercapacitors.

Regarding CO₂ removal, the adsorption method using carbon-based solid adsorbents has gained significant interest in recent years among the various methods. These adsorbents are highly selective, environmentally friendly, economical, and less energy-intensive. The adsorption of CO₂ mainly depends on the physical interactions (Lewis acid–base interactions, π - π interactions, and hydrogen bonding interactions) of the functional groups of the base materials with the CO₂ molecules. The carbonaceous materials (activated carbons, carbon nanotubes, and graphene) contain more functional groups with a large surface area, which makes them very promising adsorbents for the adsorption of carbon dioxide molecules. Moreover, the adsorption process of CO₂ is governed by van der Waals and electrostatic forces, temperature, surface area, pressure, functional groups, and vapors. Adsorption on carbonaceous adsorbents is very attractive owing to their easy availability, amenable surface properties, low moisture sensitivity, and high thermal stability. Moreover, the distribution of micropores significantly governs the adsorption of carbon dioxide, where the carbonaceous adsorbents have a significant pore volume.

The comparisons of adsorption capacities between nanotubes, graphene, and activated carbons have led to opposing views on the functionality of those particular carbonaceous materials in promoting adsorption capabilities. Moisture has a detrimental impact on adsorbent potential by reducing the active surface regions of ACs, graphene, and CNTs. It is critical to provide a sufficient set of precursors, carbonization, and activation conditions to enhance and maximize the adsorption capacities of these carbon allotropes and eliminate both organic and inorganic contaminants. There is a huge scope to develop the performance of carbonaceous materials for environmental sustainability.

Finally, it can be concluded that the 1D (carbon nanotubes), 2D (graphene), and 3D (activated carbons) carbonaceous materials are highly promising for sustainable water treatment, energy storage, and CO₂ capture.

Supplementary Materials: The following supporting information can be downloaded at: <https://www.mdpi.com/article/10.3390/su15118815/s1>, Table S1: Comparison of the adsorption capabilities of various dyes; Table S2: The activity of multifunctional CNTs in adsorption procedures; Table S3: Performance of activated carbons as supercapacitors (two-electrode cell system); Table S4: Carbon nanomaterials for CO₂ capture.

Author Contributions: Conceptualization, M.S.R., S.A., M.S.I., M.A.H. and A.K.A.; writing—original draft preparation, M.S.R., S.A., M.N.H., M.A.H., M.H., H.R. and M.S.I.; writing—review and editing, A.K., K.Z.B., S.N.I., M.H. and M.N.P.; supervision, K.K., M.N.P. and A.K.A.; funding acquisition, K.K. and K.Z.B. All authors have read and agreed to the published version of the manuscript.

Funding: The work was fulfilled in the frame of project no. AP14871005 supported by the Ministry of Science and Higher Education, Republic of Kazakhstan.

Institutional Review Board Statement: Not applicable.

Informed Consent Statement: Not applicable.

Data Availability Statement: Not applicable.

Acknowledgments: The authors are profoundly grateful to the Universiti Brunei Darussalam, Brunei; East West University, Bangladesh; the L. N. Gumilyov Eurasian National University, Kazakhstan; the Bangladesh University of Engineering and Technology, Bangladesh; and the University of Salerno, Italy.

Conflicts of Interest: The authors declare no conflict of interest.

References

1. Wang, Y.; Li, Z.; Wang, J.; Li, J.; Lin, Y. Graphene and Graphene Oxide: Biofunctionalization and Applications in Biotechnology. *Trends Biotechnol.* **2011**, *29*, 205–212. [[CrossRef](#)] [[PubMed](#)]
2. Reza, M.S.; Azad, A.K.; Bakar, M.S.A.; Karim, M.R.; Sharifpur, M.; Taweekun, J. Evaluation of Thermochemical Characteristics and Pyrolysis of Fish Processing Waste for Renewable Energy Feedstock. *Sustainability* **2022**, *14*, 1203. [[CrossRef](#)]
3. Afroze, S.; Reza, M.S.; Amin, M.R.; Taweekun, J.; Azad, A.K. Progress in Nanomaterials Fabrication and Their Prospects in Artificial Intelligence towards Solid Oxide Fuel Cells: A Review. *Int. J. Hydrogen Energy*, 2022, *in press*. [[CrossRef](#)]

4. Reza, M.S.; Taweekun, J.; Afroze, S.; Siddique, S.A.; Islam, M.S.; Wang, C.; Azad, A.K. Investigation of Thermochemical Properties and Pyrolysis of Barley Waste as a Source for Renewable Energy. *Sustainability* **2023**, *15*, 1643. [[CrossRef](#)]
5. Syazaidah, I.; Abu Bakar, M.S.; Reza, M.S.; Azad, A.K. Ex-Situ Catalytic Pyrolysis of Chicken Litter for Bio-Oil Production: Experiment and Characterization. *J. Environ. Manag.* **2021**, *297*, 113407. [[CrossRef](#)] [[PubMed](#)]
6. Mo, W.Y.; Man, Y.B.; Wong, M.H. Use of Food Waste, Fish Waste and Food Processing Waste for China's Aquaculture Industry: Needs and Challenge. *Sci. Total Environ.* **2018**, *613–614*, 635–643. [[CrossRef](#)] [[PubMed](#)]
7. Zheng, B.; Lin, X.; Zhang, X.; Wu, D.; Matyjaszewski, K. Emerging Functional Porous Polymeric and Carbonaceous Materials for Environmental Treatment and Energy Storage. *Adv. Funct. Mater.* **2020**, *30*, 1907006. [[CrossRef](#)]
8. Gupta, T. *Carbon the Black, the Gray and the Transparent*; Springer International Publishing: Cham, Switzerland, 2018; ISBN 9783319664057.
9. Mangler, C.; Meyer, J.C. Using Electron Beams to Investigate Carbonaceous Materials. *C. R. Phys.* **2014**, *15*, 241–257. [[CrossRef](#)]
10. Sheoran, K.; Thakur, V.K.; Siwal, S.S. Synthesis and Overview of Carbon-Based Materials for High Performance Energy Storage Application: A Review. *Mater. Today Proc.* **2022**, *56*, 9–17. [[CrossRef](#)]
11. Sweetman, M.; May, S.; Mebberson, N.; Pendleton, P.; Vasilev, K.; Plush, S.; Hayball, J. Activated Carbon, Carbon Nanotubes and Graphene: Materials and Composites for Advanced Water Purification. *C* **2017**, *3*, 18. [[CrossRef](#)]
12. Nazal, M.K.; Nazal, M.K. An Overview of Carbon-Based Materials for the Removal of Pharmaceutical Active Compounds. In *Carbon-Based Material for Environmental Protection and Remediation*; IntechOpen: London, UK, 2020; pp. 1–19; ISBN 978-1-78984-587-7.
13. Dhandapani, E.; Thangarasu, S.; Ramesh, S.; Ramesh, K.; Vasudevan, R.; Duraisamy, N. Recent Development and Prospective of Carbonaceous Material, Conducting Polymer and Their Composite Electrode Materials for Supercapacitor—A Review. *J. Energy Storage* **2022**, *52*, 104937. [[CrossRef](#)]
14. Reza, M.S.; Yun, C.S.; Afroze, S.; Radenahmad, N.; Bakar, M.S.A.A.; Saidur, R.; Taweekun, J.; Azad, A.K. Preparation of Activated Carbon from Biomass and Its' Applications in Water and Gas Purification, a Review. *Arab J. Basic Appl. Sci.* **2020**, *27*, 208–238. [[CrossRef](#)]
15. Gan, Y.X. Activated Carbon from Biomass Sustainable Sources. *C* **2021**, *7*, 39. [[CrossRef](#)]
16. Marco-Lozar, J.P.; Kunowsky, M.; Suárez-García, F.; Linares-Solano, A. Sorbent Design for CO₂ Capture under Different Flue Gas Conditions. *Carbon* **2014**, *72*, 125–134. [[CrossRef](#)]
17. Hussain, A.; Mehdi, S.M.; Abbas, N.; Hussain, M.; Naqvi, R.A. Synthesis of Graphene from Solid Carbon Sources: A Focused Review. *Mater. Chem. Phys.* **2020**, *248*, 122924. [[CrossRef](#)]
18. Lawal, A.T. Graphene-Based Nano Composites and Their Applications. A Review. *Biosens. Bioelectron.* **2019**, *141*, 111384. [[CrossRef](#)] [[PubMed](#)]
19. Li, Y.; Huang, X.; Zeng, L.; Li, R.; Tian, H.; Fu, X.; Wang, Y.; Zhong, W.H. A Review of the Electrical and Mechanical Properties of Carbon Nanofiller-Reinforced Polymer Composites. *J. Mater. Sci.* **2019**, *54*, 1036–1076. [[CrossRef](#)]
20. Ullah Rather, S. Preparation, Characterization and Hydrogen Storage Studies of Carbon Nanotubes and Their Composites: A Review. *Int. J. Hydrogen Energy* **2020**, *45*, 4653–4672. [[CrossRef](#)]
21. Rajabi, M.; Mahanpoor, K.; Moradi, O. Removal of Dye Molecules from Aqueous Solution by Carbon Nanotubes and Carbon Nanotube Functional Groups: Critical Review. *RSC Adv.* **2017**, *7*, 47083–47090. [[CrossRef](#)]
22. Sehrawat, P.; Julien, C.; Islam, S.S. Carbon Nanotubes in Li-Ion Batteries: A Review. *Mater. Sci. Eng. B* **2016**, *213*, 12–40. [[CrossRef](#)]
23. Singh, J.; Nayak, P.; Singh, G.; Khandai, M.; Sarangi, R.R.; Kar, M.K. Carbon Nanostructures as Therapeutic Cargoes: Recent Developments and Challenges. *C* **2022**, *9*, 3. [[CrossRef](#)]
24. Arora, B.; Attri, P. Carbon Nanotubes (CNTs): A Potential Nanomaterial for Water Purification. *J. Compos. Sci.* **2020**, *4*, 135. [[CrossRef](#)]
25. Amin, R.; Kumar, P.R.; Belharouak, I.; Amin, R.; Kumar, P.R.; Belharouak, I. Carbon Nanotubes: Applications to Energy Storage Devices. In *Carbon Nanotubes—Redefining the World of Electronics*; IntechOpen: London, UK, 2020; pp. 1–23; ISBN 978-1-83881-185-3.
26. Halada, Š.; Zlatník, J.; Mazúr, P.; Charvát, J.; Slouka, Z. Fast Screening of Carbon-Based Nanostructured Materials as Potential Electrode Materials for Vanadium Redox Flow Battery. *Electrochim. Acta* **2022**, *430*, 141043. [[CrossRef](#)]
27. Akbari, E.; Buntat, Z. Benefits of Using Carbon Nanotubes in Fuel Cells: A Review. *Int. J. Energy Res.* **2017**, *41*, 92–102. [[CrossRef](#)]
28. Shukrullah, S.; Mohamed, N.M.; Shaharun, M.S.; Ullah, S.; Naz, M.Y. Effective CO₂ Adsorption on Pristine and Chemically Functionalized MWCNTs. In Proceedings of the 4th International Conference on Fundamental and Applied Sciences (ICFAS2016), Kuala Lumpur, Malaysia, 15–17 August 2016; Volume 1787, p. 50025.
29. Hashim, H.; Shukor Salleh, M.; Zaidi Omar, M. Homogenous Dispersion and Interfacial Bonding of Carbon Nanotube Reinforced with Aluminum Matrix Composite: A Review. *Rev. Adv. Mater. Sci.* **2019**, *58*, 295–303. [[CrossRef](#)]
30. Kurbanoglu, S.; Ozkan, S.A. Electrochemical Carbon Based Nanosensors: A Promising Tool in Pharmaceutical and Biomedical Analysis. *J. Pharm. Biomed. Anal.* **2018**, *147*, 439–457. [[CrossRef](#)]
31. Jiang, Z.; Zhao, Y.; Lu, X.; Xie, J. Fullerenes for Rechargeable Battery Applications: Recent Developments and Future Perspectives. *J. Energy Chem.* **2021**, *55*, 70–79. [[CrossRef](#)]
32. Zhu, X.; Yu, S.; Xu, K.; Zhang, Y.; Zhang, L.; Lou, G.; Wu, Y.; Zhu, E.; Chen, H.; Shen, Z.; et al. Sustainable Activated Carbons from Dead Ginkgo Leaves for Supercapacitor Electrode Active Materials. *Chem. Eng. Sci.* **2018**, *181*, 36–45. [[CrossRef](#)]

33. Ould Amrouche, S.; Rekioua, D.; Rekioua, T.; Bacha, S. Overview of Energy Storage in Renewable Energy Systems. *Int. J. Hydrogen Energy* **2016**, *41*, 20914–20927. [[CrossRef](#)]
34. González, A.; Goikolea, E.; Barrena, J.A.; Mysyk, R. Review on Supercapacitors: Technologies and Materials. *Renew. Sustain. Energy Rev.* **2016**, *58*, 1189–1206. [[CrossRef](#)]
35. Zhai, Z.; Zhang, L.; Du, T.; Ren, B.; Xu, Y.; Wang, S.; Miao, J.; Liu, Z. A Review of Carbon Materials for Supercapacitors. *Mater. Des.* **2022**, *221*, 111017. [[CrossRef](#)]
36. Giri, A.; Bharti, V.K.; Kalia, S.; Arora, A.; Balaje, S.S.; Chaurasia, O.P. A Review on Water Quality and Dairy Cattle Health: A Special Emphasis on High-Altitude Region. *Appl. Water Sci.* **2020**, *10*, 79. [[CrossRef](#)]
37. Jain, C.K.; Malik, D.S.; Yadav, A.K. Applicability of Plant Based Biosorbents in the Removal of Heavy Metals: A Review. *Environ. Process.* **2016**, *3*, 495–523. [[CrossRef](#)]
38. Lata, S.; Samadder, S.R. Removal of Arsenic from Water Using Nano Adsorbents and Challenges: A Review. *J. Environ. Manag.* **2016**, *166*, 387–406. [[CrossRef](#)] [[PubMed](#)]
39. Jahan, N.; Tahmid, M.; Shoronika, A.Z.; Fariha, A.; Roy, H.; Pervez, M.N.; Cai, Y.; Naddeo, V.; Islam, M.S. A Comprehensive Review on the Sustainable Treatment of Textile Wastewater: Zero Liquid Discharge and Resource Recovery Perspectives. *Sustainability* **2022**, *14*, 15398. [[CrossRef](#)]
40. Reza, M.S.; Hasan, A.B.M.K.; Afroze, S.; Muhammad, S.; Bakar, A.; Taweekun, J.; Azad, A.K. Analysis on Preparation, Application, and Recycling of Activated Carbon to Aid in COVID-19 Protection. *Int. J. Integr. Eng.* **2020**, *12*, 233–244. [[CrossRef](#)]
41. Danish, M.; Ahmad, T.; Hashim, R.; Hafiz, M.R.; Ghazali, A.; Sulaiman, O.; Hiziroglu, S. Characterization and Adsorption Kinetic Study of Surfactant Treated Oil Palm (*Elaeis guineensis*) Empty Fruit Bunches. *Desalin. Water Treat.* **2016**, *57*, 9474–9487. [[CrossRef](#)]
42. Thekkudan, V.N.; Vaidyanathan, V.K.; Ponnusamy, S.K.; Charles, C.; Sundar, S.; Vishnu, D.; Anbalagan, S.; Vaithyanathan, V.K.; Subramanian, S. Review on Nanoadsorbents: A Solution for Heavy Metal Removal from Wastewater. *IET Nanobiotechnol.* **2017**, *11*, 213–224. [[CrossRef](#)]
43. Wang, X.; Guo, Y.; Yang, L.; Han, M.; Zhao, J.; Cheng, X. Nanomaterials as Sorbents to Remove Heavy Metal Ions in Wastewater Treatment. *J. Environ. Anal. Toxicol.* **2012**, *2*, 154–158. [[CrossRef](#)]
44. Water Pollution. Available online: http://www.informaction.org/index.php?menu=menua.txt&main=waterpol_gen.txt&s=Water+sewage (accessed on 20 September 2022).
45. UNEnvironment Greenhouse Gases Are Depriving Our Oceans of Oxygen. Available online: <https://www.unenvironment.org/news-and-stories/story/greenhouse-gases-are-depriving-our-oceans-oxygen> (accessed on 10 December 2022).
46. Chiang, Y.C.; Juang, R.S. Surface Modifications of Carbonaceous Materials for Carbon Dioxide Adsorption: A Review. *J. Taiwan Inst. Chem. Eng.* **2017**, *71*, 214–234. [[CrossRef](#)]
47. CO₂ Emissions by Year—Worldometer. Available online: <https://www.worldometers.info/co2-emissions/co2-emissions-by-year/> (accessed on 22 September 2020).
48. Gunawardene, O.H.P.; Gunathilake, C.A.; Vikrant, K.; Amaraweera, S.M. Carbon Dioxide Capture through Physical and Chemical Adsorption Using Porous Carbon Materials: A Review. *Atmosphere* **2022**, *13*, 397. [[CrossRef](#)]
49. Gao, X.; Yang, S.; Hu, L.; Cai, S.; Wu, L.; Kawi, S. Carbonaceous Materials as Adsorbents for CO₂ Capture: Synthesis and Modification. *Carbon Capture Sci. Technol.* **2022**, *3*, 100039. [[CrossRef](#)]
50. Bhatnagar, A.; Hogland, W.; Marques, M.; Sillanpää, M. An Overview of the Modification Methods of Activated Carbon for Its Water Treatment Applications. *Chem. Eng. J.* **2013**, *219*, 499–511. [[CrossRef](#)]
51. Reza, M.S.; Hasan, A.B.M.K.; Ahmed, A.S.; Afroze, S.; Bakar, M.S.A.; Islam, S.N.; Azad, A.K. COVID-19 Prevention: Role of Activated Carbon. *J. Eng. Technol. Sci.* **2021**, *53*, 210404. [[CrossRef](#)]
52. Zhang, Q.; Du, Q.; Jiao, T.; Zhang, Z.; Wang, S.; Sun, Q.; Gao, F. Rationally Designed Porous Polystyrene Encapsulated Zirconium Phosphate Nanocomposite for Highly Efficient Fluoride Uptake in Waters. *Sci. Rep.* **2013**, *3*, 2551. [[CrossRef](#)]
53. Bu, Q.; Lei, H.; Wang, L.; Wei, Y.; Zhu, L.; Liu, Y.; Liang, J.; Tang, J. Renewable Phenols Production by Catalytic Microwave Pyrolysis of Douglas Fir Sawdust Pellets with Activated Carbon Catalysts. *Bioresour. Technol.* **2013**, *142*, 546–552. [[CrossRef](#)]
54. Ahmed, M.J.; Theydan, S.K. Adsorption of Cephalexin onto Activated Carbons from Albizia Lebbeck Seed Pods by Microwave-Induced KOH and K₂CO₃ Activations. *Chem. Eng. J.* **2012**, *211–212*, 200–207. [[CrossRef](#)]
55. Chayid, M.A.; Ahmed, M.J. Amoxicillin Adsorption on Microwave Prepared Activated Carbon from Arundo Donax Linn: Isotherms, Kinetics, and Thermodynamics Studies. *J. Environ. Chem. Eng.* **2015**, *3*, 1592–1601. [[CrossRef](#)]
56. Li, J.; Dai, J.; Liu, G.; Zhang, H.; Gao, Z.; Fu, J.; He, Y.; Huang, Y. Biochar from Microwave Pyrolysis of Biomass: A Review. *Biomass Bioenergy* **2016**, *94*, 228–244. [[CrossRef](#)]
57. Gayathiri, M.; Pulingam, T.; Lee, K.T.; Sudesh, K. Activated Carbon from Biomass Waste Precursors: Factors Affecting Production and Adsorption Mechanism. *Chemosphere* **2022**, *294*, 133764. [[CrossRef](#)] [[PubMed](#)]
58. Reza, M.S.; Afroze, S.; Azad, A.K.; Sukri, R.S.; Shams, S.; Taweekun, J.; Saghir, M.; Phusunti, N.; Bakar, M.S.A. Thermochemical Characterization of Invasive Axonopus Compressus Grass as a Renewable Energy Source. In Proceedings of the 5th International Conference of Chemical Engineering and Industrial Biotechnology (ICCEIB 2020), Kuala Lumpur, Malaysia, 9–11 August 2020; pp. 1–6.
59. Reza, M.S.; Islam, S.N.; Afroze, S.; Abu Bakar, M.S.; Sukri, R.S.; Rahman, S.; Azad, A.K.; Bakar, M.S.A.; Sukri, R.S.; Rahman, S.; et al. Evaluation of the Bioenergy Potential of Invasive Pennisetum Purpureum through Pyrolysis and Thermogravimetric Analysis. *Energy Ecol. Environ.* **2020**, *5*, 118–133. [[CrossRef](#)]

60. Reza, M.S.; Afroze, S.; Bakar, M.S.A.; Saidur, R.; Aslfattahi, N.; Taweekun, J.; Azad, A.K. Biochar Characterization of Invasive Pennisetum Purpureum Grass: Effect of Pyrolysis Temperature. *Biochar* **2020**, *2*, 239–251. [[CrossRef](#)]
61. Reza, M.S.; Afroze, S.; Kuterbekov, K.; Kabyshev, A.; Bekmyrza, K.Z.; Taweekun, J.; Ja'afar, F.; Bakar, M.S.A.; Azad, A.K.; Roy, H.; et al. Ex Situ Catalytic Pyrolysis of Invasive Pennisetum Purpureum Grass with Activated Carbon for Upgrading Bio-Oil. *Sustainability* **2023**, *15*, 7628. [[CrossRef](#)]
62. Nguyen, M.-V.; Lee, B.-K. A Novel Removal of CO₂ Using Nitrogen Doped Biochar Beads as a Green Adsorbent. *Process Saf. Environ. Prot.* **2016**, *104*, 490–498. [[CrossRef](#)]
63. Rodríguez-Reinoso, F.; Silvestre-Albero, J. *Nanoporous Materials for Gas Storage*; Springer: Singapore, 2019; ISBN 9789811335037.
64. Wang, C.; Chen, P.; Li, Z. Progress in Preparation and Application of Organic Waste Based Activated Carbon. *IOP Conf. Ser. Mater. Sci. Eng.* **2018**, *392*, 042004. [[CrossRef](#)]
65. Jin, H.; Capareda, S.; Chang, Z.; Gao, J.; Xu, Y.; Zhang, J. Biochar Pyrolytically Produced from Municipal Solid Wastes for Aqueous As(V) Removal: Adsorption Property and Its Improvement with KOH Activation. *Bioresour. Technol.* **2014**, *169*, 622–629. [[CrossRef](#)] [[PubMed](#)]
66. Burhenne, L.; Aicher, T. Benzene Removal over a Fixed Bed of Wood Char: The Effect of Pyrolysis Temperature and Activation with CO₂ on the Char Reactivity. *Fuel Process. Technol.* **2014**, *127*, 140–148. [[CrossRef](#)]
67. Heidarnejad, Z.; Dehghani, M.H.; Heidari, M.; Javedan, G.; Ali, I.; Sillanpää, M. Methods for Preparation and Activation of Activated Carbon: A Review. *Environ. Chem. Lett.* **2020**, *18*, 393–415. [[CrossRef](#)]
68. Dobeles, G.; Dizhbite, T.; Gil, M.V.; Volperts, A.; Centeno, T.A. Production of Nanoporous Carbons from Wood Processing Wastes and Their Use in Supercapacitors and CO₂ Capture. *Biomass Bioenergy* **2012**, *46*, 145–154. [[CrossRef](#)]
69. Ahmed, M.J. Preparation of Activated Carbons from Date (*Phoenix dactylifera* L.) Palm Stones and Application for Wastewater Treatments: Review. *Process Saf. Environ. Prot.* **2016**, *102*, 168–182. [[CrossRef](#)]
70. Chowdhury, Z.Z.; Hamid, S.B.A.; Das, R.; Hasan, M.R.; Zain, S.M.; Khalid, K.; Uddin, M.N. Preparation of Carbonaceous Adsorbents from Lignocellulosic Biomass and Their Use in Removal of Contaminants from Aqueous Solution. *BioResources* **2013**, *8*, 6523–6555. [[CrossRef](#)]
71. Ahmed, M.J. Application of Agricultural Based Activated Carbons by Microwave and Conventional Activations for Basic Dye Adsorption: Review. *J. Environ. Chem. Eng.* **2016**, *4*, 89–99. [[CrossRef](#)]
72. Wang, Y.; Xiao, Q.; Liu, J.; Yan, H.; Wei, Y. Pilot-Scale Study of Sludge Pretreatment by Microwave and Sludge Reduction Based on Lysis-cryptic Growth. *Bioresour. Technol.* **2015**, *190*, 140–147. [[CrossRef](#)] [[PubMed](#)]
73. Nair, V.; Vinu, R. Peroxide-Assisted Microwave Activation of Pyrolysis Char for Adsorption of Dyes from Wastewater. *Bioresour. Technol.* **2016**, *216*, 511–519. [[CrossRef](#)] [[PubMed](#)]
74. Izhar, T.; Nayak, J.; Mumtaz, N. Comparative Study between Pre-Engineered RCC Structure and Usual RCC Structure. *Int. J. Sci. Res. Dev.* **2017**, *5*, 1714–1717.
75. Ao, W.; Fu, J.; Mao, X.; Kang, Q.; Ran, C.; Liu, Y.; Zhang, H.; Gao, Z.; Li, J.; Liu, G.; et al. Microwave Assisted Preparation of Activated Carbon from Biomass: A Review. *Renew. Sustain. Energy Rev.* **2018**, *92*, 958–979. [[CrossRef](#)]
76. Abraham, J.; Thomas, S.; Kalarikkal, N. *Handbook of Carbon Nanotubes*; Springer International Publishing: Cham, Switzerland, 2020; ISBN 978-3-030-91346-5.
77. Sawant, S.V.; Patwardhan, A.W.; Joshi, J.B.; Dasgupta, K. Boron Doped Carbon Nanotubes: Synthesis, Characterization and Emerging Applications—A Review. *Chem. Eng. J.* **2022**, *427*, 131616. [[CrossRef](#)]
78. Zhang, J.; Tahmasebi, A.; Omoriyekomwan, J.E.; Yu, J. Production of Carbon Nanotubes on Bio-Char at Low Temperature via Microwave-Assisted CVD Using Ni Catalyst. *Diam. Relat. Mater.* **2019**, *91*, 98–106. [[CrossRef](#)]
79. Yang, Z.; Tian, J.; Yin, Z.; Cui, C.; Qian, W.; Wei, F. Carbon Nanotube- and Graphene-Based Nanomaterials and Applications in High-Voltage Supercapacitor: A Review. *Carbon* **2019**, *141*, 467–480. [[CrossRef](#)]
80. Singh, N.P.; Gupta, V.K.; Singh, A.P. Graphene and Carbon Nanotube Reinforced Epoxy Nanocomposites: A Review. *Polymer* **2019**, *180*, 121724. [[CrossRef](#)]
81. Kumanek, B.; Janas, D. Thermal Conductivity of Carbon Nanotube Networks: A Review. *J. Mater. Sci.* **2019**, *54*, 7397–7427. [[CrossRef](#)]
82. Janas, D. From Bio to Nano: A Review of Sustainable Methods of Synthesis of Carbon Nanotubes. *Sustainability* **2020**, *12*, 4115. [[CrossRef](#)]
83. Szabó, A.; Perri, C.; Csató, A.; Giordano, G.; Vuono, D.; Nagy, J.B. Synthesis Methods of Carbon Nanotubes and Related Materials. *Materials* **2010**, *3*, 3092–3140. [[CrossRef](#)]
84. Mahto, R.K.; Kumar, S.; Mahto, R.K.; Kumar, S. Synthesis and Characterization of Low Dimensional Structure of Carbon Nanotubes. *Int. J. Sci. Res. Arch.* **2022**, *7*, 571–582. [[CrossRef](#)]
85. Ren, Z.; Lan, Y.; Wang, Y. *Aligned Carbon Nanotubes: Physics, Concepts, Fabrication and Devices*; Springer: Berlin, Germany, 2013; Volume 5. [[CrossRef](#)]
86. Rafique, M.M.A.; Iqbal, J. Production of Carbon Nanotubes by Different Routes-A Review. *J. Encapsulation Adsorpt. Sci.* **2011**, *1*, 29–34. [[CrossRef](#)]
87. Zhang, Y.; Heo, Y.J.; Son, Y.R.; In, I.; An, K.H.; Kim, B.J.; Park, S.J. Recent Advanced Thermal Interfacial Materials: A Review of Conducting Mechanisms and Parameters of Carbon Materials. *Carbon* **2019**, *142*, 445–460. [[CrossRef](#)]

88. Torres, T. Carbon Nanotubes and Related Structures. Synthesis, Characterization, Functionalization, and Applications. Edited by Dirk M. Guldi and Nazario Martín. *Angew. Chem. Int. Ed.* **2011**, *50*, 1473–1474. [[CrossRef](#)]
89. Mirabootalebi, S.O.; Akbari, G.H. Methods for Synthesis of Carbon Nanotubes-Review. *Int. J. Bio-Inorg. Hybr. Nanomater.* **2017**, *6*, 49–57.
90. Choudhury, S.; Paul, S.; Goswami, S.; Deb, K. Methods for Nanoparticle Synthesis and Drug Delivery. In *Advances in Nanotechnology-Based Drug Delivery Systems*; Elsevier: Amsterdam, The Netherlands, 2022; pp. 21–44; ISBN 9780323884501.
91. Abdullayeva, S.H. Characterization of High Quality Carbon Nanotubes Synthesized via Aerosol-CVD. *J. Adv. Phys.* **2015**, *11*, 3229–3240. [[CrossRef](#)]
92. Manawi, Y.M.; Ihsanullah; Samara, A.; Al-Ansari, T.; Atieh, M.A. A Review of Carbon Nanomaterials' Synthesis via the Chemical Vapor Deposition (CVD) Method. *Materials* **2018**, *11*, 822. [[CrossRef](#)]
93. Luo, Y.; Wang, X.; He, M.; Li, X.; Chen, H. Synthesis of High-Quality Carbon Nanotube Arrays without the Assistance of Water. *J. Nanomater.* **2012**, *2012*, 542582. [[CrossRef](#)]
94. Chen, W.; Zhao, J.; Zhang, J.; Gu, L.; Yang, Z.; Li, X.; Yu, H.; Zhu, X.; Yang, R.; Shi, D.; et al. Oxygen-Assisted Chemical Vapor Deposition Growth of Large Single-Crystal and High-Quality Monolayer MoS₂. *J. Am. Chem. Soc.* **2015**, *137*, 15632–15635. [[CrossRef](#)]
95. Dubey, R.; Dutta, D.; Sarkar, A.; Chattopadhyay, P. Functionalized Carbon Nanotubes: Synthesis, Properties and Applications in Water Purification, Drug Delivery, and Material and Biomedical Sciences. *Nanoscale Adv.* **2021**, *3*, 5722–5744. [[CrossRef](#)]
96. Manafi, S.; Rahimpour, M.R.; Mobasherpour, I.; Soltanmoradi, A. The Synthesis of Peculiar Structure of Springlike Multiwall Carbon Nanofibers/nanotubes via Mechanochemical Method. *J. Nanomater.* **2012**, *2012*, 803546. [[CrossRef](#)]
97. Kudiyarov, V.N.; Elman, R.R.; Kurdyumov, N.E. The Effect of High-Energy Ball Milling Conditions on Microstructure and Hydrogen Desorption Properties of Magnesium Hydride and Single-Walled Carbon Nanotubes. *Metals* **2021**, *11*, 1409. [[CrossRef](#)]
98. Herrera-Ramirez, J.M.; Perez-Bustamante, R.; Aguilar-Elguezabal, A. An Overview of the Synthesis, Characterization, and Applications of Carbon Nanotubes. In *Carbon-Based Nanofillers and Their Rubber Nanocomposites: Carbon Nano-Objects*; Elsevier: Amsterdam, The Netherlands, 2019; pp. 47–75. [[CrossRef](#)]
99. Dutta, S.D.; Lim, K.T.; Patel, D.K. Carbon Nanotube-Based Nanohybrids for Agricultural and Biological Applications. In *Multifunctional Hybrid Nanomaterials for Sustainable Agri-Food and Ecosystems*; Elsevier: Amsterdam, The Netherlands, 2020; pp. 505–535; ISBN 9780128213544.
100. Zhao, G.; Liu, H.Y.; Du, X.; Zhou, H.; Pan, Z.; Mai, Y.W.; Jia, Y.Y.; Yan, W. Flame Synthesis of Carbon Nanotubes on Glass Fibre Fabrics and Their Enhancement in Electrical and Thermal Properties of Glass Fibre/epoxy Composites. *Compos. Part B Eng.* **2020**, *198*, 108249. [[CrossRef](#)]
101. Wu, H.; Li, Z.; Ji, D.; Liu, Y.; Li, L.; Yuan, D.; Zhang, Z.; Ren, J.; Lefler, M.; Wang, B.; et al. One-Pot Synthesis of Nanostructured Carbon Materials from Carbon Dioxide via Electrolysis in Molten Carbonate Salts. *Carbon* **2016**, *106*, 208–217. [[CrossRef](#)]
102. Arora, N.; Sharma, N.N. Arc Discharge Synthesis of Carbon Nanotubes: Comprehensive Review. *Diam. Relat. Mater.* **2014**, *50*, 135–150. [[CrossRef](#)]
103. Bhagabati, P.; Rahaman, M.; Bhandari, S.; Roy, I.; Dey, A.; Gupta, P.; Ansari, M.A.; Dutta, A.; Chattopadhyay, D. Synthesis/Preparation of Carbon Materials. In *Carbon-Containing Polymer Composites*; Springer: Singapore, 2019; pp. 1–64.
104. Bhuyan, M.S.A.; Uddin, M.N.; Islam, M.M.; Bipasha, F.A.; Hossain, S.S. Synthesis of Graphene. *Int. Nano Lett.* **2016**, *6*, 65–83. [[CrossRef](#)]
105. Jariwala, D.; Srivastava, A.; Ajayan, P.M. Graphene Synthesis and Band Gap Opening. *J. Nanosci. Nanotechnol.* **2011**, *11*, 6621–6641. [[CrossRef](#)]
106. Rao, C.N.R.; Sood, A.K. (Eds.) *Graphene: Synthesis, Properties, and Phenomena*; Wiley-VCH Verlag GmbH & Co. KGaA: Weinheim, Germany, 2012; ISBN 9783527651122.
107. Lim, J.Y.; Mubarak, N.M.; Abdullah, E.C.; Nizamuddin, S.; Khalid, M. Inamuddin Recent Trends in the Synthesis of Graphene and Graphene Oxide Based Nanomaterials for Removal of Heavy Metals—A Review. *J. Ind. Eng. Chem.* **2018**, *66*, 29–44. [[CrossRef](#)]
108. Santhiran, A.; Iyngaran, P.; Abiman, P.; Kuganathan, N.; Bellucci, S. Graphene Synthesis and Its Recent Advances in Applications—A Review. *C* **2021**, *7*, 76. [[CrossRef](#)]
109. Park, S.; An, J.; Potts, J.R.; Velamakanni, A.; Murali, S.; Ruoff, R.S. Hydrazine-Reduction of Graphite- and Graphene Oxide. *Carbon* **2011**, *49*, 3019–3023. [[CrossRef](#)]
110. Gnanaseelan, M.; Samanta, S.; Pionteck, J.; Jehnichen, D.; Simon, F.; Pötschke, P.; Voit, B. Vanadium Salt Assisted Solvothermal Reduction of Graphene Oxide and the Thermoelectric Characterisation of the Reduced Graphene Oxide in Bulk and as Composite. *Mater. Chem. Phys.* **2019**, *229*, 319–329. [[CrossRef](#)]
111. Lavin-Lopez, M.D.P.; Romero, A.; Garrido, J.; Sanchez-Silva, L.; Valverde, J.L. Influence of Different Improved Hummers Method Modifications on the Characteristics of Graphite Oxide in Order to Make a More Easily Scalable Method. *Ind. Eng. Chem. Res.* **2016**, *55*, 12836–12847. [[CrossRef](#)]
112. Mbayachi, V.B.; Ndayiragije, E.; Sammani, T.; Taj, S.; Mbuta, E.R.; ullah Khan, A. Graphene Synthesis, Characterization and Its Applications: A Review. *Results Chem.* **2021**, *3*, 100163. [[CrossRef](#)]
113. Ikram, R.; Jan, B.M.; Ahmad, W. Advances in Synthesis of Graphene Derivatives Using Industrial Wastes Precursors; Prospects and Challenges. *J. Mater. Res. Technol.* **2020**, *9*, 15924–15951. [[CrossRef](#)]

114. Prekodravac, J.R.; Kepić, D.P.; Colmenares, J.C.; Giannakoudakis, D.A.; Jovanović, S.P. A Comprehensive Review on Selected Graphene Synthesis Methods: From Electrochemical Exfoliation through Rapid Thermal Annealing towards Biomass Pyrolysis. *J. Mater. Chem. C* **2021**, *9*, 6722–6748. [CrossRef]
115. Tetlow, H.; Posthuma de Boer, J.; Ford, I.J.; Vvedensky, D.D.; Coraux, J.; Kantorovich, L. Growth of Epitaxial Graphene: Theory and Experiment. *Phys. Rep.* **2014**, *542*, 195–295. [CrossRef]
116. Chen, X.; Zhang, L.; Chen, S. Large Area CVD Growth of Graphene. *Synth. Met.* **2015**, *210*, 95–108. [CrossRef]
117. Liu, Z.; Lin, L.; Ren, H.; Sun, X. CVD Synthesis of Graphene. In *Thermal Transport in Carbon-Based Nanomaterials*; Elsevier Inc.: Amsterdam, The Netherlands, 2017; pp. 19–56. ISBN 9780323473460.
118. Chaste, J.; Saadani, A.; Jaffre, A.; Madouri, A.; Alvarez, J.; Pierucci, D.; Ben Aziza, Z.; Ouerghi, A. Nanostructures in Suspended Mono- and Bilayer Epitaxial Graphene. *Carbon* **2017**, *125*, 162–167. [CrossRef]
119. Fogarassy, Z.; Rummeli, M.H.; Gorantla, S.; Bachmatiuk, A.; Dobrik, G.; Kamarás, K.; Biró, L.P.; Havancsák, K.; Lábár, J.L. Dominantly Epitaxial Growth of Graphene on Ni (1 1 1) Substrate. *Appl. Surf. Sci.* **2014**, *314*, 490–499. [CrossRef]
120. Wang, Q.; Wang, X.; Chai, Z.; Hu, W. Low-Temperature Plasma Synthesis of Carbon Nanotubes and Graphene Based Materials and Their Fuel Cell Applications. *Chem. Soc. Rev.* **2013**, *42*, 8821–8834. [CrossRef] [PubMed]
121. Wu, A.; Li, X.; Yang, J.; Du, C.; Shen, W.; Yan, J. Upcycling Waste Lard Oil into Vertical Graphene Sheets by Inductively Coupled Plasma Assisted Chemical Vapor Deposition. *Nanomaterials* **2017**, *7*, 318. [CrossRef] [PubMed]
122. Rashid, R.; Shafiq, I.; Akhter, P.; Iqbal, M.J.; Hussain, M. A State-of-the-Art Review on Wastewater Treatment Techniques: The Effectiveness of Adsorption Method. *Environ. Sci. Pollut. Res.* **2021**, *28*, 9050–9066. [CrossRef] [PubMed]
123. Panhwar, A.; Abro, R.; Kandhro, A.; Khaskheli, A.R.; Jalbani, N.; Gishkori, K.A.; Mahar, A.M.; Qaisar, S.; Panhwar, A.; Abro, R.; et al. Global Water Mapping, Requirements, and Concerns over Water Quality Shortages. In *Water Quality—New Perspectives [Working Title]*; IntechOpen: Rijeka, Croatia, 2022; ISBN 978-1-83969-010-5.
124. Bottero, M.; Abastante, F.; Wambui Mumbi, A.; Watanabe, T. Cost Estimations of Water Pollution for the Adoption of Suitable Water Treatment Technology. *Sustainability* **2022**, *14*, 649. [CrossRef]
125. Drinking-Water. Available online: <https://www.who.int/news-room/fact-sheets/detail/drinking-water> (accessed on 28 April 2023).
126. Pyrzynska, K. Removal of Cadmium from Wastewaters with Low-Cost Adsorbents. *J. Environ. Chem. Eng.* **2019**, *7*, 102795. [CrossRef]
127. Alcamo, J.; Henrichs, T.; Rösch, T. *World Water in 2025: Global Modeling and Scenario Analysis for the World Commission on Water for the 21st Century*; Center for Environmental Systems Research University of Kassel: Kassel, Germany, 2017.
128. Thamilselvi, V.; Radha, K.V. Silver Nanoparticle Loaded Corncob Adsorbent for Effluent Treatment. *J. Environ. Chem. Eng.* **2017**, *5*, 1843–1854. [CrossRef]
129. Rajapaksha, A.U.; Vithanage, M.; Lee, S.S.; Seo, D.-C.; Tsang, D.C.W.; Ok, Y.S. Steam Activation of Biochars Facilitates Kinetics and pH-Resilience of Sulfamethazine Sorption. *J. Soils Sediments* **2016**, *16*, 889–895. [CrossRef]
130. Zhou, Y.; Lu, J.; Zhou, Y.; Liu, Y. Recent Advances for Dyes Removal Using Novel Adsorbents: A Review. *Environ. Pollut.* **2019**, *252*, 352–365. [CrossRef]
131. Maneerung, T.; Liew, J.; Dai, Y.; Kawi, S.; Chong, C.; Wang, C.H. Activated Carbon Derived from Carbon Residue from Biomass Gasification and Its Application for Dye Adsorption: Kinetics, Isotherms and Thermodynamic Studies. *Bioresour. Technol.* **2016**, *200*, 350–359. [CrossRef] [PubMed]
132. Jung, C.; Boateng, L.K.; Flora, J.R.V.; Oh, J.; Braswell, M.C.; Son, A.; Yoon, Y. Competitive Adsorption of Selected Non-Steroidal Anti-Inflammatory Drugs on Activated Biochars: Experimental and Molecular Modeling Study. *Chem. Eng. J.* **2015**, *264*, 1–9. [CrossRef]
133. Ang, T.N.; Young, B.R.; Burrell, R.; Taylor, M.; Aroua, M.K.; Baroutian, S. Oxidative Hydrothermal Surface Modification of Activated Carbon for Sevoflurane Removal. *Chemosphere* **2021**, *264*, 128535. [CrossRef] [PubMed]
134. Kristiana, I.; Joll, C.; Heitz, A. Powdered Activated Carbon Coupled with Enhanced Coagulation for Natural Organic Matter Removal and Disinfection by-Product Control: Application in a Western Australian Water Treatment Plant. *Chemosphere* **2011**, *83*, 661–667. [CrossRef] [PubMed]
135. Jamil, S.; Loganathan, P.; Listowski, A.; Kandasamy, J.; Khourshed, C.; Vigneswaran, S. Simultaneous Removal of Natural Organic Matter and Micro-Organic Pollutants from Reverse Osmosis Concentrate Using Granular Activated Carbon. *Water Res.* **2019**, *155*, 106–114. [CrossRef] [PubMed]
136. Ho, S. Low-Cost Adsorbents for the Removal of Phenol/Phenolics, Pesticides, and Dyes from Wastewater Systems: A Review. *Water* **2022**, *14*, 3203. [CrossRef]
137. Phonlam, T.; Weerasuk, B.; Sataman, P.; Duangmanee, T.; Thongphanit, S.; Nilgumhang, K.; Anantachaisilp, S.; Chutimasakul, T.; Kwamman, T.; Chobpattana, V. Ammonia Modification of Activated Carbon Derived from Biomass via Gamma Irradiation vs. Hydrothermal Method for Methylene Blue Removal. *S. Afr. J. Chem. Eng.* **2023**, *43*, 67–78. [CrossRef]
138. Li, J.; Lv, F.; Yang, R.; Zhang, L.; Tao, W.; Liu, G.; Gao, H.; Guan, Y. N-Doped Biochar from Lignocellulosic Biomass for Preparation of Adsorbent: Characterization, Kinetics and Application. *Polymers* **2022**, *14*, 3889. [CrossRef] [PubMed]
139. Iwar, R.T.; Ogedengbe, K.; Katibi, K.K.; Oshido, L.E. Meso-Microporous Activated Carbon Derived from Raffia Palm Shells: Optimization of Synthesis Conditions Using Response Surface Methodology. *Heliyon* **2021**, *7*, e07301. [CrossRef]

140. Rattanapan, S.; Srikram, J.; Kongsune, P. Adsorption of Methyl Orange on Coffee Grounds Activated Carbon. *Energy Procedia* **2017**, *138*, 949–954. [[CrossRef](#)]
141. Nuithitikul, K.; Srikhun, S.; Hirunpraditkoon, S. Kinetics and Equilibrium Adsorption of Basic Green 4 Dye on Activated Carbon Derived from Durian Peel: Effects of Pyrolysis and Post-Treatment Conditions. *J. Taiwan Inst. Chem. Eng.* **2010**, *41*, 591–598. [[CrossRef](#)]
142. Senthilkumaar, S.; Kalaamani, P.; Porkodi, K.; Varadarajan, P.R.; Subburaam, C.V. Adsorption of Dissolved Reactive Red Dye from Aqueous Phase onto Activated Carbon Prepared from Agricultural Waste. *Bioresour. Technol.* **2006**, *97*, 1618–1625. [[CrossRef](#)]
143. Hameed, B.H.; El-Khaiary, M.I. Equilibrium, Kinetics and Mechanism of Malachite Green Adsorption on Activated Carbon Prepared from Bamboo by K_2CO_3 Activation and Subsequent Gasification with CO_2 . *J. Hazard. Mater.* **2008**, *157*, 344–351. [[CrossRef](#)] [[PubMed](#)]
144. Ahmad, A.L.; Loh, M.M.; Aziz, J.A. Preparation and Characterization of Activated Carbon from Oil Palm Wood and Its Evaluation on Methylene Blue Adsorption. *Dye Pigment* **2007**, *75*, 263–272. [[CrossRef](#)]
145. Vargas, A.M.M.; Cazetta, A.L.; Martins, A.C.; Moraes, J.C.G.; Garcia, E.E.; Gauze, G.F.; Costa, W.F.; Almeida, V.C. Kinetic and Equilibrium Studies: Adsorption of Food Dyes Acid Yellow 6, Acid Yellow 23, and Acid Red 18 on Activated Carbon from Flamboyant Pods. *Chem. Eng. J.* **2012**, *181–182*, 243–250. [[CrossRef](#)]
146. de Luna, M.D.G.; Flores, E.D.; Genuino, D.A.D.; Futralan, C.M.; Wan, M.W. Adsorption of Eriochrome Black T (EBT) Dye Using Activated Carbon Prepared from Waste Rice Hulls-Optimization, Isotherm and Kinetic Studies. *J. Taiwan Inst. Chem. Eng.* **2013**, *44*, 646–653. [[CrossRef](#)]
147. Thinakaran, N.; Pannerseelvam, P.; Baskaralingam, P.; Elango, D.; Sivanesan, S. Equilibrium and Kinetic Studies on the Removal of Acid Red 114 from Aqueous Solutions Using Activated Carbons Prepared from Seed Shells. *J. Hazard. Mater.* **2008**, *158*, 142–150. [[CrossRef](#)]
148. Uma; Banerjee, S.; Sharma, Y.C. Equilibrium and Kinetic Studies for Removal of Malachite Green from Aqueous Solution by a Low Cost Activated Carbon. *J. Ind. Eng. Chem.* **2013**, *19*, 1099–1105. [[CrossRef](#)]
149. Ahmed, M.J.; Dhedan, S.K. Equilibrium Isotherms and Kinetics Modeling of Methylene Blue Adsorption on Agricultural Wastes-Based Activated Carbons. *Fluid Phase Equilib.* **2012**, *317*, 9–14. [[CrossRef](#)]
150. Kaouah, F.; Boumaza, S.; Berrama, T.; Trari, M.; Bendjama, Z. Preparation and Characterization of Activated Carbon from Wild Olive Cores (Oleaster) by H_3PO_4 for the Removal of Basic Red 46. *J. Clean. Prod.* **2013**, *54*, 296–306. [[CrossRef](#)]
151. Mahamad, M.N.; Zaini, M.A.A.; Zakaria, Z.A. Preparation and Characterization of Activated Carbon from Pineapple Waste Biomass for Dye Removal. *Int. Biodeterior. Biodegrad.* **2015**, *102*, 274–280. [[CrossRef](#)]
152. Kumar, M.; Tamilarasan, R. Modeling Studies for the Removal of Methylene Blue from Aqueous Solution Using Acacia Fumosa Seed Shell Activated Carbon. *J. Environ. Chem. Eng.* **2013**, *1*, 1108–1116. [[CrossRef](#)]
153. Akar, E.; Altinişik, A.; Seki, Y. Using of Activated Carbon Produced from Spent Tea Leaves for the Removal of Malachite Green from Aqueous Solution. *Ecol. Eng.* **2013**, *52*, 19–27. [[CrossRef](#)]
154. Angin, D. Utilization of Activated Carbon Produced from Fruit Juice Industry Solid Waste for the Adsorption of Yellow 18 from Aqueous Solutions. *Bioresour. Technol.* **2014**, *168*, 259–266. [[CrossRef](#)] [[PubMed](#)]
155. Li, J.; Ng, D.H.L.; Song, P.; Kong, C.; Song, Y. Synthesis of SnO_2 -Activated Carbon Fiber Hybrid Catalyst for the Removal of Methyl Violet from Water. *Mater. Sci. Eng. B Solid-State Mater. Adv. Technol.* **2015**, *194*, 1–8. [[CrossRef](#)]
156. Nethaji, S.; Sivasamy, A. Adsorptive Removal of an Acid Dye by Lignocellulosic Waste Biomass Activated Carbon: Equilibrium and Kinetic Studies. *Chemosphere* **2011**, *82*, 1367–1372. [[CrossRef](#)]
157. Hajati, S.; Ghaedi, M.; Yaghoubi, S. Local, Cheep and Nontoxic Activated Carbon as Efficient Adsorbent for the Simultaneous Removal of Cadmium Ions and Malachite Green: Optimization by Surface Response Methodology. *J. Ind. Eng. Chem.* **2015**, *21*, 760–767. [[CrossRef](#)]
158. Altenor, S.; Carene, B.; Emmanuel, E.; Lambert, J.; Ehrhardt, J.-J.; Gaspard, S. Adsorption Studies of Methylene Blue and Phenol onto Vetiver Roots Activated Carbon Prepared by Chemical Activation. *J. Hazard. Mater.* **2009**, *165*, 1029–1039. [[CrossRef](#)]
159. Santhi, T.; Manonmani, S.; Smitha, T. Removal of Malachite Green from Aqueous Solution by Activated Carbon Prepared from the Epicarp of Ricinus Communis by Adsorption. *J. Hazard. Mater.* **2010**, *179*, 178–186. [[CrossRef](#)]
160. Garg, R.; Garg, R.; Sillanpää, M.; Khan, M.A.; Mubarak, N.M.; Tan, Y.H. Rapid Adsorptive Removal of Chromium from Wastewater Using Walnut—Derived Biosorbents. *Sci. Rep.* **2023**, *13*, 6859. [[CrossRef](#)]
161. Bumajdad, A.; Hasila, P. Surface Modification of Date Palm Activated Carbonaceous Materials for Heavy Metal Removal and CO_2 Adsorption. *Arab. J. Chem.* **2023**, *16*, 104403. [[CrossRef](#)]
162. Jimenez-Paz, J.; Lozada-Castro, J.J.; Lester, E.; Williams, O.; Stevens, L.; Barraza-Burgos, J. Solutions to Hazardous Wastes Issues in the Leather Industry: Adsorption of Chromium Iii and vi from Leather Industry Wastewaters Using Activated Carbons Produced from Leather Industry Solid Wastes. *J. Environ. Chem. Eng.* **2023**, *11*, 109715. [[CrossRef](#)]
163. Hassan, A.F.; Abdel-Mohsen, A.M.; Elhadidy, H. Adsorption of Arsenic by Activated Carbon, Calcium Alginate and Their Composite Beads. *Int. J. Biol. Macromol.* **2014**, *68*, 125–130. [[CrossRef](#)] [[PubMed](#)]
164. St. Vassileva, P.; Detcheva, A. Adsorption of Some Transition Metal Ions [Cu(II), Fe(III), Cr(III) and Au(III)] onto Lignite-Based Activated Carbons Modified by Oxidation. *Adsorpt. Sci. Technol.* **2010**, *28*, 229–242. [[CrossRef](#)]
165. Imamoglu, M.; Tekir, O. Removal of Copper (II) and Lead (II) Ions from Aqueous Solutions by Adsorption on Activated Carbon from a New Precursor Hazelnut Husks. *Desalination* **2008**, *228*, 108–113. [[CrossRef](#)]

166. Giraldo-Gutiérrez, L.; Moreno-Piraján, J.C. Pb(II) and Cr(VI) Adsorption from Aqueous Solution on Activated Carbons Obtained from Sugar Cane Husk and Sawdust. *J. Anal. Appl. Pyrolysis* **2008**, *81*, 278–284. [[CrossRef](#)]
167. Depci, T.; Kul, A.R.; Önal, Y. Competitive Adsorption of Lead and Zinc from Aqueous Solution on Activated Carbon Prepared from Van Apple Pulp: Study in Single- and Multi-Solute Systems. *Chem. Eng. J.* **2012**, *200–202*, 224–236. [[CrossRef](#)]
168. Huang, Y.; Li, S.; Lin, H.; Chen, J. Fabrication and Characterization of Mesoporous Activated Carbon from Lemna Minor Using One-Step H₃PO₄ Activation for Pb(II) Removal. *Appl. Surf. Sci.* **2014**, *317*, 422–431. [[CrossRef](#)]
169. Boudrahem, F.; Aissani-Benissad, F.; Aït-Amar, H. Batch Sorption Dynamics and Equilibrium for the Removal of Lead Ions from Aqueous Phase Using Activated Carbon Developed from Coffee Residue Activated with Zinc Chloride. *J. Environ. Manag.* **2009**, *90*, 3031–3039. [[CrossRef](#)]
170. Sugashini, S.; Begum, K.M.M.S. Preparation of Activated Carbon from Carbonized Rice Husk by Ozone Activation for Cr(VI) Removal. *New Carbon Mater.* **2015**, *30*, 252–261. [[CrossRef](#)]
171. Demiral, H.; Demiral, İ.; Tümsel, F.; Karabacakoglu, B. Adsorption of chromium(VI) from Aqueous Solution by Activated Carbon Derived from Olive Bagasse and Applicability of Different Adsorption Models. *Chem. Eng. J.* **2008**, *144*, 188–196. [[CrossRef](#)]
172. Yang, J.; Yu, M.; Chen, W. Adsorption of Hexavalent Chromium from Aqueous Solution by Activated Carbon Prepared from Longan Seed: Kinetics, Equilibrium and Thermodynamics. *J. Ind. Eng. Chem.* **2015**, *21*, 414–422. [[CrossRef](#)]
173. El Nemr, A.; Khaled, A.; Abdelwahab, O.; El-Sikaily, A. Treatment of Wastewater Containing Toxic Chromium Using New Activated Carbon Developed from Date Palm Seed. *J. Hazard. Mater.* **2008**, *152*, 263–275. [[CrossRef](#)] [[PubMed](#)]
174. AL-Othman, Z.A.; Ali, R.; Naushad, M. Hexavalent Chromium Removal from Aqueous Medium by Activated Carbon Prepared from Peanut Shell: Adsorption Kinetics, Equilibrium and Thermodynamic Studies. *Chem. Eng. J.* **2012**, *184*, 238–247. [[CrossRef](#)]
175. Zabihi, M.; Haghighi Asl, A.; Ahmadpour, A. Studies on Adsorption of Mercury from Aqueous Solution on Activated Carbons Prepared from Walnut Shell. *J. Hazard. Mater.* **2010**, *174*, 251–256. [[CrossRef](#)] [[PubMed](#)]
176. Mashhadi, S.; Sohrabi, R.; Javadian, H.; Ghasemi, M.; Tyagi, I.; Agarwal, S.; Gupta, V.K. Rapid Removal of Hg (II) from Aqueous Solution by Rice Straw Activated Carbon Prepared by Microwave-Assisted H₂SO₄ Activation: Kinetic, Isotherm and Thermodynamic Studies. *J. Mol. Liq.* **2016**, *215*, 144–153. [[CrossRef](#)]
177. Kadirvelu, K.; Kavipriya, M.; Karthika, C.; Vennilamani, N.; Pattabhi, S. Mercury (II) Adsorption by Activated Carbon Made from Sago Waste. *Carbon* **2004**, *42*, 745–752. [[CrossRef](#)]
178. Asasian, N.; Kaghazchi, T.; Soleimani, M. Elimination of Mercury by Adsorption onto Activated Carbon Prepared from the Biomass Material. *J. Ind. Eng. Chem.* **2012**, *18*, 283–289. [[CrossRef](#)]
179. Saman, N.; Abdul Aziz, A.; Johari, K.; Song, S.T.; Mat, H. Adsorptive Efficacy Analysis of Lignocellulosic Waste Carbonaceous Adsorbents toward Different Mercury Species. *Process Saf. Environ. Prot.* **2015**, *96*, 33–42. [[CrossRef](#)]
180. Alslaibi, T.M.; Abustan, I.; Ahmad, M.A.; Foul, A.A. Cadmium Removal from Aqueous Solution Using Microwaved Olive Stone Activated Carbon. *J. Environ. Chem. Eng.* **2013**, *1*, 589–599. [[CrossRef](#)]
181. Fouladi Tajar, A.; Kaghazchi, T.; Soleimani, M. Adsorption of Cadmium from Aqueous Solutions on Sulfurized Activated Carbon Prepared from Nut Shells. *J. Hazard. Mater.* **2009**, *165*, 1159–1164. [[CrossRef](#)] [[PubMed](#)]
182. Obregón-Valencia, D.; del Rosario Sun-Kou, M. Comparative Cadmium Adsorption Study on Activated Carbon Prepared from Aguaje (*Mauritia flexuosa*) and Olive Fruit Stones (*Olea europaea* L.). *J. Environ. Chem. Eng.* **2014**, *2*, 2280–2288. [[CrossRef](#)]
183. Singh, A.; Sharma, A.; Verma, R.K.; Chopade, R.L.; Pandit, P.P.; Nagar, V.; Aseri, V.; Choudhary, S.K.; Awasthi, G.; Awasthi, K.K.; et al. Heavy Metal Contamination of Water and Their Toxic Effect on Living Organisms. In *The Toxicity of Environmental Pollutants*; IntechOpen: London, UK, 2022; ISBN 978-1-80355-580-5.
184. Kumar, A.; Kumar, A.; Cabral-Pinto, M.; Chaturvedi, A.K.; Shabnam, A.A.; Subrahmanyam, G.; Mondal, R.; Gupta, D.K.; Malyan, S.K.; Kumar, S.S.; et al. Lead Toxicity: Health Hazards, Influence on Food Chain, and Sustainable Remediation Approaches. *Int. J. Environ. Res. Public Health* **2020**, *17*, 2179. [[CrossRef](#)]
185. Hossini, H.; Shafie, B.; Niri, A.D.; Nazari, M.; Esfahlan, A.J.; Ahmadpour, M.; Nazmara, Z.; Ahmadimanesh, M.; Makhdoumi, P.; Mirzaei, N.; et al. A Comprehensive Review on Human Health Effects of Chromium: Insights on Induced Toxicity. *Environ. Sci. Pollut. Res. Int.* **2022**, *29*, 70686–70705. [[CrossRef](#)] [[PubMed](#)]
186. Salman, J.M.; Hussein, F.H. Batch Adsorber Design for Different Solution Volume/ Adsorbate Mass Ratios of Bentazon, Carbofuran and 2,4-D Adsorption on to Date Seeds Activated Carbon. *J. Environ. Anal. Chem.* **2014**, *2*, 2. [[CrossRef](#)]
187. El Bakouri, H.; Usero, J.; Morillo, J.; Rojas, R.; Ouassini, A. Drin Pesticides Removal from Aqueous Solutions Using Acid-Treated Date Stones. *Bioresour. Technol.* **2009**, *100*, 2676–2684. [[CrossRef](#)]
188. Salman, J.M.; Njoku, V.O.; Hameed, B.H. Bentazon and Carbofuran Adsorption onto Date Seed Activated Carbon: Kinetics and Equilibrium. *Chem. Eng. J.* **2011**, *173*, 361–368. [[CrossRef](#)]
189. Ioannidou, O.A.; Zabaniotou, A.A.; Stavropoulos, G.G.; Islam, M.A.; Albanis, T.A. Preparation of Activated Carbons from Agricultural Residues for Pesticide Adsorption. *Chemosphere* **2010**, *80*, 1328–1336. [[CrossRef](#)] [[PubMed](#)]
190. Ahmed, M.J.; Theydan, S.K. Equilibrium Isotherms, Kinetics and Thermodynamics Studies of Phenolic Compounds Adsorption on Palm-Tree Fruit Stones. *Ecotoxicol. Environ. Saf.* **2012**, *84*, 39–45. [[CrossRef](#)]
191. Zbair, M.; Ainassaari, K.; Drif, A.; Ojala, S.; Bottlinger, M.; Pirilä, M.; Keiski, R.L.; Bensitel, M.; Brahmi, R. Toward New Benchmark Adsorbents: Preparation and Characterization of Activated Carbon from Argan Nut Shell for Bisphenol A Removal. *Environ. Sci. Pollut. Res.* **2018**, *25*, 1869–1882. [[CrossRef](#)]

192. Min, H.S.; Abbas, M.; Kanthasamy, R.; Abdul Aziz, H.; Tay, C.C. *Activated Carbon: Prepared from Various Precursors*; Ideal International E—Publication Pvt. Ltd.: Indore, India, 2017; ISBN 9789386675071.
193. Alam, M.G.; Danish, M.; Alanazi, A.M.; Ahmad, T.; Khalil, H.P.S.A. Response Surface Methodology Approach of Phenol Removal Study Using High-Quality Activated Carbon Derived from H₃PO₄ Activation of Acacia Mangium Wood. *Diam. Relat. Mater.* **2023**, *132*, 109632. [[CrossRef](#)]
194. Dat, N.D.; Huynh, Q.S.; Tran, K.A.T.; Nguyen, M.L. Performance of Heterogeneous Fenton Catalyst from Solid Wastes for Removal of Emerging Contaminant in Water: A Potential Approach to Circular Economy. *Results Eng.* **2023**, *18*, 101086. [[CrossRef](#)]
195. Wei, X.; Huang, S.; Yang, J.; Liu, P.; Li, X.; Wu, Y.; Wu, S. Adsorption of Phenol from Aqueous Solution on Activated Carbons Prepared from Antibiotic Mycelial Residues and Traditional Biomass. *Fuel Process. Technol.* **2023**, *242*, 107663. [[CrossRef](#)]
196. González-García, P. Activated Carbon from Lignocellulosics Precursors: A Review of the Synthesis Methods, Characterization Techniques and Applications. *Renew. Sustain. Energy Rev.* **2018**, *82*, 1393–1414. [[CrossRef](#)]
197. Kecira, Z.; Benturki, A.; Daoud, M.; Benturki, O. Effect of Chemical Activation on the Surface Properties of Apricot Stones Based Activated Carbons and Its Adsorptive Properties Toward Aniline. In *Proceedings of the Third International Symposium on Materials and Sustainable Development*; Springer: New York, NY, USA, 2018; pp. 228–240.
198. Tchikuala, E.F.; Mourão, P.A.M.; Nabais, J.M.V. Removal of Phenol by Adsorption on Activated Carbon from Aqueous Solution. In *Proceedings of the WASTES 2017 International Conference: Solutions, Treatments and Opportunities*, Porto, Portugal, 25–26 September 2017; Faculty of Engineering of the University of Porto: Porto, Portugal, 2017; pp. 1–3.
199. Fan, J.; Zhang, J.; Zhang, C.; Ren, L.; Shi, Q. Adsorption of 2,4,6-Trichlorophenol from Aqueous Solution onto Activated Carbon Derived from Loosestrife. *Desalination* **2011**, *267*, 139–146. [[CrossRef](#)]
200. Kodali, J.; Talasila, S.; Arunraj, B.; Nagarathnam, R. Activated Coconut Charcoal as a Super Adsorbent for the Removal of Organophosphorous Pesticide Monocrotophos from Water. *Case Stud. Chem. Environ. Eng.* **2021**, *3*, 100099. [[CrossRef](#)]
201. Hussain, O.A.; Hathout, A.S.; Abdel-Mobdy, Y.E.; Rashed, M.M.; Abdel Rahim, E.A.; Fouzy, A.S.M. Preparation and Characterization of Activated Carbon from Agricultural Wastes and Their Ability to Remove Chlorpyrifos from Water. *Toxicol. Rep.* **2023**, *10*, 146–154. [[CrossRef](#)] [[PubMed](#)]
202. Bansal, R.C.; Aggarwal, D.; Goyal, M.; Kaistha, B.C. Influence of Carbon-Oxygen Surface Groups on the Adsorption of Phenol by Activated Carbons. *Indian J. Chem. Technol.* **2002**, *9*, 290–296.
203. Ma, R.; Xue, Y.; Ma, Q.; Chen, Y.; Yuan, S.; Fan, J. Recent Advances in Carbon-Based Materials for Adsorptive and Photocatalytic Antibiotic Removal. *Nanomaterials* **2022**, *12*, 4045. [[CrossRef](#)]
204. Ahmed, M.J. Adsorption of Non-Steroidal Anti-Inflammatory Drugs from Aqueous Solution Using Activated Carbons: Review. *J. Environ. Manag.* **2017**, *190*, 274–282. [[CrossRef](#)]
205. Boudrahem, N.; Delpoux-Ouldriane, S.; Khenniche, L.; Boudrahem, F.; Aissani-Benissad, F.; Gineys, M. Single and Mixture Adsorption of Clofibrac Acid, Tetracycline and Paracetamol onto Activated Carbon Developed from Cotton Cloth Residue. *Process Saf. Environ. Prot.* **2017**, *111*, 544–559. [[CrossRef](#)]
206. Pereira, D.; Gil, M.V.; Esteves, V.I.; Silva, N.J.O.; Otero, M.; Calisto, V. Ex-Situ Magnetic Activated Carbon for the Adsorption of Three Pharmaceuticals with Distinct Physicochemical Properties from Real Wastewater. *J. Hazard. Mater.* **2023**, *443*, 130258. [[CrossRef](#)] [[PubMed](#)]
207. Al-sareji, O.J.; Meiczinger, M.; Somogyi, V.; Al-Juboori, R.A.; Grmasha, R.A.; Stenger-Kovács, C.; Jakab, M.; Hashim, K.S. Removal of Emerging Pollutants from Water Using Enzyme-Immobilized Activated Carbon from Coconut Shell. *J. Environ. Chem. Eng.* **2023**, *11*, 109803. [[CrossRef](#)]
208. Rueda-Márquez, J.J.; Moreno-Andrés, J.; Rey, A.; Corada-Fernández, C.; Mikola, A.; Manzano, M.A.; Levchuk, I. Post-Treatment of Real Municipal Wastewater Effluents by Means of Granular Activated Carbon (GAC) Based Catalytic Processes: A Focus on Abatement of Pharmaceutically Active Compounds. *Water Res.* **2021**, *192*, 116833. [[CrossRef](#)] [[PubMed](#)]
209. Wong, S.; Ngadi, N.; Inuwa, I.M.; Hassan, O. Recent Advances in Applications of Activated Carbon from Biowaste for Wastewater Treatment: A Short Review. *J. Clean. Prod.* **2018**, *175*, 361–375. [[CrossRef](#)]
210. Mansour, F.; Al-Hindi, M.; Yahfoufi, R.; Ayoub, G.M.; Ahmad, M.N. The Use of Activated Carbon for the Removal of Pharmaceuticals from Aqueous Solutions: A Review. *Rev. Environ. Sci. Biotechnol.* **2018**, *17*, 109–145. [[CrossRef](#)]
211. Jaria, G.; Silva, C.P.; Oliveira, J.A.B.P.; Santos, S.M.; Gil, M.V.; Otero, M.; Calisto, V.; Esteves, V.I. Production of Highly Efficient Activated Carbons from Industrial Wastes for the Removal of Pharmaceuticals from Water—A Full Factorial Design. *J. Hazard. Mater.* **2019**, *370*, 212–218. [[CrossRef](#)] [[PubMed](#)]
212. Li, R.; Zhang, L.; Wang, P. Rational Design of Nanomaterials for Water Treatment. *Nanoscale* **2015**, *7*, 17167–17194. [[CrossRef](#)]
213. Yang, K.; Xing, B. Adsorption of Organic Compounds by Carbon Nanomaterials in Aqueous Phase: Polanyi Theory and Its Application. *Chem. Rev.* **2010**, *110*, 5989–6008. [[CrossRef](#)]
214. Ohnishi, M.; Shiga, T.; Shiomi, J. Effects of Defects on Thermoelectric Properties of Carbon Nanotubes. *Phys. Rev. B* **2017**, *95*, 155405. [[CrossRef](#)]
215. Zeng, Y.; Zhao, L.; Wu, W.; Lu, G.; Xu, F.; Tong, Y.; Liu, W.; Du, J. Enhanced Adsorption of Malachite Green onto Carbon Nanotube/polyaniline Composites. *J. Appl. Polym. Sci.* **2013**, *127*, 2475–2482. [[CrossRef](#)]
216. Robati, D.; Mirza, B.; Ghazisaeidi, R.; Rajabi, M.; Moradi, O.; Tyagi, I.; Agarwal, S.; Gupta, V.K. Adsorption Behavior of Methylene Blue Dye on Nanocomposite Multi-Walled Carbon Nanotube Functionalized Thiol (MWCNT-SH) as New Adsorbent. *J. Mol. Liq.* **2016**, *216*, 830–835. [[CrossRef](#)]

217. Royer, B.; Cardoso, N.F.; Lima, E.C.; Vaghetti, J.C.P.; Simon, N.M.; Calvete, T.; Veses, R.C. Applications of Brazilian Pine-Fruit Shell in Natural and Carbonized Forms as Adsorbents to Removal of Methylene Blue from Aqueous Solutions-Kinetic and Equilibrium Study. *J. Hazard. Mater.* **2009**, *164*, 1213–1222. [[CrossRef](#)]
218. Moradi, O. Adsorption Behavior of Basic Red 46 by Single-Walled Carbon Nanotubes Surfaces. *Fuller. Nanotub. Carbon Nanostruct.* **2013**, *21*, 286–301. [[CrossRef](#)]
219. Alkaim, A.F.; Sadik, Z.; Mahdi, D.K.; Alshrefi, S.M.; Al-Sammarraie, A.M.; Alamgir, F.M.; Singh, P.M.; Aljeboree, A.M. Preparation, Structure and Adsorption Properties of Synthesized Multiwall Carbon Nanotubes for Highly Effective Removal of Maxilon Blue Dye. *Korean J. Chem. Eng.* **2015**, *32*, 2456–2462. [[CrossRef](#)]
220. Gupta, V.K.; Nayak, A.; Agarwal, S. Bioadsorbents for Remediation of Heavy Metals: Current Status and Their Future Prospects. *Environ. Eng. Res.* **2015**, *20*, 1–18. [[CrossRef](#)]
221. Zhu, H.Y.; Jiang, R.; Xiao, L.; Zeng, G.M. Preparation, Characterization, Adsorption Kinetics and Thermodynamics of Novel Magnetic Chitosan Enwrapping Nanosized γ -Fe₂O₃ and Multi-Walled Carbon Nanotubes with Enhanced Adsorption Properties for Methyl Orange. *Bioresour. Technol.* **2010**, *101*, 5063–5069. [[CrossRef](#)]
222. Machado, F.M.; Bergmann, C.P.; Lima, E.C.; Adebayo, M.A.; Fagan, S.B. Adsorption of a Textile Dye from Aqueous Solutions by Carbon Nanotubes. *Mater. Res.* **2014**, *17*, 153–160. [[CrossRef](#)]
223. Bazrafshan, E.; Kord Mostafapour, F.; Rahdar, S.; Mahvi, A.H. Equilibrium and Thermodynamics Studies for Decolorization of Reactive Black 5 (RB5) by Adsorption onto MWCNTs. *Desalin. Water Treat.* **2015**, *54*, 2241–2251. [[CrossRef](#)]
224. Machado, F.M.; Bergmann, C.P.; Fernandes, T.H.M.; Lima, E.C.; Royer, B.; Calvete, T.; Fagan, S.B. Adsorption of Reactive Red M-2BE Dye from Water Solutions by Multi-Walled Carbon Nanotubes and Activated Carbon. *J. Hazard. Mater.* **2011**, *192*, 1122–1131. [[CrossRef](#)]
225. Wu, C.H. Adsorption of Reactive Dye onto Carbon Nanotubes: Equilibrium, Kinetics and Thermodynamics. *J. Hazard. Mater.* **2007**, *144*, 93–100. [[CrossRef](#)] [[PubMed](#)]
226. Prola, L.D.T.; Machado, F.M.; Bergmann, C.P.; de Souza, F.E.; Gally, C.R.; Lima, E.C.; Adebayo, M.A.; Dias, S.L.P.; Calvete, T. Adsorption of Direct Blue 53 Dye from Aqueous Solutions by Multi-Walled Carbon Nanotubes and Activated Carbon. *J. Environ. Manag.* **2013**, *130*, 166–175. [[CrossRef](#)] [[PubMed](#)]
227. Geyikçi, F. Adsorption of Acid Blue 161 (AB 161) Dye from Water by Multi-Walled Carbon Nanotubes. *Fuller. Nanotub. Carbon Nanostruct.* **2013**, *21*, 579–593. [[CrossRef](#)]
228. Exley, J.M.; Hunter, T.N.; Pugh, T.; Tillotson, M.R. Influence of Flake Size and Electrolyte Conditions on Graphene Oxide Adsorption of Ionic Dyes. *Powder Technol.* **2023**, *421*, 118387. [[CrossRef](#)]
229. Ramutshatsha-Makhwedzha, D.; Mavhungu, A.; Moropeng, M.L.; Mbaya, R. Activated Carbon Derived from Waste Orange and Lemon Peels for the Adsorption of Methyl Orange and Methylene Blue Dyes from Wastewater. *Heliyon* **2022**, *8*, e09930. [[CrossRef](#)]
230. Ahmad, N.; Suryani Arsyad, F.; Royani, I.; Lesbani, A. Charcoal Activated as Template Mg/Al Layered Double Hydroxide for Selective Adsorption of Direct Yellow on Anionic Dyes. *Results Chem.* **2023**, *5*, 100766. [[CrossRef](#)]
231. Yu, J.G.; Zhao, X.H.; Yang, H.; Chen, X.H.; Yang, Q.; Yu, L.Y.; Jiang, J.H.; Chen, X.Q. Aqueous Adsorption and Removal of Organic Contaminants by Carbon Nanotubes. *Sci. Total Environ.* **2014**, *482–483*, 241–251. [[CrossRef](#)] [[PubMed](#)]
232. Khani, H.; Moradi, O. Influence of Surface Oxidation on the Morphological and Crystallographic Structure of Multi-Walled Carbon Nanotubes via Different Oxidants. *J. Nanostruct. Chem.* **2013**, *3*, 73. [[CrossRef](#)]
233. Usman Farid, M.; Luan, H.Y.; Wang, Y.; Huang, H.; An, A.K.; Jalil Khan, R. Increased Adsorption of Aqueous Zinc Species by Ar/O₂ Plasma-Treated Carbon Nanotubes Immobilized in Hollow-Fiber Ultrafiltration Membrane. *Chem. Eng. J.* **2017**, *325*, 239–248. [[CrossRef](#)]
234. Ihsanullah; Al-Khalidi, F.A.; Abu-Sharkh, B.; Abulkibash, A.M.; Qureshi, M.I.; Laoui, T.; Atieh, M.A. Effect of Acid Modification on Adsorption of Hexavalent Chromium (Cr(VI)) from Aqueous Solution by Activated Carbon and Carbon Nanotubes. *Desalin. Water Treat.* **2016**, *57*, 7232–7244. [[CrossRef](#)]
235. Ihsanullah; Al Amer, A.M.; Laoui, T.; Abbas, A.; Al-Aqeeli, N.; Patel, F.; Khraisheh, M.; Atieh, M.A.; Hilal, N. Fabrication and Antifouling Behaviour of a Carbon Nanotube Membrane. *Mater. Des.* **2016**, *89*, 549–558. [[CrossRef](#)]
236. Pyrzynska, K. Recent Applications of Carbon Nanotubes for Separation and Enrichment of Lead Ions. *Separations* **2023**, *10*, 152. [[CrossRef](#)]
237. Šolic, M.; Maletic, S.; Isakovski, M.K.; Nikic, J.; Watson, M.; Kónya, Z.; Trickovic, J. Comparing the Adsorption Performance of Multiwalled Carbon Nanotubes Oxidized by Varying Degrees for Removal of Low Levels of Copper, Nickel and Chromium(VI) from Aqueous Solutions. *Water* **2020**, *12*, 723. [[CrossRef](#)]
238. Ihsanullah; Abbas, A.; Al-Amer, A.M.; Laoui, T.; Al-Marri, M.J.; Nasser, M.S.; Khraisheh, M.; Atieh, M.A. Heavy Metal Removal from Aqueous Solution by Advanced Carbon Nanotubes: Critical Review of Adsorption Applications. *Sep. Purif. Technol.* **2016**, *157*, 141–161. [[CrossRef](#)]
239. Ali, S.; Rehman, S.A.U.; Luan, H.Y.; Farid, M.U.; Huang, H. Challenges and Opportunities in Functional Carbon Nanotubes for Membrane-Based Water Treatment and Desalination. *Sci. Total Environ.* **2019**, *646*, 1126–1139. [[CrossRef](#)] [[PubMed](#)]
240. Li, J.; Chen, S.; Sheng, G.; Hu, J.; Tan, X.; Wang, X. Effect of Surfactants on Pb(II) Adsorption from Aqueous Solutions Using Oxidized Multiwall Carbon Nanotubes. *Chem. Eng. J.* **2011**, *166*, 551–558. [[CrossRef](#)]
241. Addo Ntim, S.; Mitra, S. Removal of Trace Arsenic to Meet Drinking Water Standards Using Iron Oxide Coated Multiwall Carbon Nanotubes. *J. Chem. Eng. Data* **2011**, *56*, 2077–2083. [[CrossRef](#)]

242. Al-Kadhi, N.S.; Pashameah, R.A.; Ahmed, H.A.; Alrefae, S.H.; Alamro, F.S.; Faqih, H.H.; Mwafy, E.A.; Mostafa, A.M. Preparation of NiO/MWCNTs Nanocomposite for the Removal of Cadmium Ions. *J. Mater. Res. Technol.* **2022**, *19*, 1961–1971. [[CrossRef](#)]
243. Dobrzyńska, J.; Mróz, A.; Olchowski, R.; Zięba, E.; Dobrowolski, R. Modified Multi-Walled Carbon Nanotubes as Effective Pt(IV) Ions Adsorbent with Respect to Analytical Application. *Appl. Surf. Sci.* **2022**, *602*, 154388. [[CrossRef](#)]
244. Moghaddam, H.K.; Pakizeh, M. Experimental Study on Mercury Ions Removal from Aqueous Solution by MnO₂/CNTs Nanocomposite Adsorbent. *J. Ind. Eng. Chem.* **2015**, *21*, 221–229. [[CrossRef](#)]
245. Ji, L.; Zhou, L.; Bai, X.; Shao, Y.; Zhao, G.; Qu, Y.; Wang, C.; Li, Y. Facile Synthesis of Multiwall Carbon Nanotubes/iron Oxides for Removal of Tetrabromobisphenol A and Pb(II). *J. Mater. Chem.* **2012**, *22*, 15853–15862. [[CrossRef](#)]
246. Sankararamkrishnan, N.; Jaiswal, M.; Verma, N. Composite Nanofloral Clusters of Carbon Nanotubes and Activated Alumina: An Efficient Sorbent for Heavy Metal Removal. *Chem. Eng. J.* **2014**, *235*, 1–9. [[CrossRef](#)]
247. Moradi, O. The Removal of Ions by Functionalized Carbon Nanotube: Equilibrium, Isotherms and Thermodynamic Studies. *Chem. Biochem. Eng. Q.* **2011**, *25*, 229–240.
248. Dichiaro, A.B.; Webber, M.R.; Gorman, W.R.; Rogers, R.E. Removal of Copper Ions from Aqueous Solutions via Adsorption on Carbon Nanocomposites. *ACS Appl. Mater. Interfaces* **2015**, *7*, 15674–15680. [[CrossRef](#)] [[PubMed](#)]
249. Lu, C.; Chiu, H.; Liu, C. Removal of zinc(II) from Aqueous Solution by Purified Carbon Nanotubes: Kinetics and Equilibrium Studies. *Ind. Eng. Chem. Res.* **2006**, *45*, 2850–2855. [[CrossRef](#)]
250. Tofighy, M.A.; Mohammadi, T. Adsorption of Divalent Heavy Metal Ions from Water Using Carbon Nanotube Sheets. *J. Hazard. Mater.* **2011**, *185*, 140–147. [[CrossRef](#)] [[PubMed](#)]
251. Pütün, A.E.; Özbay, N.; Önal, E.P.; Pütün, E. Fixed-Bed Pyrolysis of Cotton Stalk for Liquid and Solid Products. *Fuel Process. Technol.* **2005**, *86*, 1207–1219. [[CrossRef](#)]
252. Das, R.; Ali, M.E.; Hamid, S.B.A.; Ramakrishna, S.; Chowdhury, Z.Z. Carbon Nanotube Membranes for Water Purification: A Bright Future in Water Desalination. *Desalination* **2014**, *336*, 97–109. [[CrossRef](#)]
253. Li, Y.H.; Zhao, Y.M.; Hu, W.B.; Ahmad, I.; Zhu, Y.Q.; Peng, X.J.; Luan, Z.K. Carbon Nanotubes—The Promising Adsorbent in Wastewater Treatment. *J. Phys. Conf. Ser.* **2007**, *61*, 698–702. [[CrossRef](#)]
254. Mubarak, N.M.; Daniel, S.; Khalid, M.; Tan, J. Comparative Study of Functionalize and Non- Functionalized Carbon Nanotube for Removal of Copper from Polluted Water. *Int. J. Chem. Environ. Eng.* **2012**, *3*, 6–9.
255. Rao, G.P.; Lu, C.; Su, F. Sorption of Divalent Metal Ions from Aqueous Solution by Carbon Nanotubes: A Review. *Sep. Purif. Technol.* **2007**, *58*, 224–231. [[CrossRef](#)]
256. Kang, M.S.; Kwon, M.; Jang, H.J.; Jeong, S.J.; Han, D.W.; Kim, K.S. Biosafety of Inorganic Nanomaterials for Theranostic Applications. *Emergent Mater.* **2022**, *5*, 1995–2029. [[CrossRef](#)]
257. Bassyouni, M.; Mansi, A.E.; Elgabry, A.; Ibrahim, B.A.; Kassem, O.A.; Alhebeshy, R. Utilization of Carbon Nanotubes in Removal of Heavy Metals from Wastewater: A Review of the CNTs' Potential and Current Challenges. *Appl. Phys. A Mater. Sci. Process.* **2020**, *126*, 38. [[CrossRef](#)]
258. Teixeira-Santos, R.; Gomes, M.; Gomes, L.C.; Mergulhão, F.J. Antimicrobial and Anti-Adhesive Properties of Carbon Nanotube-Based Surfaces for Medical Applications: A Systematic Review. *iScience* **2021**, *24*, 102001. [[CrossRef](#)] [[PubMed](#)]
259. Indarto, A.; Ikhsan, N.A.; Wibowo, I. Applications of Carbon Nanotubes for Controlling Waterborne Pathogens. In *Waterborne Pathogens: Detection and Treatment*; Butterworth-Heinemann: Oxford, UK, 2020; pp. 433–461. ISBN 9780128187838.
260. Kang, S.; Pinault, M.; Pfefferle, L.D.; Elimelech, M. Single-Walled Carbon Nanotubes Exhibit Strong Antimicrobial Activity. *Langmuir* **2007**, *23*, 8670–8673. [[CrossRef](#)] [[PubMed](#)]
261. Ihsanullah; Asmaly, H.A.; Saleh, T.A.; Laoui, T.; Gupta, V.K.; Atieh, M.A. Enhanced Adsorption of Phenols from Liquids by Aluminum Oxide/carbon Nanotubes: Comprehensive Study from Synthesis to Surface Properties. *J. Mol. Liq.* **2015**, *206*, 176–182. [[CrossRef](#)]
262. Rananga, L.E.; Magadzu, T. Interaction of Silver Doped Carbon Nanotubes-Cyclodextrin Nanocomposites with Escherichia Coli Bacteria during Water Purification. *Water Sci. Technol. Water Supply* **2014**, *14*, 367–375. [[CrossRef](#)]
263. Sheng, L.; Huang, S.; Sui, M.; Zhang, L.; She, L.; Chen, Y. Deposition of Copper Nanoparticles on Multiwalled Carbon Nanotubes Modified with Poly (Acrylic Acid) and Their Antimicrobial Application in Water Treatment. *Front. Environ. Sci. Eng.* **2015**, *9*, 625–633. [[CrossRef](#)]
264. Liu, C.; Xie, X.; Zhao, W.; Liu, N.; Maraccini, P.A.; Sassoubre, L.M.; Boehm, A.B.; Cui, Y. Conducting Nanosponge Electroporation for Affordable and High-Efficiency Disinfection of Bacteria and Viruses in Water. *Nano Lett.* **2013**, *13*, 4288–4293. [[CrossRef](#)]
265. Sui, M.; Zhang, L.; Sheng, L.; Huang, S.; She, L. Synthesis of ZnO Coated Multi-Walled Carbon Nanotubes and Their Antibacterial Activities. *Sci. Total Environ.* **2013**, *452–453*, 148–154. [[CrossRef](#)]
266. Lilly, M.; Dong, X.; McCoy, E.; Yang, L. Inactivation of Bacillus Anthracis Spores by Single-Walled Carbon Nanotubes Coupled with Oxidizing Antimicrobial Chemicals. *Environ. Sci. Technol.* **2012**, *46*, 13417–13424. [[CrossRef](#)] [[PubMed](#)]
267. Zalipour, Z.; Lashanizadegan, A.; Sadeghfar, F.; Ghaedi, M.; Asfaram, A.; Sadegh, F. Electrochemical Synthesis of CNTs-Zn: ZnO@SDS/PEG@Ni₂P Nanocomposite and Its Application for Ultrasound-Assisted Removal of Methylene Blue and Investigation of Its Antibacterial Property. *Environ. Nanotechnol. Monit. Manag.* **2022**, *18*, 100721. [[CrossRef](#)]
268. Zhang, W.; Li, Z.; Luo, R.; Guo, Q.; Xu, F.; Yang, F.; Zhang, M.; Jia, L.; Yuan, S. Design of Tandem CuO/CNTs Composites for Enhanced Tetracycline Degradation and Antibacterial Activity. *Sep. Purif. Technol.* **2023**, *306*, 122548. [[CrossRef](#)]

269. Liu, J.R.; Wang, X.Y.; Saberi, A.; Heydari, Z. The Effect of Co-Encapsulated GNPs-CNTs Nanofillers on Mechanical Properties, Degradation and Antibacterial Behavior of Mg-Based Composite. *J. Mech. Behav. Biomed. Mater.* **2023**, *138*, 105601. [[CrossRef](#)] [[PubMed](#)]
270. Das, R.; Abd Hamid, S.B.; Ali, M.E.; Ismail, A.F.; Annuar, M.S.M.; Ramakrishna, S. Multifunctional Carbon Nanotubes in Water Treatment: The Present, Past and Future. *Desalination* **2014**, *354*, 160–179. [[CrossRef](#)]
271. Bhatnagar, A.; Sillanpää, M. Removal of Natural Organic Matter (NOM) and Its Constituents from Water by Adsorption—A Review. *Chemosphere* **2017**, *166*, 497–510. [[CrossRef](#)] [[PubMed](#)]
272. Xu, L.; Shahid, S.; Shen, J.; Emanuelsson, E.A.C.; Patterson, D.A. A Wide Range and High Resolution One-Filtration Molecular Weight Cut-off Method for Aqueous Based Nanofiltration and Ultrafiltration Membranes. *J. Memb. Sci.* **2017**, *525*, 304–311. [[CrossRef](#)]
273. Ajmani, G.S.; Goodwin, D.; Marsh, K.; Fairbrother, D.H.; Schwab, K.J.; Jacangelo, J.G.; Huang, H. Modification of Low Pressure Membranes with Carbon Nanotube Layers for Fouling Control. *Water Res.* **2012**, *46*, 5645–5654. [[CrossRef](#)]
274. Wang, Y.; Zhu, J.; Huang, H.; Cho, H.H. Carbon Nanotube Composite Membranes for Microfiltration of Pharmaceuticals and Personal Care Products: Capabilities and Potential Mechanisms. *J. Memb. Sci.* **2015**, *479*, 165–174. [[CrossRef](#)]
275. Engel, M.; Chefetz, B. Adsorption and Desorption of Dissolved Organic Matter by Carbon Nanotubes: Effects of Solution Chemistry. *Environ. Pollut.* **2016**, *213*, 90–98. [[CrossRef](#)]
276. Yang, X.; Lee, J.; Yuan, L.; Chae, S.R.; Peterson, V.K.; Minett, A.I.; Yin, Y.; Harris, A.T. Removal of Natural Organic Matter in Water Using Functionalised Carbon Nanotube Buckypaper. *Carbon* **2013**, *59*, 160–166. [[CrossRef](#)]
277. Yin, S.; López, J.F.; Solís, J.J.C.; Wong, M.S.; Villagrán, D. Enhanced Adsorption of PFOA with Nano MgAl₂O₄@CNTs: Influence of pH and Dosage, and Environmental Conditions. *J. Hazard. Mater. Adv.* **2023**, *9*, 100252. [[CrossRef](#)]
278. Nagorzanski, M.; Qian, J.; Martinez, A.; Cwiertny, D.M. Electrospun Nanofiber Mats as Sorbents for Polar Emerging Organic Contaminants: Demonstrating Tailorable Material Performance for Uptake of Neonicotinoid Insecticides from Water. *J. Hazard. Mater. Adv.* **2023**, *9*, 100219. [[CrossRef](#)] [[PubMed](#)]
279. Jiang, L.; Rastgar, M.; Wang, C.; Ke, S.; He, L.; Chen, X.; Song, Y.; He, C.; Wang, J.; Sadrzadeh, M. Robust PANI-Entangled CNTs Electro-Responsive Membranes for Enhanced In-Situ Generation of H₂O₂ and Effective Separation of Charged Contaminants. *Sep. Purif. Technol.* **2022**, *303*, 122274. [[CrossRef](#)]
280. Wang, Y.; Ma, J.; Zhu, J.; Ye, N.; Zhang, X.; Huang, H. Multi-Walled Carbon Nanotubes with Selected Properties for Dynamic Filtration of Pharmaceuticals and Personal Care Products. *Water Res.* **2016**, *92*, 104–112. [[CrossRef](#)] [[PubMed](#)]
281. Li, S.; He, M.; Li, Z.; Li, D.; Pan, Z. Removal of Humic Acid from Aqueous Solution by Magnetic Multi-Walled Carbon Nanotubes Decorated with Calcium. *J. Mol. Liq.* **2017**, *230*, 520–528. [[CrossRef](#)]
282. Khalid, A.; Al-Juhani, A.A.; Al-Hamouz, O.C.; Laoui, T.; Khan, Z.; Atieh, M.A. Preparation and Properties of Nanocomposite Polysulfone/multi-Walled Carbon Nanotubes Membranes for Desalination. *Desalination* **2015**, *367*, 134–144. [[CrossRef](#)]
283. Shao, D.; Sheng, G.; Chen, C.; Wang, X.; Nagatsu, M. Removal of Polychlorinated Biphenyls from Aqueous Solutions Using β -Cyclodextrin Grafted Multiwalled Carbon Nanotubes. *Chemosphere* **2010**, *79*, 679–685. [[CrossRef](#)]
284. Wang, Y.; Huang, H.; Wei, X. Influence of Wastewater Precoagulation on Adsorptive Filtration of Pharmaceutical and Personal Care Products by Carbon Nanotube Membranes. *Chem. Eng. J.* **2018**, *333*, 66–75. [[CrossRef](#)]
285. Zhao, J.; Wang, Z.; White, J.C.; Xing, B. Graphene in the Aquatic Environment: Adsorption, Dispersion, Toxicity and Transformation. *Environ. Sci. Technol.* **2014**, *48*, 9995–10009. [[CrossRef](#)] [[PubMed](#)]
286. Zhao, G.; Li, J.; Ren, X.; Chen, C.; Wang, X. Few-Layered Graphene Oxide Nanosheets as Superior Sorbents for Heavy Metal Ion Pollution Management. *Environ. Sci. Technol.* **2011**, *45*, 10454–10462. [[CrossRef](#)]
287. Li, M.F.; Liu, Y.G.; Zeng, G.M.; Liu, N.; Liu, S.B. Graphene and Graphene-Based Nanocomposites Used for Antibiotics Removal in Water Treatment: A Review. *Chemosphere* **2019**, *226*, 360–380. [[CrossRef](#)] [[PubMed](#)]
288. Sitko, R.; Turek, E.; Zawisza, B.; Malicka, E.; Talik, E.; Heimann, J.; Gagor, A.; Feist, B.; Wrzalik, R. Adsorption of Divalent Metal Ions from Aqueous Solutions Using Graphene Oxide. *Dalton Trans.* **2013**, *42*, 5682–5689. [[CrossRef](#)] [[PubMed](#)]
289. Huang, Z.H.; Zheng, X.; Lv, W.; Wang, M.; Yang, Q.H.; Kang, F. Adsorption of lead(II) Ions from Aqueous Solution on Low-Temperature Exfoliated Graphene Nanosheets. *Langmuir* **2011**, *27*, 7558–7562. [[CrossRef](#)] [[PubMed](#)]
290. Lee, Y.C.; Yang, J.W. Self-Assembled Flower-like TiO₂ on Exfoliated Graphite Oxide for Heavy Metal Removal. *J. Ind. Eng. Chem.* **2012**, *18*, 1178–1185. [[CrossRef](#)]
291. Santhosh, C.; Velmurugan, V.; Jacob, G.; Jeong, S.K.; Grace, A.N.; Bhatnagar, A. Role of Nanomaterials in Water Treatment Applications: A Review. *Chem. Eng. J.* **2016**, *306*, 1116–1137. [[CrossRef](#)]
292. Kumar, S.; Nair, R.R.; Pillai, P.B.; Gupta, S.N.; Iyengar, M.A.R.; Sood, A.K. Graphene Oxide-MnFe₂O₄ Magnetic Nanohybrids for Efficient Removal of Lead and Arsenic from Water. *ACS Appl. Mater. Interfaces* **2014**, *6*, 17426–17436. [[CrossRef](#)] [[PubMed](#)]
293. Al-Mhyawi, S.R.; Bader, D.M.D.; Bajaber, M.A.; El Dayem, S.M.A.; Ragab, A.H.; Abd El-Rahem, K.A.; Gado, M.A.; Atia, B.M.; Cheira, M.F. Zirconium Oxide with Graphene Oxide Anchoring for Improved Heavy Metal Ions Adsorption: Isotherm and Kinetic Study. *J. Mater. Res. Technol.* **2023**, *22*, 3058–3074. [[CrossRef](#)]
294. Li, J.; Zhang, S.; Chen, C.; Zhao, G.; Yang, X.; Li, J.; Wang, X. Removal of Cu(II) and Fulvic Acid by Graphene Oxide Nanosheets Decorated with Fe₃O₄ Nanoparticles. *ACS Appl. Mater. Interfaces* **2012**, *4*, 4991–5000. [[CrossRef](#)]

295. Hu, X.J.; Liu, Y.G.; Zeng, G.M.; You, S.H.; Wang, H.; Hu, X.; Guo, Y.M.; Tan, X.F.; Guo, F.Y. Effects of Background Electrolytes and Ionic Strength on Enrichment of Cd(II) Ions with Magnetic Graphene Oxide-Supported Sulfanilic Acid. *J. Colloid Interface Sci.* **2014**, *435*, 138–144. [[CrossRef](#)] [[PubMed](#)]
296. Bukhari, A.; Ijaz, I.; Zain, H.; Mehmood, U.; Mudassir Iqbal, M.; Gilani, E.; Nazir, A. Introduction of CdO Nanoparticles into Graphene and Graphene Oxide Nanosheets for Increasing Adsorption Capacity of Cr from Wastewater Collected from Petroleum Refinery. *Arab. J. Chem.* **2023**, *16*, 104445. [[CrossRef](#)]
297. Zhang, Y.; Yan, L.; Xu, W.; Guo, X.; Cui, L.; Gao, L.; Wei, Q.; Du, B. Adsorption of Pb(II) and Hg(II) from Aqueous Solution Using Magnetic CoFe₂O₄-Reduced Graphene Oxide. *J. Mol. Liq.* **2014**, *191*, 177–182. [[CrossRef](#)]
298. Nandi, D.; Basu, T.; Debnath, S.; Ghosh, A.K.; De, A.; Ghosh, U.C. Mechanistic Insight for the Sorption of Cd(II) and Cu(II) from Aqueous Solution on Magnetic Mn-Doped Fe(III) Oxide Nanoparticle Implanted Graphene. *J. Chem. Eng. Data* **2013**, *58*, 2809–2818. [[CrossRef](#)]
299. Dan, S.; Bagheri, H.; Shahidzadeh, A.; Hashemipour, H. Performance of Graphene Oxide/SiO₂ Nanocomposite-Based: Antibacterial Activity, Dye and Heavy Metal Removal. *Arab. J. Chem.* **2023**, *16*, 104450. [[CrossRef](#)]
300. Hu, X.J.; Liu, Y.G.; Wang, H.; Chen, A.W.; Zeng, G.M.; Liu, S.M.; Guo, Y.M.; Hu, X.; Li, T.T.; Wang, Y.Q.; et al. Removal of Cu(II) Ions from Aqueous Solution Using Sulfonated Magnetic Graphene Oxide Composite. *Sep. Purif. Technol.* **2013**, *108*, 189–195. [[CrossRef](#)]
301. Hur, J.; Shin, J.; Yoo, J.; Seo, Y.S. Competitive Adsorption of Metals onto Magnetic Graphene Oxide: Comparison with Other Carbonaceous Adsorbents. *Sci. World J.* **2015**, *2015*, 836287. [[CrossRef](#)] [[PubMed](#)]
302. Hao, L.; Song, H.; Zhang, L.; Wan, X.; Tang, Y.; Lv, Y. SiO₂/graphene Composite for Highly Selective Adsorption of Pb(II) Ion. *J. Colloid Interface Sci.* **2012**, *369*, 381–387. [[CrossRef](#)]
303. Thu, V.T.; Trieu, M.H.; An, N.H.T.; Dat, N.T.; Linh, N.D.; Manh, N.B. Mussel-Inspired Biosorbent Combined with Graphene Oxide for Removal of Organic Pollutants from Aqueous Solutions. *Ecotoxicol. Environ. Saf.* **2023**, *255*, 114793. [[CrossRef](#)] [[PubMed](#)]
304. An, J.; Wang, S.; Huang, M.; Zhang, J.; Wang, P. Removal of Water-Soluble Lignin Model Pollutants with Graphene Oxide Loaded Ironic Sulfide as an Efficient Adsorbent and Heterogeneous Fenton Catalyst. *Arab. J. Chem.* **2022**, *15*, 104338. [[CrossRef](#)]
305. Khalil, S.; Bianchi, A.; Kovtun, A.; Tunioli, F.; Boschi, A.; Zambianchi, M.; Paci, D.; Bocchi, L.; Valsecchi, S.; Polesello, S.; et al. Graphene Oxide Nanosheets for Drinking Water Purification by Tandem Adsorption and Microfiltration. *Sep. Purif. Technol.* **2022**, *300*, 121826. [[CrossRef](#)]
306. Zhang, X.; Cheng, C.; Zhao, J.; Ma, L.; Sun, S.; Zhao, C. Polyethersulfone Enwrapped Graphene Oxide Porous Particles for Water Treatment. *Chem. Eng. J.* **2013**, *215–216*, 72–81. [[CrossRef](#)]
307. Xie, G.; Xi, P.; Liu, H.; Chen, F.; Huang, L.; Shi, Y.; Hou, F.; Zeng, Z.; Shao, C.; Wang, J. A Facile Chemical Method to Produce Superparamagnetic Graphene Oxide-Fe₃O₄ Hybrid Composite and Its Application in the Removal of Dyes from Aqueous Solution. *J. Mater. Chem.* **2012**, *22*, 1033–1039. [[CrossRef](#)]
308. Bai, S.; Shen, X.; Zhong, X.; Liu, Y.; Zhu, G.; Xu, X.; Chen, K. One-Pot Solvothermal Preparation of Magnetic Reduced Graphene Oxide-Ferrite Hybrids for Organic Dye Removal. *Carbon* **2012**, *50*, 2337–2346. [[CrossRef](#)]
309. Liu, F.; Chung, S.; Oh, G.; Seo, T.S. A Three-Dimensional Graphene Oxide Nanostructure for Fast and Efficient Dye Removal. *ACS Appl. Mater. Interfaces* **2012**, *4*, 922–927. [[CrossRef](#)] [[PubMed](#)]
310. Yao, Y.; Miao, S.; Liu, S.; Ma, L.P.; Sun, H.; Wang, S. Synthesis, Characterization, and Adsorption Properties of Magnetic Fe₃O₄@graphene Nanocomposite. *Chem. Eng. J.* **2012**, *184*, 326–332. [[CrossRef](#)]
311. Bradder, P.; Ling, S.K.; Wang, S.; Liu, S. Dye Adsorption on Layered Graphite Oxide. *J. Chem. Eng. Data* **2011**, *56*, 138–141. [[CrossRef](#)]
312. Jahan, N.; Roy, H.; Reaz, A.H.; Arshi, S.; Rahman, E.; Firoz, S.H.; Islam, M.S. A Comparative Study on Sorption Behavior of Graphene Oxide and Reduced Graphene Oxide towards Methylene Blue. *Case Stud. Chem. Environ. Eng.* **2022**, *6*, 100239. [[CrossRef](#)]
313. Liu, T.; Li, Y.; Du, Q.; Sun, J.; Jiao, Y.; Yang, G.; Wang, Z.; Xia, Y.; Zhang, W.; Wang, K.; et al. Adsorption of Methylene Blue from Aqueous Solution by Graphene. *Colloids Surf. B Biointerfaces* **2012**, *90*, 197–203. [[CrossRef](#)]
314. Carmalin Sophia, A.; Lima, E.C.; Allaudeen, N.; Rajan, S. Application of Graphene Based Materials for Adsorption of Pharmaceutical Traces from Water and Wastewater—a Review. *Desalin. Water Treat.* **2016**, *57*, 27573–27586. [[CrossRef](#)]
315. Ghaedi, M.; Zeinali, N.; Ghaedi, A.M.; Teimuori, M.; Tashkhourian, J. Artificial Neural Network-Genetic Algorithm Based Optimization for the Adsorption of Methylene Blue and Brilliant Green from Aqueous Solution by Graphite Oxide Nanoparticle. *Spectrochim. Acta-Part A Mol. Biomol. Spectrosc.* **2014**, *125*, 264–277. [[CrossRef](#)] [[PubMed](#)]
316. Shen, Y.; Fang, Q.; Chen, B. Environmental Applications of Three-Dimensional Graphene-Based Macrostructures: Adsorption, Transformation, and Detection. *Environ. Sci. Technol.* **2015**, *49*, 67–84. [[CrossRef](#)] [[PubMed](#)]
317. Sabzevari, M.; Cree, D.E.; Wilson, L.D. Graphene Oxide-Chitosan Composite Material for Treatment of a Model Dye Effluent. *ACS Omega* **2018**, *3*, 13045–13054. [[CrossRef](#)] [[PubMed](#)]
318. Mahmoodi, N.M.; Bakhtiari, M.; Oveisi, M.; Mahmoodi, B.; Hayati, B. Green Synthesis of Eco-Friendly Magnetic Metal-Organic Framework Nanocomposites (AlFum-Graphene Oxide) and Pollutants (Dye and Pharmaceuticals) Removal Capacity from Water. *Mater. Chem. Phys.* **2023**, *302*, 127720. [[CrossRef](#)]
319. Thamaraiselvan, C.; Bandyopadhyay, D.; Powell, C.D.; Arnusch, C.J. Electrochemical Degradation of Emerging Pollutants via Laser-Induced Graphene Electrodes. *Chem. Eng. J. Adv.* **2021**, *8*, 100195. [[CrossRef](#)]

320. Gao, Y.; Li, Y.; Zhang, L.; Huang, H.; Hu, J.; Shah, S.M.; Su, X. Adsorption and Removal of Tetracycline Antibiotics from Aqueous Solution by Graphene Oxide. *J. Colloid Interface Sci.* **2012**, *368*, 540–546. [[CrossRef](#)] [[PubMed](#)]
321. Lin, Y.; Xu, S.; Li, J. Fast and Highly Efficient Tetracyclines Removal from Environmental Waters by Graphene Oxide Functionalized Magnetic Particles. *Chem. Eng. J.* **2013**, *225*, 679–685. [[CrossRef](#)]
322. Ghadim, E.E.; Manouchehri, F.; Soleimani, G.; Hosseini, H.; Kimiagar, S.; Nafisi, S. Adsorption Properties of Tetracycline onto Graphene Oxide: Equilibrium, Kinetic and Thermodynamic Studies. *PLoS ONE* **2013**, *8*, e79254. [[CrossRef](#)]
323. Chen, H.; Gao, B.; Li, H. Removal of Sulfamethoxazole and Ciprofloxacin from Aqueous Solutions by Graphene Oxide. *J. Hazard. Mater.* **2015**, *282*, 201–207. [[CrossRef](#)]
324. Yu, F.; Ma, J.; Bi, D. Enhanced Adsorptive Removal of Selected Pharmaceutical Antibiotics from Aqueous Solution by Activated Graphene. *Environ. Sci. Pollut. Res.* **2015**, *22*, 4715–4724. [[CrossRef](#)]
325. Ma, J.; Yang, M.; Yu, F.; Zheng, J. Water-Enhanced Removal of Ciprofloxacin from Water by Porous Graphene Hydrogel. *Sci. Rep.* **2015**, *5*, 13578. [[CrossRef](#)]
326. Wu, S.; Zhao, X.; Li, Y.; Du, Q.; Sun, J.; Wang, Y.; Wang, X.; Xia, Y.; Wang, Z.; Xia, L. Adsorption Properties of Doxorubicin Hydrochloride onto Graphene Oxide: Equilibrium, Kinetic and Thermodynamic Studies. *Materials* **2013**, *6*, 2026–2042. [[CrossRef](#)] [[PubMed](#)]
327. Dong, S.; Sun, Y.; Wu, J.; Wu, B.; Creamer, A.E.; Gao, B. Graphene Oxide as Filter Media to Remove Levofloxacin and Lead from Aqueous Solution. *Chemosphere* **2016**, *150*, 759–764. [[CrossRef](#)] [[PubMed](#)]
328. Elanchezhian, S.S.; Muthu Prabhu, S.; Kim, Y.; Park, C.M. Lanthanum-Substituted Bimetallic Magnetic Materials Assembled Carboxylate-Rich Graphene Oxide Nanohybrids as Highly Efficient Adsorbent for Perfluorooctanoic Acid Adsorption from Aqueous Solutions. *Appl. Surf. Sci.* **2020**, *509*, 144716. [[CrossRef](#)]
329. Jones, S.; Pramanik, A.; Kanchanapally, R.; Viraka Nellore, B.P.; Begum, S.; Sweet, C.; Ray, P.C. Multifunctional Three-Dimensional Chitosan/Gold Nanoparticle/Graphene Oxide Architecture for Separation, Label-Free SERS Identification of Pharmaceutical Contaminants, and Effective Killing of Superbugs. *ACS Sustain. Chem. Eng.* **2017**, *5*, 7175–7187. [[CrossRef](#)]
330. Tian, T.; Shi, X.; Cheng, L.; Luo, Y.; Dong, Z.; Gong, H.; Xu, L.; Zhong, Z.; Peng, R.; Liu, Z. Graphene-Based Nanocomposite as an Effective, Multifunctional, and Recyclable Antibacterial Agent. *ACS Appl. Mater. Interfaces* **2014**, *6*, 8542–8548. [[CrossRef](#)] [[PubMed](#)]
331. Nasrollahzadeh, M.; Sajjadi, M.; Irvani, S.; Varma, R.S. Carbon-Based Sustainable Nanomaterials for Water Treatment: State-of-Art and Future Perspectives. *Chemosphere* **2020**, *263*, 128005. [[CrossRef](#)]
332. Fera, M.; Macchiaroli, R.; Iannone, R.; Miranda, S.; Riemma, S. Economic Evaluation Model for the Energy Demand Response. *Energy* **2016**, *112*, 457–468. [[CrossRef](#)]
333. Reza, M.S.; Ahmad, N.B.H.; Afroze, S.; Taweekun, J.; Sharifpur, M.; Azad, A.K. Hydrogen Production from Water Splitting Through Photocatalytic Activity of Carbon-Based Materials, A Review. *Chem. Eng. Technol.* **2023**, *46*, 420–434. [[CrossRef](#)]
334. Singh, S.; Jain, S.; PS, V.; Tiwari, A.K.; Nouni, M.R.; Pandey, J.K.; Goel, S. Hydrogen: A Sustainable Fuel for Future of the Transport Sector. *Renew. Sustain. Energy Rev.* **2015**, *51*, 623–633. [[CrossRef](#)]
335. Kalair, A.; Abas, N.; Saleem, M.S.; Kalair, A.R.; Khan, N. Role of Energy Storage Systems in Energy Transition from Fossil Fuels to Renewables. *Energy Storage* **2021**, *3*, e135. [[CrossRef](#)]
336. Zhang, L.; Xu, M.; Chen, H.; Li, Y.; Chen, S. Globalization, Green Economy and Environmental Challenges: State of the Art Review for Practical Implications. *Front. Environ. Sci.* **2022**, *10*, 199. [[CrossRef](#)]
337. Radenahmad, N.; Reza, S.; Saifullah, M.; Bakar, A.; Shams, S.; Tesfai, A.; Taweekun, J.; Khalilpoor, N.; Azad, A.K.; Issakhov, A. Evaluation of the Bioenergy Potential of Temer Musa: An Invasive Tree from the African Desert. *Int. J. Chem. Eng.* **2021**, *2021*, 6693071. [[CrossRef](#)]
338. Zhao, Y.-Q.; Lu, M.; Tao, P.-Y.; Zhang, Y.-J.; Gong, X.-T.; Yang, Z.; Zhang, G.-Q.; Li, H.-L. Hierarchically Porous and Heteroatom Doped Carbon Derived from Tobacco Rods for Supercapacitors. *J. Power Sources* **2016**, *307*, 391–400. [[CrossRef](#)]
339. Azcárate, C.; Mallor, F.; Mateo, P. Tactical and Operational Management of Wind Energy Systems with Storage Using a Probabilistic Forecast of the Energy Resource. *Renew. Energy* **2017**, *102*, 445–456. [[CrossRef](#)]
340. Holze, R.F.; Béguin, E. Frackowiak (Eds): Supercapacitors—Materials, Systems, and Applications. *J. Solid State Electrochem.* **2015**, *19*, 1253. [[CrossRef](#)]
341. Zhang, Q.; Uchaker, E.; Candelaria, S.L.; Cao, G. Nanomaterials for Energy Conversion and Storage. *Chem. Soc. Rev.* **2013**, *42*, 3127. [[CrossRef](#)]
342. Borenstein, A.; Hanna, O.; Attias, R.; Luski, S.; Brousse, T.; Aurbach, D. Carbon-Based Composite Materials for Supercapacitor Electrodes: A Review. *J. Mater. Chem. A* **2017**, *5*, 12653–12672. [[CrossRef](#)]
343. Ferrero, G.A.; Fuertes, A.B.; Sevilla, M. From Soybean Residue to Advanced Supercapacitors. *Sci. Rep.* **2015**, *5*, 16618. [[CrossRef](#)]
344. Dai, L.; Chang, D.W.; Baek, J.B.; Lu, W. Carbon Nanomaterials for Advanced Energy Conversion and Storage. *Small* **2012**, *8*, 1130–1166. [[CrossRef](#)]
345. Ayinla, R.T.; Dennis, J.O.O.; Zaid, H.M.M.; Sanusi, Y.K.K.; Usman, F.; Adebayo, L.L.L. A Review of Technical Advances of Recent Palm Bio-Waste Conversion to Activated Carbon for Energy Storage. *J. Clean. Prod.* **2019**, *229*, 1427–1442. [[CrossRef](#)]
346. Winter, M.; Brodd, R.J. What Are Batteries, Fuel Cells, and Supercapacitors? *Chem. Rev.* **2004**, *104*, 4245–4269. [[CrossRef](#)]
347. Wang, X.; Wang, D.; Liang, J. Performance of Electric Double Layer Capacitors Using Active Carbons Prepared from Petroleum Coke by KOH and Vapor Re-Etching. *J. Mater. Sci. Technol.* **2003**, *19*, 265–269.

348. Zhang, C.; Long, D.; Xing, B.; Qiao, W.; Zhang, R.; Zhan, L.; Liang, X.; Ling, L. The Superior Electrochemical Performance of Oxygen-Rich Activated Carbons Prepared from Bituminous Coal. *Electrochem. Commun.* **2008**, *10*, 1809–1811. [[CrossRef](#)]
349. Hasegawa, G.; Aoki, M.; Kanamori, K.; Nakanishi, K.; Hanada, T.; Tadanaga, K. Monolithic Electrode for Electric Double-Layer Capacitors Based on Macro/meso/microporous S-Containing Activated Carbon with High Surface Area. *J. Mater. Chem.* **2011**, *21*, 2060–2063. [[CrossRef](#)]
350. Fang, B.; Wei, Y.Z.; Maruyama, K.; Kumagai, M. High Capacity Supercapacitors Based on Modified Activated Carbon Aerogel. *J. Appl. Electrochem.* **2005**, *35*, 229–233. [[CrossRef](#)]
351. Toupin, M.; Bélanger, D.; Hill, I.R.; Quinn, D. Performance of Experimental Carbon Blacks in Aqueous Supercapacitors. *J. Power Sources* **2005**, *140*, 203–210. [[CrossRef](#)]
352. Zhao, J.; Lai, C.; Dai, Y.; Xie, J. Synthesis of Mesoporous Carbon as Electrode Material for SC. *J. Cent. South Univ.* **2005**, *12*, 647–652. [[CrossRef](#)]
353. Jin, J.; Tanaka, S.; Egashira, Y.; Nishiyama, N. KOH Activation of Ordered Mesoporous Carbons Prepared by a Soft-Templating Method and Their Enhanced Electrochemical Properties. *Carbon* **2010**, *48*, 1985–1989. [[CrossRef](#)]
354. Li, X.; Han, C.; Chen, X.; Shi, C. Preparation and Performance of Straw Based Activated Carbon for Supercapacitor in Non-Aqueous Electrolytes. *Microporous Mesoporous Mater.* **2010**, *131*, 303–309. [[CrossRef](#)]
355. Jiang, J.; Gao, Q.; Xia, K.; Hu, J. Enhanced Electrical Capacitance of Porous Carbons by Nitrogen Enrichment and Control of the Pore Structure. *Microporous Mesoporous Mater.* **2009**, *118*, 28–34. [[CrossRef](#)]
356. Yun, Y.S.; Cho, S.Y.; Shim, J.; Kim, B.H.; Chang, S.J.; Baek, S.J.; Huh, Y.S.; Tak, Y.; Park, Y.W.; Park, S.; et al. Microporous Carbon Nanoplates from Regenerated Silk Proteins for Supercapacitors. *Adv. Mater.* **2013**, *25*, 1993–1998. [[CrossRef](#)]
357. Jiang, Q.; Qu, M.Z.; Zhou, G.M.; Zhang, B.L.; Yu, Z.L. A Study of Activated Carbon Nanotubes as Electrochemical Super Capacitors Electrode Materials. *Mater. Lett.* **2002**, *57*, 988–991. [[CrossRef](#)]
358. Rufford, T.E.; Hulicova-Jurcakova, D.; Zhu, Z.; Lu, G.Q. Nanoporous Carbon Electrode from Waste Coffee Beans for High Performance Supercapacitors. *Electrochem. Commun.* **2008**, *10*, 1594–1597. [[CrossRef](#)]
359. Sun, L.; Tian, C.; Li, M.; Meng, X.; Wang, L.; Wang, R.; Yin, J.; Fu, H. From Coconut Shell to Porous Graphene-like Nanosheets for High-Power Supercapacitors. *J. Mater. Chem. A* **2013**, *1*, 6462–6470. [[CrossRef](#)]
360. Asfaw, H.D.; Kucernak, A.; Greenhalgh, E.S.; Shaffer, M.S.P. Electrochemical Performance of Supercapacitor Electrodes Based on Carbon Aerogel-Reinforced Spread Tow Carbon Fiber Fabrics. *Compos. Sci. Technol.* **2023**, *238*, 110042. [[CrossRef](#)]
361. Priya, D.S.; Kennedy, L.J.; Anand, G.T. Effective Conversion of Waste Banana Bract into Porous Carbon Electrode for Supercapacitor Energy Storage Applications. *Results Surf. Interfaces* **2023**, *10*, 100096. [[CrossRef](#)]
362. Tu, J.; Qiao, Z.; Wang, Y.; Li, G.; Zhang, X.; Li, G.; Ruan, D. American Ginseng Biowaste-Derived Activated Carbon for High-Performance Supercapacitors. *Int. J. Electrochem. Sci.* **2023**, *18*, 16–24. [[CrossRef](#)]
363. Shrestha, D. Activated Carbon and Its Hybrid Composites with Manganese (IV) Oxide as Effectual Electrode Materials for High Performance Supercapacitor. *Arab. J. Chem.* **2022**, *15*, 103946. [[CrossRef](#)]
364. Taberna, P.-L.; Gaspard, S. Chapter 9 Nanoporous Carbons for High Energy Density Supercapacitors. In *Biomass for Sustainable Applications: Pollution Remediation and Energy*; The Royal Society of Chemistry: London, UK, 2014; pp. 366–399; ISBN 978-1-84973-600-8.
365. Gupta, R.K.; Dubey, M.; Kharel, P.; Gu, Z.; Fan, Q.H. Biochar Activated by Oxygen Plasma for Supercapacitors. *J. Power Sources* **2015**, *274*, 1300–1305. [[CrossRef](#)]
366. Li, X.; Jiang, X.; Xu, H.; Xu, Q.; Jiang, L.; Shi, Y.; Zhang, Q. Scandium-Doped PrBaCo_{2-x}Sc_xO_{6-δ} Oxides as Cathode Material for Intermediate-Temperature Solid Oxide Fuel Cells. *Int. J. Hydrogen Energy* **2013**, *38*, 12035–12042. [[CrossRef](#)]
367. Jiang, J.; Zhang, L.; Wang, X.; Holm, N.; Rajagopalan, K.; Chen, F.; Ma, S. Highly Ordered Macroporous Woody Biochar with Ultra-High Carbon Content as Supercapacitor Electrodes. *Electrochim. Acta* **2013**, *113*, 481–489. [[CrossRef](#)]
368. Tan, X.F.; Liu, S.B.; Liu, Y.G.; Gu, Y.L.; Zeng, G.M.; Hu, X.J.; Wang, X.; Liu, S.H.; Jiang, L.H. Biochar as Potential Sustainable Precursors for Activated Carbon Production: Multiple Applications in Environmental Protection and Energy Storage. *Bioresour. Technol.* **2017**, *227*, 359–372. [[CrossRef](#)] [[PubMed](#)]
369. Hecht, D.S.; Hu, L.; Irvin, G. Emerging Transparent Electrodes Based on Thin Films of Carbon Nanotubes, Graphene, and Metallic Nanostructures. *Adv. Mater.* **2011**, *23*, 1482–1513. [[CrossRef](#)] [[PubMed](#)]
370. Sun, L.; Fan, Y.; Wang, X.; Agung Susantyoko, R.; Zhang, Q. Large Scale Low Cost Fabrication of Diameter Controllable Silicon Nanowire Arrays. *Nanotechnology* **2014**, *25*, 255302. [[CrossRef](#)]
371. Baughman, R.H.; Zakhidov, A.A.; De Heer, W.A. Carbon Nanotubes—The Route toward Applications. *Science* **2002**, *297*, 787–792. [[CrossRef](#)] [[PubMed](#)]
372. An, K.H.; Kim, W.S.; Park, Y.S.; Moon, J.M.; Bae, D.J.; Lim, S.C.; Lee, Y.S.; Lee, Y.H. Electrochemical Properties of High-Power Supercapacitors Using Single-Walled Carbon Nanotube Electrodes. *Adv. Funct. Mater.* **2001**, *11*, 387–392. [[CrossRef](#)]
373. Islam, M.R.; Pias, S.M.N.S.; Alam, R.B.; Khondaker, S.I. Enhanced Electrochemical Performance of Solution-Processed Single-Wall Carbon Nanotube Reinforced Polyvinyl Alcohol Nanocomposite Synthesized via Solution-Cast Method. *Nano Express* **2020**, *1*, 30013. [[CrossRef](#)]
374. Picó, F.; Rojo, J.M.; Sanjuán, M.L.; Ansón, A.; Benito, A.M.; Callejas, M.A.; Maser, W.K.; Martínez, M.T. Single-Walled Carbon Nanotubes as Electrodes in Supercapacitors. *J. Electrochem. Soc.* **2004**, *151*, A831. [[CrossRef](#)]
375. Frackowiak, E.; Jurewicz, K.; Delpeux, S.; Béguin, F. Nanotubular Materials for Supercapacitors. *J. Power Sources* **2001**, 97–98, 822–825. [[CrossRef](#)]

376. Khomenko, V.; Raymundo-Piñero, E.; Béguin, F. Optimisation of an Asymmetric Manganese Oxide/activated Carbon Capacitor Working at 2 V in Aqueous Medium. *J. Power Sources* **2006**, *153*, 183–190. [[CrossRef](#)]
377. Lal, M.S.; Badam, R.; Matsumi, N.; Ramaprabhu, S. Hydrothermal Synthesis of Single-Walled Carbon nanotubes/TiO₂ for Quasi-Solid-State Composite-Type Symmetric Hybrid Supercapacitors. *J. Energy Storage* **2021**, *40*, 102794. [[CrossRef](#)]
378. Chen, Y.; Tong, L.; Lin, G.; Liu, X. SWCNTs/phthalocyanine Polymer Composite Derived Nitrogen Self-Doped Graphene-like Carbon for High-Performance Supercapacitors Electrodes. *Mater. Chem. Phys.* **2022**, *277*, 125433. [[CrossRef](#)]
379. Ma, S.B.; Nam, K.W.; Yoon, W.S.; Yang, X.Q.; Ahn, K.Y.; Oh, K.H.; Kim, K.B. Electrochemical Properties of Manganese Oxide Coated onto Carbon Nanotubes for Energy-Storage Applications. *J. Power Sources* **2008**, *178*, 483–489. [[CrossRef](#)]
380. Wang, G.X.; Ahn, J.H.; Yao, J.; Lindsay, M.; Liu, H.K.; Dou, S.X. Preparation and Characterization of Carbon Nanotubes for Energy Storage. *J. Power Sources* **2003**, *119–121*, 16–23. [[CrossRef](#)]
381. Zhang, Z.; Feng, L.; Jing, P.; Hou, X.; Suo, G.; Ye, X.; Zhang, L.; Yang, Y.; Zhai, C. In Situ Construction of Hierarchical polyaniline/SnS₂@carbon Nanotubes on Carbon Fibers for High-Performance Supercapacitors. *J. Colloid Interface Sci.* **2021**, *588*, 84–93. [[CrossRef](#)] [[PubMed](#)]
382. Wang, Z.; Wang, M.; Hao, Y.; Chen, C. Facile Synthesis of N-Doped NiCo₂S₄/CNTs with Coordinated Effects as Cathode Materials for High-Performance Supercapacitors. *Ionics* **2021**, *27*, 3567–3578. [[CrossRef](#)]
383. Akbar, A.R.; Wu, J.; Tahir, M.; Hu, H.; Yu, C.; Qadir, M.B.; Mateen, F.; Xiong, C.; Yang, Q. Synthesis of the Novel Binary Composite of Self-Suspended Polyaniline (S-PANI) and Functionalized Multi-Walled Carbon Nanotubes for High-Performance Supercapacitors. *Ionics* **2021**, *27*, 1743–1755. [[CrossRef](#)]
384. Solgi, M.; Cheraghali, R.; Aghazadeh, M. Self-Assembled Co(OH)₂/functionalized MWNTs/porous Graphene Ternary Binder-Free Hybrid for Supercapacitors. *J. Mater. Sci. Mater. Electron.* **2021**, *32*, 151–167. [[CrossRef](#)]
385. Ma, S.B.; Nam, K.W.; Yoon, W.S.; Bak, S.M.; Yang, X.Q.; Cho, B.W.; Kim, K.B. Nano-Sized Lithium Manganese Oxide Dispersed on Carbon Nanotubes for Energy Storage Applications. *Electrochem. Commun.* **2009**, *11*, 1575–1578. [[CrossRef](#)]
386. Yan, L.; Xu, Y.; Zhou, M.; Chen, G.; Deng, S.; Smirnov, S.; Luo, H.; Zou, G. Porous TiO₂ Conformal Coating on Carbon Nanotubes as Energy Storage Materials. *Electrochim. Acta* **2015**, *169*, 73–81. [[CrossRef](#)]
387. Sathiya, M.; Prakash, A.S.; Ramesha, K.; Tarascon, J.M.; Shukla, A.K. V₂O₅-Anchored Carbon Nanotubes for Enhanced Electrochemical Energy Storage. *J. Am. Chem. Soc.* **2011**, *133*, 16291–16299. [[CrossRef](#)] [[PubMed](#)]
388. Dang, A.; Sun, Y.; Fang, C.; Li, T.; Liu, X.; Xia, Y.; Ye, F.; Zada, A.; Khan, M. Rational Design of Ti₃C₂/carbon nanotubes/MnCo₂S₄ Electrodes for Symmetric Supercapacitors with High Energy Storage. *Appl. Surf. Sci.* **2022**, *581*, 152432. [[CrossRef](#)]
389. Shi, K.; Ren, M.; Zhitomirsky, I. Activated Carbon-Coated Carbon Nanotubes for Energy Storage in Supercapacitors and Capacitive Water Purification. *ACS Sustain. Chem. Eng.* **2014**, *2*, 1289–1298. [[CrossRef](#)]
390. Decruyenaere, J.G.; Holt, J.S. Seasonality of Clonal Propagation in Giant Reed. *Weed Sci.* **2006**, *49*, 760–767. [[CrossRef](#)]
391. Dunn, B.; Kamath, H.; Tarascon, J.M. Electrical Energy Storage for the Grid: A Battery of Choices. *Science* **2011**, *334*, 928–935. [[CrossRef](#)] [[PubMed](#)]
392. Wang, X.; Lu, X.; Liu, B.; Chen, D.; Tong, Y.; Shen, G. Flexible Energy-Storage Devices: Design Consideration and Recent Progress. *Adv. Mater.* **2014**, *26*, 4763–4782. [[CrossRef](#)]
393. Kitajima, K.; Joseph Wright, S.; Westbrook, J.W. Leaf Cellulose Density as the Key Determinant of Inter-and Intra-Specific Variation in Leaf Fracture Toughness in a Species-Rich Tropical Forest. *Interface Focus* **2016**, *6*, 20150100. [[CrossRef](#)]
394. Zhang, Q.; Huang, J.Q.; Qian, W.Z.; Zhang, Y.Y.; Wei, F. The Road for Nanomaterials Industry: A Review of Carbon Nanotube Production, Post-Treatment, and Bulk Applications for Composites and Energy Storage. *Small* **2013**, *9*, 1237–1265. [[CrossRef](#)] [[PubMed](#)]
395. Yamazaki, S.; Obata, K.; Okuhama, Y.; Matsuda, Y.; Ishikawa, M. Activated Carbon/DNA Composite Electrodes for Electric Double Layer Capacitors with Neutral Aqueous Electrolytes. *Electrochemistry* **2007**, *75*, 592–594. [[CrossRef](#)]
396. Dai, L.; Patil, A.; Gong, X.; Guo, Z.; Liu, L.; Liu, Y.; Zhu, D. Aligned Nanotubes. *ChemPhysChem* **2003**, *4*, 1150–1169. [[CrossRef](#)] [[PubMed](#)]
397. Chen, D.; Feng, H.; Li, J. Graphene Oxide: Preparation, Functionalization, and Electrochemical Applications. *Chem. Rev.* **2012**, *112*, 6027–6053. [[CrossRef](#)] [[PubMed](#)]
398. Ai, Y.; Lou, Z.; Chen, S.; Chen, D.; Wang, Z.M.; Jiang, K.; Shen, G. All rGO-on-PVDF-Nanofibers Based Self-Powered Electronic Skins. *Nano Energy* **2017**, *35*, 121–127. [[CrossRef](#)]
399. Lou, Z.; Chen, S.; Wang, L.; Jiang, K.; Shen, G. An Ultra-Sensitive and Rapid Response Speed Graphene Pressure Sensors for Electronic Skin and Health Monitoring. *Nano Energy* **2016**, *23*, 7–14. [[CrossRef](#)]
400. El-Kady, M.F.; Shao, Y.; Kaner, R.B. Graphene for Batteries, Supercapacitors and beyond. *Nat. Rev. Mater.* **2016**, *1*, 16033. [[CrossRef](#)]
401. Qin, Y.; Li, J.; Jin, X.; Jiao, S.; Chen, Y.; Cai, W.; Cao, R. Anthraquinone-Functionalized Graphene Framework for Supercapacitors and Lithium Batteries. *Ceram. Int.* **2020**, *46*, 15379–15384. [[CrossRef](#)]
402. He, X.; Tang, Z.; Gao, L.L.; Wang, F.; Zhao, J.; Miao, Z.; Wu, X.; Zhou, J.; Su, Y.; Zhuo, S. Facile and Controllable Synthesis N-Doping Porous Graphene for High-Performance Supercapacitor. *J. Electroanal. Chem.* **2020**, *871*, 114311. [[CrossRef](#)]
403. Kang, D.N.; Li, J.; Xu, Y.H.; Huang, W.X. Synthesis of MnO₂ Nanoparticle Decorated Graphene-Based Porous Composite Electrodes for High-Performance Supercapacitors. *Int. J. Electrochem. Sci.* **2020**, *15*, 6091–6108. [[CrossRef](#)]

404. Khawaja, M.K.; Khanfar, M.F.; Oghlenian, T.; Alnahar, W. Fabrication and Electrochemical Characterization of Graphene-Oxide Supercapacitor Electrodes with Activated Carbon Current Collectors on Graphite Substrates. *Comput. Electr. Eng.* **2020**, *85*, 106678. [[CrossRef](#)]
405. Wang, C.; Liu, F.; Chen, J.; Yuan, Z.; Liu, C.; Zhang, X.; Xu, M.; Wei, L.; Chen, Y. A Graphene-Covalent Organic Framework Hybrid for High-Performance Supercapacitors. *Energy Storage Mater.* **2020**, *32*, 448–457. [[CrossRef](#)]
406. Wang, H.; Tran, D.; Moussa, M.; Stanley, N.; Tung, T.T.; Yu, L.; Yap, P.L.; Ding, F.; Qian, J.; Losic, D. Improved Preparation of MoS₂/graphene Composites and Their Inks for Supercapacitors Applications. *Mater. Sci. Eng. B Solid-State Mater. Adv. Technol.* **2020**, *262*, 114700. [[CrossRef](#)]
407. Hamra, A.A.B.; Lim, H.N.; Huang, N.M.; Gowthaman, N.S.K.; Nakajima, H.; Rahman, M.M. Microwave Exfoliated Graphene-Based Materials for Flexible Solid-State Supercapacitor. *J. Mol. Struct.* **2020**, *1220*, 128710. [[CrossRef](#)]
408. Mondal, A.K.; Wang, B.; Su, D.; Wang, Y.; Chen, S.; Zhang, X.; Wang, G. Graphene/MnO₂ Hybrid Nanosheets as High Performance Electrode Materials for Supercapacitors. *Mater. Chem. Phys.* **2014**, *143*, 740–746. [[CrossRef](#)]
409. Pan, D.; Zhang, M.; Wang, Y.; Yan, Z.; Jing, J.; Xie, J. In Situ Fabrication of Nickel Based Oxide on Nitrogen-Doped Graphene for High Electrochemical Performance Supercapacitors. *Chem. Phys. Lett.* **2017**, *685*, 457–464. [[CrossRef](#)]
410. Chen, Y.; Huang, Z.; Zhang, H.; Chen, Y.; Cheng, Z.; Zhong, Y.; Ye, Y.; Lei, X. Synthesis of the Graphene/nickel Oxide Composite and Its Electrochemical Performance for Supercapacitors. *Int. J. Hydrogen Energy* **2014**, *39*, 16171–16178. [[CrossRef](#)]
411. Zhao, P.; Li, W.; Wang, G.; Yu, B.; Li, X.; Bai, J.; Ren, Z. Facile Hydrothermal Fabrication of Nitrogen-Doped graphene/Fe₂O₃ Composites as High Performance Electrode Materials for Supercapacitor. *J. Alloys Compd.* **2014**, *604*, 87–93. [[CrossRef](#)]
412. Tsai, W.Y.; Lin, R.; Murali, S.; Li Zhang, L.; McDonough, J.K.; Ruoff, R.S.; Taberna, P.L.; Gogotsi, Y.; Simon, P. Outstanding Performance of Activated Graphene Based Supercapacitors in Ionic Liquid Electrolyte from –50 to 80 °C. *Nano Energy* **2013**, *2*, 403–411. [[CrossRef](#)]
413. Lai, L.; Li, R.; Su, S.; Zhang, L.; Cui, Y.; Guo, N.; Shi, W.; Zhu, X. Controllable Synthesis of Reduced Graphene Oxide/nickel Hydroxide Composites with Different Morphologies for High Performance Supercapacitors. *J. Alloys Compd.* **2020**, *820*, 153120. [[CrossRef](#)]
414. Xu, T.; Yang, D.; Zhang, S.; Zhao, T.; Zhang, M.; Yu, Z.-Z. Antifreezing and Stretchable All-Gel-State Supercapacitor with Enhanced Capacitances Established by graphene/PEDOT-Polyvinyl Alcohol Hydrogel Fibers with Dual Networks. *Carbon* **2021**, *171*, 201–210. [[CrossRef](#)]
415. Abdallah, L.; El-Shennawy, T. Reducing Carbon Dioxide Emissions from Electricity Sector Using Smart Electric Grid Applications. *J. Eng.* **2013**, *2013*, 845051. [[CrossRef](#)]
416. Mohamad Nor, N.; Lau, L.C.; Lee, K.T.; Mohamed, A.R. Synthesis of Activated Carbon from Lignocellulosic Biomass and Its Applications in Air Pollution Control—A Review. *J. Environ. Chem. Eng.* **2013**, *1*, 658–666. [[CrossRef](#)]
417. Plaza, M.G.; González, A.S.; Pis, J.J.; Rubiera, F.; Pevida, C. Production of Microporous Biochars by Single-Step Oxidation: Effect of Activation Conditions on CO₂ Capture. *Appl. Energy* **2014**, *114*, 551–562. [[CrossRef](#)]
418. Abd, A.A.; Naji, S.Z.; Hashim, A.S.; Othman, M.R. Carbon Dioxide Removal through Physical Adsorption Using Carbonaceous and Non-Carbonaceous Adsorbents: A Review. *J. Environ. Chem. Eng.* **2020**, *8*, 104142. [[CrossRef](#)]
419. Kammerer, S.; Borho, I.; Jung, J.; Schmidt, M.S. Review: CO₂ Capturing Methods of the Last Two Decades. *Int. J. Environ. Sci. Technol.* **2022**, *1*–18. [[CrossRef](#)]
420. Wang, M.; Lawal, A.; Stephenson, P.; Sidders, J.; Ramshaw, C. Post-Combustion CO₂ Capture with Chemical Absorption: A State-of-the-Art Review. *Chem. Eng. Res. Des.* **2011**, *89*, 1609–1624. [[CrossRef](#)]
421. Tlili, N.; Grévillet, G.; Vallières, C. Carbon Dioxide Capture and Recovery by Means of TSA And/or VSA. *Int. J. Greenh. Gas Control* **2009**, *3*, 519–527. [[CrossRef](#)]
422. Dillon, E.P.; Crouse, C.A.; Barron, A.R. Synthesis, Characterization, and Carbon Dioxide Adsorption of Covalently Attached Polyethyleneimine-Functionalized Single-Wall Carbon Nanotubes. *ACS Nano* **2008**, *2*, 156–164. [[CrossRef](#)]
423. Abuelnoor, N.; AlHajaj, A.; Khaleel, M.; Vega, L.F.; Abu-Zahra, M.R.M. Activated Carbons from Biomass-Based Sources for CO₂ Capture Applications. *Chemosphere* **2021**, *282*, 131111. [[CrossRef](#)] [[PubMed](#)]
424. Ogungbenro, A.E.; Quang, D.V.; Al-Ali, K.A.; Vega, L.F.; Abu-Zahra, M.R.M. Synthesis and Characterization of Activated Carbon from Biomass Date Seeds for Carbon Dioxide Adsorption. *J. Environ. Chem. Eng.* **2020**, *8*, 104257. [[CrossRef](#)]
425. Wei, H.; Deng, S.; Hu, B.; Chen, Z.; Wang, B.; Huang, J.; Yu, G. Granular Bamboo-Derived Activated Carbon for High CO₂ Adsorption: The Dominant Role of Narrow Micropores. *ChemSusChem* **2012**, *5*, 2354–2360. [[CrossRef](#)]
426. Luo, L.; Chen, T.; Li, Z.; Zhang, Z.; Zhao, W.; Fan, M. Heteroatom Self-Doped Activated Biocarbons from Fir Bark and Their Excellent Performance for Carbon Dioxide Adsorption. *J. CO₂ Util.* **2018**, *25*, 89–98. [[CrossRef](#)]
427. Wei, H.; Chen, H.; Fu, N.; Chen, J.; Lan, G.; Qian, W.; Liu, Y.; Lin, H.; Han, S. Excellent Electrochemical Properties and Large CO₂ Capture of Nitrogen-Doped Activated Porous Carbon Synthesised from Waste Longan Shells. *Electrochim. Acta* **2017**, *231*, 403–411. [[CrossRef](#)]
428. Sevilla, M.; Fuertes, A.B. Sustainable Porous Carbons with a Superior Performance for CO₂ Capture. *Energy Environ. Sci.* **2011**, *4*, 1765. [[CrossRef](#)]
429. Zhu, X.-L.; Wang, P.-Y.; Peng, C.; Yang, J.; Yan, X.-B. Activated Carbon Produced from Paulownia Sawdust for High-Performance CO₂ Sorbents. *Chin. Chem. Lett.* **2014**, *25*, 929–932. [[CrossRef](#)]

430. Hong, S.-M.; Jang, E.; Dysart, A.D.; Pol, V.G.; Lee, K.B. CO₂ Capture in the Sustainable Wheat-Derived Activated Microporous Carbon Compartments. *Sci. Rep.* **2016**, *6*, 34590. [[CrossRef](#)] [[PubMed](#)]
431. Zhang, C.; Song, W.; Ma, Q.; Xie, L.; Zhang, X.; Guo, H. Enhancement of CO₂ Capture on Biomass-Based Carbon from Black Locust by KOH Activation and Ammonia Modification. *Energy Fuels* **2016**, *30*, 4181–4190. [[CrossRef](#)]
432. Wang, R.; Wang, P.; Yan, X.; Lang, J.; Peng, C.; Xue, Q. Promising Porous Carbon Derived from Celtsuce Leaves with Outstanding Supercapacitance and CO₂ Capture Performance. *ACS Appl. Mater. Interfaces* **2012**, *4*, 5800–5806. [[CrossRef](#)] [[PubMed](#)]
433. Jing, J.; Zhao, Z.; Zhang, X.; Feng, J.; Li, W. CO₂ Capture over Activated Carbon Derived from Pulverized Semi-Coke. *Separations* **2022**, *9*, 174. [[CrossRef](#)]
434. Sreńscek-Nazzal, J.; Narkiewicz, U.; Morawski, A.W.; Wróbel, R.J.; Michalkiewicz, B. Comparison of Optimized Isotherm Models and Error Functions for Carbon Dioxide Adsorption on Activated Carbon. *J. Chem. Eng. Data* **2015**, *60*, 3148–3158. [[CrossRef](#)]
435. Liu, C.; Xing, W.; Zhou, J.; Zhuo, S.P. N-Containing Activated Carbons for CO₂ Capture. *Int. J. Smart Nano Mater.* **2013**, *4*, 55–61. [[CrossRef](#)]
436. Przepiórski, J.; Skrodzewicz, M.; Morawski, A.W. High Temperature Ammonia Treatment of Activated Carbon for Enhancement of CO₂ Adsorption. *Appl. Surf. Sci.* **2004**, *225*, 235–242. [[CrossRef](#)]
437. Acevedo, S.; Giraldo, L.; Moreno-Piraján, J.C. Adsorption of CO₂ on Activated Carbons Prepared by Chemical Activation with Cupric Nitrate. *ACS Omega* **2020**, *5*, 10423–10432. [[CrossRef](#)] [[PubMed](#)]
438. Lu, C.; Bai, H.; Wu, B.; Su, F.; Hwang, J.F. Comparative Study of CO₂ Capture by Carbon Nanotubes, Activated Carbons, and Zeolites. *Energy Fuels* **2008**, *22*, 3050–3056. [[CrossRef](#)]
439. Songolzadeh, M.; Soleimani, M.; Takht Ravanchi, M.; Songolzadeh, R. Carbon Dioxide Separation from Flue Gases: A Technological Review Emphasizing Reduction in Greenhouse Gas Emissions. *Sci. World J.* **2014**, *2014*, 828131. [[CrossRef](#)] [[PubMed](#)]
440. Lee, A.; Nikraz, H. BOD: COD Ratio as an Indicator for River Pollution. *Int. Proc. Chem. Biol. Environ. Eng.* **2015**, *51*, 139–142. [[CrossRef](#)]
441. Dantas, T.L.; Rodrigues, A.E.; Moreira, R.F.P.M. Separation of Carbon Dioxide from Flue Gas Using Adsorption on Porous Solids. In *Greenhouse Gases—Capturing, Utilization and Reduction*; IntechOpen: London, UK, 2012; pp. 57–80.
442. Raganati, F.; Ammendola, P.; Chirone, R. CO₂ capture by Adsorption on Fine Activated Carbon in a Sound Assisted Fluidized Bed. *Chem. Eng. Trans.* **2015**, *43*, 1033–1038. [[CrossRef](#)]
443. Plaza, M.G.; Pevida, C.; Arenillas, A.; Rubiera, F.; Pis, J.J. CO₂ Capture by Adsorption with Nitrogen Enriched Carbons. *Fuel* **2007**, *86*, 2204–2212. [[CrossRef](#)]
444. Nasri, N.S.; Hamza, U.D.; Ismail, S.N.; Ahmed, M.M.; Mohsin, R. Assessment of Porous Carbons Derived from Sustainable Palm Solid Waste for Carbon Dioxide Capture. *J. Clean. Prod.* **2014**, *71*, 148–157. [[CrossRef](#)]
445. Li, Y.; Ruan, G.; Jalilov, A.S.; Tarkunde, Y.R.; Fei, H.; Tour, J.M. Biochar as a Renewable Source for High-Performance CO₂ Sorbent. *Carbon* **2016**, *107*, 344–351. [[CrossRef](#)]
446. Zhang, X.; Zhang, S.; Yang, H.; Shao, J.; Chen, Y.; Liao, X.; Wang, X.; Chen, H. Generalized Two-Dimensional Correlation Infrared Spectroscopy to Reveal Mechanisms of CO₂ Capture in Nitrogen Enriched Biochar. *Proc. Combust. Inst.* **2017**, *36*, 3933–3940. [[CrossRef](#)]
447. Zhang, X.; Zhang, S.; Yang, H.; Shao, J.; Chen, Y.; Feng, Y.; Wang, X.; Chen, H. Effects of Hydrofluoric Acid Pre-Deashing of Rice Husk on Physicochemical Properties and CO₂ Adsorption Performance of Nitrogen-Enriched Biochar. *Energy* **2015**, *91*, 903–910. [[CrossRef](#)]
448. Madejski, P.; Chmiel, K.; Subramanian, N.; Kuś, T. Methods and Techniques for CO₂ Capture: Review of Potential Solutions and Applications in Modern Energy Technologies. *Energies* **2022**, *15*, 887. [[CrossRef](#)]
449. Sabzehmeidani, M.M.; Mahnaee, S.; Ghaedi, M.; Heidari, H.; Roy, V.A.L. Carbon Based Materials: A Review of Adsorbents for Inorganic and Organic Compounds. *Mater. Adv.* **2021**, *2*, 598–627. [[CrossRef](#)]
450. Samanta, A.; Zhao, A.; Shimizu, G.K.H.; Sarkar, P.; Gupta, R. Post-Combustion CO₂ Capture Using Solid Sorbents: A Review. *Ind. Eng. Chem. Res.* **2012**, *51*, 1438–1463. [[CrossRef](#)]
451. Grondein, A.; Bélanger, D. Chemical Modification of Carbon Powders with Aminophenyl and Aryl-Aliphatic Amine Groups by Reduction of in Situ Generated Diazonium Cations: Applicability of the Grafted Powder towards CO₂ Capture. *Fuel* **2011**, *90*, 2684–2693. [[CrossRef](#)]
452. Ye, Q.; Jiang, J.; Wang, C.; Liu, Y.; Pan, H.; Shi, Y. Adsorption of Low-Concentration Carbon Dioxide on Amine-Modified Carbon Nanotubes at Ambient Temperature. *Energy Fuels* **2012**, *26*, 2497–2504. [[CrossRef](#)]
453. Liu, Y.; Ye, Q.; Shen, M.; Shi, J.; Chen, J.; Pan, H.; Shi, Y. Carbon Dioxide Capture by Functionalized Solid Amine Sorbents with Simulated Flue Gas Conditions. *Environ. Sci. Technol.* **2011**, *45*, 5710–5716. [[CrossRef](#)] [[PubMed](#)]
454. Su, F.; Lu, C.; Cnen, W.; Bai, H.; Hwang, J.F. Capture of CO₂ from Flue Gas via Multiwalled Carbon Nanotubes. *Sci. Total Environ.* **2009**, *407*, 3017–3023. [[CrossRef](#)] [[PubMed](#)]
455. Cinke, M.; Li, J.; Bauschlicher, C.W.; Ricca, A.; Meyyappan, M. CO₂ Adsorption in Single-Walled Carbon Nanotubes. *Chem. Phys. Lett.* **2003**, *376*, 761–766. [[CrossRef](#)]
456. Osler, K.; Twala, N.; Oluwasina, O.O.; Daramola, M.O. Synthesis and Performance Evaluation of Chitosan/Carbon Nanotube (Chitosan/MWCNT) Composite Adsorbent for Post-Combustion Carbon Dioxide Capture. *Energy Procedia* **2017**, *114*, 2330–2335. [[CrossRef](#)]

457. Salehi, S.; Anbia, M.; Hosseiny, A.H.; Sepehrian, M. Enhancement of CO₂ Adsorption on Polyethylenimine Functionalized Multiwalled Carbon nanotubes/Cd-Nanozeolite Composites. *J. Mol. Struct.* **2018**, *1173*, 792–800. [[CrossRef](#)]
458. Keller, L.; Ohs, B.; Lenhart, J.; Abduly, L.; Blanke, P.; Wessling, M. High Capacity Polyethylenimine Impregnated Microtubes Made of Carbon Nanotubes for CO₂ Capture. *Carbon* **2018**, *126*, 338–345. [[CrossRef](#)]
459. Ngoy, J.M.; Wagner, N.; Riboldi, L.; Bolland, O. A CO₂ Capture Technology Using Multi-Walled Carbon Nanotubes with Polyaspartamide Surfactant. *Energy Procedia* **2014**, *63*, 2230–2248. [[CrossRef](#)]
460. Irani, M.; Jacobson, A.T.; Gasem, K.A.M.; Fan, M. Modified Carbon Nanotubes/tetraethylenepentamine for CO₂ Capture. *Fuel* **2017**, *206*, 10–18. [[CrossRef](#)]
461. Gunathilake, C.; Dassanayake, R.S.; Abidi, N.; Jaroniec, M. Amidoxime-Functionalized Microcrystalline Cellulose–mesoporous Silica Composites for Carbon Dioxide Sorption at Elevated Temperatures. *J. Mater. Chem. A* **2016**, *4*, 4808–4819. [[CrossRef](#)]
462. Yu, B.; Cong, H.; Li, Z.; Tang, J.; Zhao, X.S. Pebax-1657 Nanocomposite Membranes Incorporated with Nanoparticles/colloids/carbon Nanotubes for CO₂/N₂ and CO₂/H₂ Separation. *J. Appl. Polym. Sci.* **2013**, *130*, 2867–2876. [[CrossRef](#)]
463. Su, F.; Lu, C.; Chung, A.J.; Liao, C.H. CO₂ Capture with Amine-Loaded Carbon Nanotubes via a Dual-Column Temperature/vacuum Swing Adsorption. *Appl. Energy* **2014**, *113*, 706–712. [[CrossRef](#)]
464. Sun, Q.; Wang, M.; Li, Z.; Ma, Y.; Du, A. CO₂ Capture and Gas Separation on Boron Carbon Nanotubes. *Chem. Phys. Lett.* **2013**, *575*, 59–66. [[CrossRef](#)]
465. Jiao, Y.; Zheng, Y.; Smith, S.C.; Du, A.; Zhu, Z. Electrocatalytically Switchable CO₂ Capture: First Principle Computational Exploration of Carbon Nanotubes with Pyridinic Nitrogen. *ChemSusChem* **2014**, *7*, 435–441. [[CrossRef](#)]
466. Lu, A.-H.; Hao, G.-P.; Zhang, X.-Q. Porous Carbons for Carbon Dioxide Capture. In *Green Chemistry and Sustainable Technology*; Springer: Berlin/Heidelberg, Germany, 2014; pp. 15–77.
467. Chowdhury, S.; Parshetti, G.K.; Balasubramanian, R. Post-Combustion CO₂ Capture Using Mesoporous TiO₂/graphene Oxide Nanocomposites. *Chem. Eng. J.* **2015**, *263*, 374–384. [[CrossRef](#)]
468. Alhwaige, A.A.; Agag, T.; Ishida, H.; Qutubuddin, S. Biobased Chitosan Hybrid Aerogels with Superior Adsorption: Role of Graphene Oxide in CO₂ Capture. *RSC Adv.* **2013**, *3*, 16011–16020. [[CrossRef](#)]
469. Yang, S.; Zhan, L.; Xu, X.; Wang, Y.; Ling, L.; Feng, X. Graphene-Based Porous Silica Sheets Impregnated with Polyethyleneimine for Superior CO₂ Capture. *Adv. Mater.* **2013**, *25*, 2130–2134. [[CrossRef](#)] [[PubMed](#)]
470. Srinivas, G.; Burrell, J.; Yildirim, T. Graphene Oxide Derived Carbons (GODCs): Synthesis and Gas Adsorption Properties. *Energy Environ. Sci.* **2012**, *5*, 6453–6459. [[CrossRef](#)]
471. Chandra, V.; Yu, S.U.; Kim, S.H.; Yoon, Y.S.; Kim, D.Y.; Kwon, A.H.; Meyyappan, M.; Kim, K.S. Highly Selective CO₂ Capture on N-Doped Carbon Produced by Chemical Activation of Polypyrrole Functionalized Graphene Sheets. *Chem. Commun.* **2012**, *48*, 735–737. [[CrossRef](#)] [[PubMed](#)]
472. Szczeńniak, B.; Choma, J. Graphene-Containing Microporous Composites for Selective CO₂ Adsorption. *Microporous Mesoporous Mater.* **2020**, *292*, 109761. [[CrossRef](#)]
473. Arifutzzaman, A.; Musa, I.N.; Aroua, M.K.; Saidur, R. MXene Based Activated Carbon Novel Nano-Sandwich for Efficient CO₂ Adsorption in Fixed-Bed Column. *J. CO₂ Util.* **2023**, *68*, 102353. [[CrossRef](#)]
474. Creamer, A.E.; Gao, B. Carbon-Based Adsorbents for Postcombustion CO₂ Capture: A Critical Review. *Environ. Sci. Technol.* **2016**, *50*, 7276–7289. [[CrossRef](#)] [[PubMed](#)]

Disclaimer/Publisher’s Note: The statements, opinions and data contained in all publications are solely those of the individual author(s) and contributor(s) and not of MDPI and/or the editor(s). MDPI and/or the editor(s) disclaim responsibility for any injury to people or property resulting from any ideas, methods, instructions or products referred to in the content.